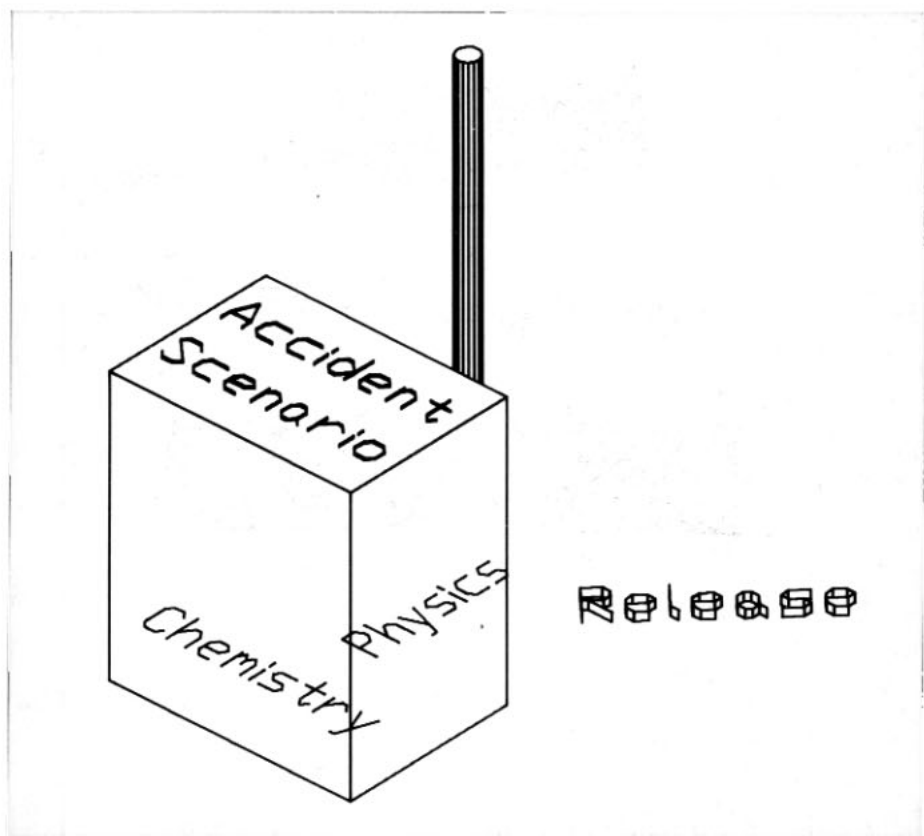


# THE INFLUENCE OF CHEMISTRY ON CORE MELT ACCIDENTS



# **THE INFLUENCE OF CHEMISTRY ON CORE MELT ACCIDENTS**

**Final Report of the NKA Project AKTI-150**

**R. Alenljung, L.G. Johansson and O. Lindquist  
Department of Inorganic Chemistry,  
Chalmers University of Technology and University of Göteborg,  
Sweden**

**L. Hammar  
Swedish Nuclear Power Inspectorate**

**A. Hautojärvi and Jorma Jokiniemi  
Nuclear Engineering Laboratory,  
Technical Research Center of Finland**

**J.O. Liljenzin and J.P. Omtvedt  
Department of Chemistry, University of Oslo, Norway**

**T. Raunemaa, K. Koistinen and P. Pasanen  
Laboratory for Atmospheric Physics and Chemistry,  
Department of Environmental Health, University of Kuopio, Finland**

**U. Steiner Jensen  
ELSAM, Denmark**

**Edited by J.O. Liljenzin**

**September 1990**

This report is available on request from:

The Swedish Nuclear Power Inspectorate  
Box 27106  
S-10252 Stockholm  
Sweden

This report is part of the Nordic nuclear safety programme 1985-89 sponsored by NKA, the Nordic Liaison Committee for Atomic Energy. The work has been financed in part by the Nordic Council of Ministers, in part by national sources through the participating organizations.

ISBN 87 7303 452 5  
NORD 1990:56

Graphic Systems AB, Malmö 1990

## SUMMARY

Chemical reactions play an important role in many of the accident sequences which have to be analyzed in order to assess the safety of nuclear power plants.

The progression of hypothetical accidents in which it is assumed that the reactor core melts is to-day routinely modeled in mathematical terms. These models are expressed as various computer codes. Such codes have been used in the Nordic countries in the safety analysis of the four Finnish and twelve Swedish nuclear power reactors. One of the most frequently used models is the MAAP code, developed in the USA.

The processes included in these codes are mainly of a physical nature and their description is by necessity approximate. The main source of heat in the early stage of an accident is, however, due to a chemical reaction between steam and the zirconium encapsulating the nuclear fuel. The heating and melting of fuel leads to a release of fission products which rapidly condense to form particles suspended in the surrounding gas, so called aerosols. Aerosols are the main carriers of radioactivity as they may transport active material from the reactor vessel into the reactor containment building where it is deposited.

The content of fission products in the aerosol particles and their chemical form determine their interaction with water molecules. Chemical forces lead to an absorption of water in the particles which transforms them into droplets with increased mass. Thereby the particles become spherical and hence deposit more rapidly on surrounding surfaces. This phenomenon has been studied in the AKTI-150 project and its importance verified, thus permitting a mathematical modeling of this effect.

Contrary to earlier assumptions it was found that boron carbide present in the control blades of boiling water reactors do not primarily form boric acid by reaction with steam. Instead there is a rapid reaction between boron carbide and stainless steel in the blades. Consequently, there is only a small formation of boric acid which reduces the importance of its chemical reactions. This in turn leads to a smaller formation of volatile iodine compounds. On the other hand, the alloying process is likely to cause melting of the control blades so they are removed from the reactor core, a process which may have secondary effects to take into account in the safety analysis.

A mathematical description of chemical reactions and of their velocity has been introduced in a slightly modified version of the MAAP code. This permits an inclusion of pertinent chemical effects in the analysis of a hypothetical accident. The code version developed within this project is called CHMAAP.

It has also been found that a series of materials that are present in the reactor containment are likely to participate in various chemical reactions during an accident. Among the important materials

are electric cables, motors, thermal insulation, surface coatings and sheet metal. Metallic surface coatings and sheet metal can be some of the main sources of hydrogen.

The work performed within the AKTI-150 project has underlined the importance of including chemical phenomena in reactor accident analysis to improve its realism. The accuracy of predictions from the chemical models depend on the availability of reliable data on reaction rates and on chemical thermodynamic properties. The need for better data is great. Once such data become available the effects from chemical reactions can be more accurately predicted by the new CHMAAP code which combines thermal, hydraulic and chemical phenomena.

It should be noted that, at the present state of knowledge, no effects have been observed that are likely to change the major conclusions drawn from recent safety analyses of the nuclear power reactors operating in Scandinavia.

## SAMMANFATTNING

Kemiska reaktioner spelar en betydelsefull roll i många av de olyckssekvenser som måste analyseras i samband med bedömning av säkerheten hos kärnkraftverk.

Förloppet av hypotetiska svåra olyckor där man antar att reaktorhärden smälter modelleras i dag rutinmässigt med hjälp av matematiska samband. Dessa samband utnyttjas sedan i form av olika datorprogram. Sådana program har använts i de nordiska länderna vid säkerhetsanalys av de 4 finska och de 12 svenska kärnkraftreaktorerna. En av de mest utnyttjade koderna är det i USA utvecklade MAAP programmet.

De processer som behandlas i dessa koder omfattar i huvudsak fysikaliska fenomen och beskrivningen av verkligheten måste med nödvändighet vara förenklad. Huvudorsak till den stora värmeutvecklingen under början av en stor olycka är emellertid en kemisk reaktion mellan vattenånga och det zirkonium som utgör kapsling för kärnbränslet. Upphettnings och nedsmältning av bränsle medför att klyvningsprodukter frigörs. Dessa kondenserar snabbt till partiklar som svävar i omgivande gas, så kallade aerosoler. Dessa aerosoler innehåller radioaktiva ämnen och de är huvudsakligen i denna form som dessa ämnen kan transporteras från reaktortanken till inneslutningen.

Innehållet av fissionsprodukter i aerosolpartiklarna och dessas kemiska form styr växelverkan mellan partiklarna och omgivande vattenmolekyler. Kemiska krafter leder till att vatten absorberas av aerosolpartiklarna som därigenom övergår i droppform. Härigenom ökar partiklarnas massa och de blir droppformade. Detta leder till en snabbare avsättning av aerosolen på närliggande ytor. Dessa fenomen har studerats inom AKTI-150 projektet varvid fenomenens betydelse fastställts och en matematisk modellering kunnat göras.

I motsats till tidigare antaganden upptäcktes att den borkarbid som ingår i reaktorernas rostfria styrstavar inte i första hand oxideras av omgivande ånga till borsyra utan snabbt legerar sig med stålet i styrstavarna. Följaktligen blir bildningen av borsyra betydligt mindre än som vad tidigare antagits, vilket minskar betydelsen av borsyrans kemiska reaktioner. I sin tur leder detta till en mindre bildning av flyktiga jodföreningar. Å andra sidan medför denna legeringsbildning att styrstavarna kan försvinna ur härden, vilket kan ha sekundära effekter som bör behandlas vid säkerhetsanalysen.

En matematisk beskrivning av kemiska reaktioner och deras hastighet har införts i en något modifierad form av MAAP koden. Detta gör det möjligt att inkludera viktigare kemiska effekter i analyser av hypotetiska olyckor. Den version av koden som utvecklats inom projektet kallas CHMAAP.

Man har även upptäckt att en hel serie av material som förekommer i reaktorinneslutningen kan delta i olika kemiska reaktioner under ett stort haveri. Bland dessa material märks särskilt elektriska kablar, motorer, värmeisolering, ytbeläggningar och tunna plåtar.

Metalliska ytbeläggningar och tunna plåtar kan utgöra några av huvudkällorna till vätgas.

Det arbete som utförts inom AKTI-150 projektet har understrukt betydelsen av att kemiska fenomen inkluderas vid analysen av hypotetiska svåra olyckor för att deras behandling skall bli mer realistisk. Värdet av de kemiska modellernas förutsägelser avhänger av tillgången på pålitliga data för reaktionshastigheter och kemisk termodynamik. Behovet av bättre data är stort. När sådana data blir tillgängliga är det möjligt att förutsäga effekterna av kemin med större tillförlitlighet genom användning av den nya CHMAAP koden som kombinerar termiska, hydrauliska och kemiska fenomen.

Med dagens kunskaper har dock inga nya fenomen identifierats som leder till omvärdering av de säkerhetsanalyser som har gjorts för kärnkraftverken i Norden.

TABLE OF CONTENTS

1	INTRODUCTION	1
2	CHEMICAL SPECIES AND CHEMICAL BEHAVIOR IN CORE MELT ACCIDENTS - AN OVERVIEW	3
3	SPECIFIC STUDIES PERFORMED WITHIN AKTI-150	7
3.1	Studies of the hygroscopicity of cesium hydroxide by measurement of the vapor pressure in the system H <sub>2</sub> O-CsOH	7
3.1.1	<u>Introduction</u>	7
3.1.2	<u>Experimental</u>	8
3.1.3	<u>Results and discussion</u>	9
3.1.4	<u>References</u>	10
3.2	Studies of hygroscopic aerosols	13
3.2.1	<u>Sedimentation in tubes</u>	13
3.2.1.1	<u>Introduction</u>	13
3.2.1.2	<u>Test matrix</u>	13
3.2.1.3	<u>Experimental</u>	14
3.2.1.4	<u>Deposition characteristics of mixed cesium hydroxide/zinc aerosol</u>	15
3.2.1.5	<u>Analysis of results and discussion</u>	17
3.2.1.6	<u>References</u>	19
3.2.2	<u>Condensational growth of hygroscopic aerosols in moist air</u>	19
3.2.2.1	<u>Introduction</u>	19
3.2.2.2	<u>Behavior of hygroscopic aerosols</u>	20
3.2.2.2.1	Water activity	20
3.2.2.2.2	Mass and heat transfer	21
3.2.2.2.3	The equilibrium radius	21
3.2.2.3	<u>Experimental</u>	23
3.2.2.4	<u>Measurements</u>	25
3.2.2.5	<u>Results</u>	27
3.2.2.5.1	Facility testing	27
3.2.2.5.2	Theoretical calculations	27
3.2.2.5.3	Experiments with hygroscopic CsOH	29
3.2.2.5.3.1	After 10 minutes travel time	30
3.2.2.5.3.2	After 5 minutes and 2 minutes travel time	30
3.2.2.6	<u>Discussion</u>	32
3.2.2.6.1	Cesium hydroxide aerosol	33
3.2.2.7	<u>Conclusions</u>	35
3.2.2.8	<u>Nomenclature</u>	35
3.2.2.9	<u>References</u>	36
3.2.3	<u>Conclusions</u>	37
3.3	Reactions of boron carbide with steam and stainless steel	38
3.3.1	<u>Introduction</u>	38
3.3.2	<u>Experimental</u>	38
3.3.3	<u>Kinetics of boron carbide oxidation in steam</u>	40
3.3.4	<u>Kinetics of reaction between boron carbide and steel</u>	42
3.3.5	<u>Results and discussion</u>	43
3.3.6	<u>References</u>	44
3.4	Stickiness and flow properties of a deposited wet slurry	45
3.4.1	<u>References</u>	46

3.5	Acidity/basicity of water solutions in the containment during some selected accident sequences	46
3.5.1	<u>Pyrolysis of insulating materials</u>	47
3.5.2	<u>Corrosion of aluminium and zinc</u>	50
3.5.3	<u>Copper</u>	51
3.5.4	<u>Conclusions</u>	52
3.5.5	<u>References</u>	53
3.6	Assessment of the contribution to formation of hydrogen to be expected in the primary system under core melt accident conditions due to corrosion of steels	53
4	DISCUSSION OF POSSIBLE INFLUENCES OF CHEMICAL BEHAVIOR ON SPECIFIC PROCESSES AFFECTING THE COURSE OF EVENTS IN CORE MELT ACCIDENTS	55
4.1	Melt progression	55
4.2	Hydrogen formation	55
4.3	Evaporation and nucleation	56
4.4	Reactions in the reactor coolant system	57
4.5	Aerosol nucleation	57
4.6	Condensation and chemisorption on aerosol particles	60
4.7	Agglomeration of aerosol particles	61
4.8	Condensation on surfaces in the reactor coolant system	63
4.9	Reevaporation	63
4.10	Resuspension	63
4.11	Fission product release from melt-concrete reaction	64
4.12	Acid-base balance (pH) in the containment	64
4.13	Speciation of iodine in the primary system	66
4.13.1	<u>Possible iodine chemical forms following an accident</u>	67
4.13.2	<u>Formation of hydrogen iodide</u>	67
4.13.3	<u>Radiolytic reactions in the primary system</u>	68
4.14	Speciation of iodine in the aqueous phase	68
4.14.1	<u>Transport of iodine from the primary system to the containment</u>	69
4.14.2	<u>Hydrolysis of I<sub>2</sub></u>	69
4.14.3	<u>Formation of CH<sub>3</sub>I</u>	70
4.14.4	<u>Conditions under which iodine may be released to the environment</u>	70
4.15	References	70
5	THE MODELING OF CHEMICAL BEHAVIOR IN ACCIDENT ANALYSIS CODES	73
5.1	Release from fuel and structural materials	73
5.1.1	<u>GRASS codes</u>	73
5.1.2	<u>VICTORIA</u>	74
5.1.3	<u>CORSOR (STCP)</u>	75
5.1.4	<u>FAEREL</u>	76
5.2	Chemical reactions within the primary system	77
5.2.1	<u>VICTORIA</u>	77
5.2.2	<u>RAFT (Reactor Aerosol Formation and Transport Code)</u>	79
5.2.3	<u>HORN</u>	80
5.3	Core - concrete interaction	81
5.4	Chemical reactions within the containment	83
5.5	Integrated severe reactor accident codes	83
5.6	Concluding remarks	83

5.7	References	84
6	GENERAL RECOMMENDATIONS FOR MODELING OF CHEMICAL BEHAVIOR IN ACCIDENT ANALYSIS CODES	87
6.1	Overview	87
6.2	Overview of what needs to be done	88
6.3	Chemical aspects on the feedback	89
6.4	A chemists view of accident analysis codes	90
6.5	Chemical phenomena which ought to be modeled	91
6.6	Reasons for the chosen considerations	92
6.6.1	<u>Formation of chemical systems</u>	92
6.6.1.1	<u>A model for formation of chemical systems</u>	92
6.6.1.2	<u>Chemical change</u>	93
6.6.1.3	<u>A model for prediction of chemical change</u>	93
6.6.1.4	<u>The time aspect</u>	94
6.6.1.5	<u>A model for the time aspect of change</u>	94
6.6.1.6	<u>Initialization of matter transport</u>	94
6.6.1.7	<u>A model for initialization of matter transport</u>	95
6.6.2	<u>Modeling of chemistry in the containment</u>	95
6.6.2.1	<u>The containment after the slump</u>	96
7	RECOMMENDED MODELING OF AEROSOL BEHAVIOR IN ACCIDENT ANALYSIS CODES WITH REGARD TO HYGROSCOPICITY	99
7.1	Introduction	99
7.2	Requirements for modeling hygroscopic particles	99
7.3	References	100
8	DESCRIPTION OF THE MODELING OF CHEMICAL BEHAVIOR USED IN THE MAAP CODE. ASSESSMENT OF THE SIGNIFICANCE OF SIMPLIFICATIONS AND APPROXIMATIONS	103
8.1	The core	103
8.2	The rest of the reactor vessel	103
8.3	The region below the vessel when corium flows through this region	104
8.4	The bottom of the containment when the corium is situated there	104
8.5	The containment, excluding the bottom, after the slump	104
8.6	Interaction between thermal hydraulics and chemistry	104
8.7	Shortcomings of the chemical model in MAAP	105
8.8	Identified errors in MAAP	106
8.9	Conclusions	107
8.10	Reference	107
9	THE SOLGASMIX DATA BASE - SUITABILITY AS A BASIS FOR THE MODELING OF CHEMICAL BEHAVIOR IN CORE MELT ACCIDENTS	109
9.1	The extent of the data base	109
9.2	Limitations of a data base of only pure chemical compounds	109
9.3	Consistency of the JANAF tables	110
9.4	Recommendations for future improvements	110
9.5	References	110

10	CELSOL ANALYSES OF SEVERE LWR REACTOR ACCIDENTS	111
10.1	The CELSOL code	111
10.2	CELSOL analyses of the TB accident sequence	112
10.2.1	<u>TB Accident sequence with automatic depressurization</u>	114
10.2.1.1	<u>TB with ADS and no boron release</u>	114
10.2.1.2	<u>TB with ADS and new boron data from Winfrith</u>	115
10.2.1.3	<u>TB with ADS and JANAF boron data</u>	117
10.2.2	<u>TB accidents without automatic depressurization</u>	119
10.2.2.1	<u>TB without ADS and no boron release</u>	119
10.2.2.2	<u>TB without ADS and with new boron data from Winfrith</u>	121
10.2.2.3	<u>TB without ADS and with JANAF boron data</u>	123
10.2.3	<u>Analysis of the chemical importance of plate out</u>	124
10.3	Conclusions concerning CELSOL analyses	125
10.4	Recommendations for the future	127
10.5	References	127
11	EXTENDED CHEMISTRY MODEL FOR THE MAAP CODE, BASED ON SOLGASMIX AND SIMPLISTIC SIMULATION OF REACTION RATE LIMITATIONS, FOR APPLICATIONS IN SENSITIVITY ANALYSIS	129
11.1	Strategy for development and implementation	129
11.2	Some thoughts about the modeling of chemistry during severe accident conditions	129
11.2.1	<u>Fulfillment of condition 1</u>	130
11.2.2	<u>Fulfillment of condition 2</u>	130
11.2.3	<u>Fulfillment of condition 3</u>	130
11.3	The modeling of chemical phenomena	130
11.4	How to speed up the execution of the chemical model	131
11.5	The specific descriptions for the main system	132
11.6	Summary of the chemical model	132
11.7	Functional description of the MAAP chemistry extension	133
11.7.1	<u>Gas phase reactions</u>	133
11.7.2	<u>Reactions between gas and aerosol</u>	135
11.7.3	<u>Reactions between deposited substances</u>	135
11.7.4	<u>Aerosol deposition</u>	136
11.7.4.1	<u>Nodes with liquid water present</u>	136
11.7.4.2	<u>Dry nodes</u>	136
11.7.5	<u>Reactions between gas and surfaces</u>	137
11.7.6	<u>Formation of new amounts in the MAAP groups</u>	137
11.7.7	<u>Mass rate-of-change calculation</u>	138
11.8	Applications	138
11.9	Recommendations for future development	139
12	COMPARISON BETWEEN THE CHMAAP AND MAAP CODES	141
12.1	How the comparison was performed	141
12.1.1	<u>Description of some of the differences observed</u>	141
12.2	Conclusions	143
12.3	Recommendations for the future	144
13	CONCLUSIONS AND RECOMMENDATIONS	183

## 1 INTRODUCTION

The Nordic Nuclear Safety Research (NKA) Program was conducted jointly by the Nordic countries Denmark, Finland, Norway and Sweden with the main purpose to form unified views on the safety of the Nordic nuclear power installations, located exclusively in Finland and Sweden, and to contribute to maintaining an adequate level of competence in all the Nordic countries so as to enable continued discussions of nuclear safety matters creating concern across the borders. The most recent NKA Program, which commenced in 1985 and presently is completed (1990), comprised projects on severe core melt accidents (the so-called AKT program), nuclear waste management, general nuclear risk analysis, materials science related to nuclear safety and advanced information technology applied to nuclear emergency preparedness. This research program is the third of its kind, the first one started already in 1977, i.e. before the TMI accident.

The AKT program was concerned with the source term in the event of severe core accidents (the AKTI Projects) and the consequences in the environment (the AKTU Projects). The present report covers one of the AKTI projects (AKTI-150), dealing with the chemical aspects of the accidents.

An increasing realization of the importance of considerations related to chemistry and chemical behavior forms the background to the project to be reported below. While the phenomena prevailing under severe accident conditions were in the past mainly described in terms of thermal hydraulics and aerosol physics, accounting for the chemical behavior of a great variety of fission products and other matter only in a very crude manner, modeling of the chemistry in recent versions of the 'mechanistic' accident analysis codes is becoming more realistic. At the same time it is becoming obvious that there is a definite practical limit to what can be achieved in this regard, i.e. in terms of increasingly complex and slow-running codes and lack of thermodynamic data of the chemical species and non ideal mixtures concerned - not to mention the reaction rate (kinetic) data.

However, in order to enable practical risk- and safety analyses of the nuclear power plants, as well as various systems considered for accident consequence mitigation (like filtered containment venting) and prepared schemes for accident management, there is a need for much simpler and more fast-running accident analysis codes. Such codes - usually called 'risk analysis codes' - obviously need efficient, simplistic chemical modeling. The preferred risk analysis code in Sweden and Finland is the so-called MAAP code (Modular Accident Analysis Program) which was developed in the IDCOR program in the USA, in which Finland and Sweden participated and which was specifically adapted to the Nordic reactors.

It has been a main concern of the AKTI-150 project to provide an assessment of the MAAP code in regard of the uncertainty of calculated source term data likely to be related to the poor chemical

modeling used in the code. As the code is not aimed for accurate predictions of the source term, but for providing necessary understanding of the possible course of events in an accident, the aim has not been, in the first place, to try to improve the chemical modeling used in the code but to provide indications of possible great uncertainties of practical significance, if any. Such indications could then serve a useful purpose in practical interpretations of results obtained using the code.

Accordingly, the main purpose of the AKTI-150 project has been to develop an improved understanding of the severe accident phenomena, particularly in regard of the possible significance of aspects of chemical behavior. This was attempted partly by performing studies of certain particular issues related to chemical behavior and partly by studies of certain chemical model implementations in codes used for analyzing accident sequences.

The main working goals for the projects were:

- \* Review of chemical phenomena with potential influence on the course of core melt accidents, on the practicability of accident management procedures and on the source term
- \* Assessment of the significance, if any, of the poor representation of chemical behavior in the MAAP code
- \* Improving the knowledge of certain selected issues concerning chemical behavior of assumed significance, particularly related to the chemistry of cesium, iodine and boron
- \* Compilation of relevant chemical data and recommendations to form a basis for a handbook concerning core melt accidents

The following tasks were formulated and distributed between research institutions in the participating countries:

Denmark: Development and application of the CELSOL code for accident analysis with regard to chemical behavior of the fission products.

Finland: The behavior of hygroscopic aerosols under severe accident conditions: experimental simulation and theoretical assessment.

Norway: Studies of the reactions between boron carbide, steam and stainless steel.

Sweden: Studies of the hygroscopicity of cesium hydroxide by measurement of the water vapor pressure in the system  $H_2O - CsOH$ .

Development of a general chemical model for transport of matter which includes simple modeling of formation and disruption of chemical systems and a simplistic simulation of reaction rate limitations. The modeling of chemical reactions are based on the SOLGASMIX code. Sensitivity studies using the modified MAAP code containing a model of chemistry.

2 CHEMICAL SPECIES AND CHEMICAL BEHAVIOR IN CORE MELT ACCIDENTS -  
AN OVERVIEW

The release of activity to the environment at a nuclear reactor core meltdown is critically dependent upon plant design and type of accident. It follows that any estimate of those releases using e.g. various computer codes will be plant specific and will only apply to a certain accident sequence. The complexity of the nuclear reactor and the many possible event trees imply that any calculation of the radioactive source term will contain large uncertainties.

Chemical reactions and chemical speciation is important to the release and transport of radio nuclides. Part of the uncertainty in the calculation of releases at a core meltdown stems from the fact that the existing codes and code packages cover the chemistry of the radio nuclides very incompletely.

It is probable that the thermohydraulics of a number of accident sequences is modeled fairly well by existing computer codes (e.g. MAAP).

Even if we would know the temperature and pressure everywhere in the system as a function of time, the release of activity from the core, the transport of this activity through the primary system to the containment and further into the environment are still difficult to predict.

The release of activity from the core (the core source term) is governed by a number of factors besides temperature and pressure. These factors include melt progression, melt composition, the surface area of the melt and convection within the melt and in the gas phase.

To some extent the core source term depends on the chemistry of the melt. The equilibrium vapor pressure of the different elements, some of which contain important radioactive isotopes, will be greatly reduced if they dissolve in the melt. The equilibrium vapor pressures of the fission products also changes due to the formation of compounds with substances in the melt.

The melt will not be a single phase but an oxidic melt and a metallic melt will tend to separate. These will have different density and different tendency to dissolve and react with the radioactive elements.

The radioactive substances may vaporize as elements or as compounds, depending on chemical affinity.

In the reactor vessel and in other parts of the primary system temperatures will be lower than in the melted core where temperatures may reach 2300°C. As the vapors cool down they will start to condense, plate out on surfaces and/or form one or more aerosols.

The substances released in the primary system will be partly in

gaseous and partly in particulate form. This means that gaseous transport (e.g. convection, condensation, agglomeration, sedimentation and resuspension) need to be considered.

The condensation of a gas to form particles is a process that involves much chemistry. The vaporized species will tend to react with the surrounding gas. As mentioned above, some elements may vaporize as compounds or form compounds in the gas phase. Much of the iodine will be present in the form of cesium iodide ( $\text{CsI(g)}$ ) while tellurium may be present as e.g. tin telluride ( $\text{SnTe(g)}$ ). Depending on the hydrogen/steam ratio and on the temperature some elements may form oxides or hydroxides, e.g.  $\text{Cs}_2\text{MoO}_4\text{(g)}$  and  $\text{CsOH(g)}$ , while others may stay in elemental form, e.g. Ru.<sup>4</sup> The chemical speciation will fundamentally affect the condensation of the elements as the vapor cools down. Thus cesium hydroxide is much more easily condensed than cesium while molybdenum has a low vapor pressure in the form of Mo or  $\text{MoO}_2$  while it has a rather high vapor pressure in the form of  $\text{Cs}_2\text{MoO}_4$  or  $\text{MoO}_3$ .

Much of the material vaporized will be non-radioactive. The condensation of this material will influence the transport of radioactive species because of co-condensation, agglomeration, adsorption and chemical reaction.

Radioactive material in the primary system will deposit on the relatively cool walls of the reactor vessel. Gaseous substances may condense on, adsorb on or react chemically with the surface, e.g. tellurium with stainless steel. Radioactive material in particulate form will also settle on these surfaces and may also react with the substrate to some extent. Reheating of these deposits due to radioactive decay energy may revaporize some substances. The deposition of radioactive matter on cooler surfaces in the vessel will tend to retain part of the radio nuclides in the primary system.

At some stage in most serious accidents the melt will penetrate the bottom of the pressure vessel to be ejected into the containment. This will cause a large part of the radioactive inventory to enter the containment.

Not only will the melt itself with all its radioactive species leave the vessel, in addition a large fraction of the radioactive material that has already been released within the vessel will also enter the containment. However, upon entering the containment atmosphere elementary cesium will immediately reconvert to cesium hydroxide.

As most of the water will leave the pressure vessel together with the melt or soon thereafter the vessel atmosphere will become more reducing. Thus radioactive elements may be reduced to elemental form which will affect their transport properties e.g. cesium hydroxide may form elemental cesium, which has a much higher vapor pressure than cesium hydroxide, causing much of the deposited cesium in the vessel to enter the containment.

Heat from the exiting melt will cause pyrolysis and vaporization of electric equipment and cables present immediately below the vessel

bottom. This will inject copper, aluminium and iron vapor and a large number of organic and inorganic vapors and gases into the containment atmosphere. Quite complicated chemical reactions may then occur between these and the containment atmosphere.

The ejected melt will come in contact with concrete structures in the containment. The heated concrete will release much water vapor which will cause sparging of the melt and may lead to the evolution of extra radioactive substances from the melt.

The melt - concrete interaction will also release acidic substances, e.g.  $\text{CO}_2(\text{g})$ ,  $\text{SO}_2(\text{g})$ ,  $\text{SiO}_2(\text{s})$ , and basic substances, e.g.  $\text{NaOH}$ ,  $\text{CaO}$ , from the concrete that may significantly influence the chemical environment in the containment.

As in the case of the primary system, the transport properties and chemical reactions of both gaseous and particulate, radioactive and non-radioactive, matter need to be considered in the containment.

Since the reactor containment wall forms the last barrier between the released radioactive materials and the environment, the transport and deposition of radioactive matter within the containment becomes crucial.

Temperatures in the containment are relatively low so that most radioactive elements will be present in condensed form. The major gaseous radioactive species being the noble gases, hydrogen iodide, iodine, organic iodides and the corresponding bromine species.

The amount of radioactive material suspended in the containment atmosphere either in particulate or in gaseous form will largely determine the amount of activity released to the environment if and when the containment fails. However, also some of the vapor and aerosols still in the vessel will enter into the containment when the total pressure drops. This is also true if the containment is vented via a filter.

The chemistry of the gaseous radioactive substances is obviously important because, together with gas-phase transport, it will determine their deposition rate on solid and aqueous surfaces.

Gaseous iodine species,  $\text{HI}$ ,  $\text{I}_2$  and  $\text{R-I}$ , will dissolve and react in aqueous solution. The reactions involved are all pH dependent so that an increased pH generally increases the rate of reaction as well as the maximum attainable partitioning coefficient between aqueous phase and gas. The presence of acidic substances,  $\text{B}_2\text{O}_3$ ,  $\text{CO}_2$ ,  $\text{SO}_2$  and  $\text{SO}_3$ , will therefore tend to increase the relative amount of gaseous iodine containing species in the containment.

The attenuation of suspended aerosol mass in the containment as a function of time is also a critical factor in the calculation of radioactivity release. The settling of aerosol particles depend on e.g. convection, thermophoresis and on factors pertaining to the particles such as mass, diameter and shape. The same factors also apply to the filtering out of aerosols. Chemical considerations are

important to the formation of these aerosol particles and to their equilibria with species in the gas phase. Thus the behavior of cesium in the containment will be very different depending on whether it condenses mainly in hydroxide form or if it condenses to form e.g. a borate, carbonate, sulfite or silicate.

The behavior of a cesium hydroxide containing particle in the containment is influenced by its reactions with gaseous species and with other particles. Thus cesium hydroxide will attract water from the gas. This will increase the rate of sedimentation of the particle. The uptake of water is especially important close to the dew point. In the presence of more than 123 millibar of water vapor, no solids appear in the CsOH - H<sub>2</sub>O system. This means that cesium that has already settled, e.g. on walls, may be relocated by flowing. It also means that surface tension will be important.

The presence of a radiation field is important to the chemistry in the containment and to the source term. Radiation will tend to break chemical bonds of all types. This will create many reactive radicals, both in solution and in the gas phase. These radicals are shortlived but their presence is nevertheless important because their rather indiscriminate reactions creates a large number of metastable substances whose formation cannot be predicted from thermodynamics. Thus hydrocarbons, from the pyrolysis of organic matter, will form e.g. methyl radical that in turn willingly reacts with e.g. cesium iodide to form methyl iodide or with tellurium to form organic tellurides with high vapor pressures and low solubilities in water. It is also possible that nitrogen, hydrogen and steam in the containment atmosphere will react to form varying amounts of ammonia, nitrous acid or nitric acid depending on the proportions of reactants, pressure, temperature, catalysts and scavengers.

The metastable compounds decompose with time, e.g. methyl iodide will be undergoing hydrolysis in water. However, the continued presence of the radiation field generates new metastable species all the time so that a significant steady state concentration is upheld.

A series of experiments were performed within the AKTI-150 project in the participating countries in order to improve the understanding of important phenomena and to provide additional data on important chemical effects and chemical systems. The results are summarized in this section.

3.1 Studies of the hygroscopicity of cesium hydroxide by measurement of the vapor pressure in the system  $H_2O-CsOH$

This section summarizes work performed by L. G. Johansson and S. Kazikowski of the Department of Inorganic Chemistry, Chalmers University of Technology and the University of Gothenburg, Sweden, on equilibrium water vapor pressures in the cesium hydroxide - water system in the temperature range 50 to 300°C and water vapor pressures from 6.1 to 500 millibar.

3.1.1 Introduction

One of the problems in aerosol chemistry when applied to core melt accidents is the scarcity of data on many of the species that may be present in aerosol form.

Large amounts of cesium will be released from the reactor core. In most environments, except under very dry and reducing conditions, cesium will react with steam and water to form cesium hydroxide. The hydroxide will also certainly react with acid substances present producing e.g. cesium iodide, borates, silicates and carbonate. It is, however, probable that a large fraction of the total cesium inventory will remain as cesium hydroxide during at least part of most accident sequences.

As the aerosol cools down, cesium hydroxide will condense either homogeneously or heterogeneously and form particles. The sedimentation rate of these particles is influenced by their mass and shape. Both these factors are fundamentally influenced by the ability of cesium hydroxide to attract water. It is obvious that the absorption of water leads to increased particle mass, but it is also true that the uptake of water narrows the temperature range within which cesium hydroxide forms a solid. The conversion of a solid particle to a droplet will tend to increase its sedimentation rate due to decreased drag. The presence of liquid cesium hydroxide solutions also influences resuspension and later relocation of deposited material within the containment.

The work presented here aims at new reliable data on the vapor pressure of water over the system  $CsOH - H_2O$ . Hopefully the new data will contribute to better predictions of the releases of radioactive materials in reactor accidents.

### 3.1.2 Experimental

The experiments were performed using a Cahn recording vacuum microbalance. The weighed  $\text{CsOH}\cdot\text{H}_2\text{O}$  sample (about 0.25 g) was placed in a silver weighing pan suspended in the vacuum microbalance. Using a resistance furnace connected to a programmable temperature controller the temperature of the sample was varied. A Pt/Pt-10% Rh thermocouple was used for temperature measurements. The hot end of the thermocouple was situated about 5 mm below the weighing pan. The temperature measurement was checked using the melting point of tin ( $231.9^\circ\text{C}$ ). The calibration was performed under the same experimental conditions as used in the actual experiments. The accuracy of the temperature determination was  $\pm 1^\circ\text{C}$ . A schematic view of the experimental setup is shown in Figure 3.1.1.

The sample was exposed to an atmosphere consisting of pure nitrogen with a known amount of water vapor added. The steam of nitrogen was saturated with water by bubbling through three consecutive flasks immersed in a thermostated water bath. The tubes leading the humidified nitrogen to the sample were heated to avoid condensation.

The gas flowed upwards through the cylindrical weighing compartment (45 mm diameter), in the middle of which the sample was suspended. Condensation of water within the microbalance proper, where temperatures were close to ambient, was avoided using a flow of dry nitrogen for protection. The flow-rate of humid nitrogen past the sample

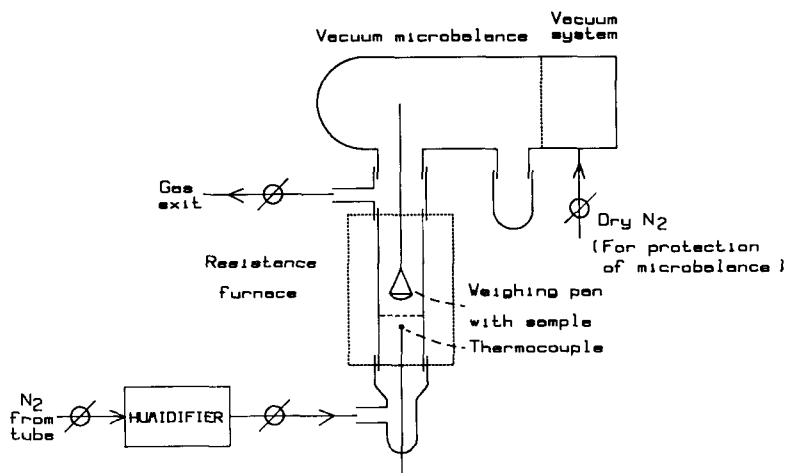


Figure 3.1.1. Schematic view of the experimental setup.

was 350 ml/minute at STP. The equilibrium sample mass was not influenced by changes in the flow-rate of humid nitrogen past the sample nor by changes in the flow-rate of dry nitrogen through the microbalance proper. Convection within the sample compartment was minimized by a metal net inserted below the sample.

After placing the sample in position the microbalance was evacuated to less than 1 millibar and flushed repeatedly with dry nitrogen. The sample temperature was then increased to 300°C. The sample weight became constant after one hour of pumping at this temperature. Gravimetric analysis showed that all water was removed from the sample by this treatment.

After the evacuation, dry nitrogen was introduced into the weighing compartment and the sample mass was recorded. The flow of humid nitrogen was then started. Introduction of water vapor resulted in an increase of sample mass. After reaching a stable equilibrium value, generally after 1 to 4 hours, the new sample mass was recorded. The procedure was repeated for a series of sample temperatures at the same water vapor pressure. The equilibrium composition of the sample, corresponding to a given temperature and water vapor pressure, was calculated from the initial and equilibrium sample masses. Seven different water vapor partial pressures from 6.1 to 500 millibar were investigated.

The attainment of a stable mass was very slow in some cases, notably in the  $\text{CsOH}(\text{aq}) + \text{CsOH}\cdot\text{H}_2\text{O}(\text{s})$  region. The data recorded in this region are therefore rather less precise than in other regions.

The error in the water mole fractions given is in the order of 0.005.

The  $\text{CsOH}\cdot\text{H}_2\text{O}$  used was of P.A. quality but contained 5% cesium carbonate. The carbonate mass was accounted for in the calculation of sample composition. However, the slight ability of the carbonate to attract water was neglected at the relatively low water activities studied.

### 3.1.3 Results and discussion

The results are summarized in Table 3.1.1. In addition to the measured quantities (temperature, composition, and  $p(\text{H}_2\text{O})$ ), the activity of water  $a_w = p(\text{H}_2\text{O})/p_0(\text{H}_2\text{O})$  is given. The activity coefficient of water,  $f_w \equiv a_w/x_w$ , in the  $\text{CsOH} - \text{H}_2\text{O}$  system is also given in the single-phase regions.

Figure 3.1.2 shows the isobaric plots in the  $\text{CsOH} - \text{H}_2\text{O}$  diagram. For comparison, the phase diagram by Rollet *et al.* /1/ is included.

The isobaric lines should become horizontal in the two-phase regions of the  $x - T$  diagram. The isobars for 6.1, 20.6 and 42.4 millibar show such horizontal regions and are clearly seen to enter the  $\text{CsOH}(\text{aq}) + \text{CsOH}\cdot\text{H}_2\text{O}(\text{s})$  and  $\text{CsOH}\cdot\text{H}_2\text{O}(\text{s}) + \text{CsOH}(\text{l})$  areas. However, no such horizontal regions appear at higher water vapor partial pres

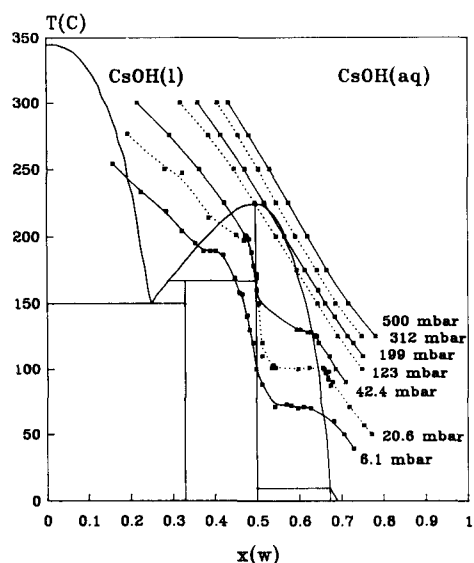


Figure 3.1.2. Isobaric plots in the CsOH - H<sub>2</sub>O system. The CsOH - H<sub>2</sub>O phase diagram, adapted from Rollet *et al.*, is included for comparison.

tures. The conclusion is that no solids appear in this system at water vapor partial pressures above 123 millibar.

A comparison with the phase diagram of Rollet *et al.* suggests that they may have given a too high value for the melting point of the monohydrate (226°C). Jacobs *et al.* /2/ gives a melting point of 205°C based on single crystal Cp measurements. This value may be in better agreement with our data.

Figure 3.1.3 shows the influence of temperature on the activity coefficient of water in CsOH at different compositions. The family of curves all show an activity coefficient increasing with temperature at all compositions studied. This is in accordance with Krey's data on the NaOH - H<sub>2</sub>O system. However, the water activity coefficients are in general much lower in the CsOH - H<sub>2</sub>O system than in the NaOH - H<sub>2</sub>O system.

Figure 3.1.4 shows the activity coefficient of water in CsOH as a function of composition at different temperatures.

#### 3.1.4 References

- /1/ A.-P. Rollet, R. Cohen - Adad and C. Ferlin, *Compt. Rend.*, 256 (1963) 5580.
- /2/ H. von Jacobs, B. Harbercht, P Mueller and W. Bronger, *Z. anorg. allg. Chem.*, 491 (1982) 154.
- /3/ J. Krey, *Z. physik. Chemie, Neue Folge*, 81 (1972) 252.

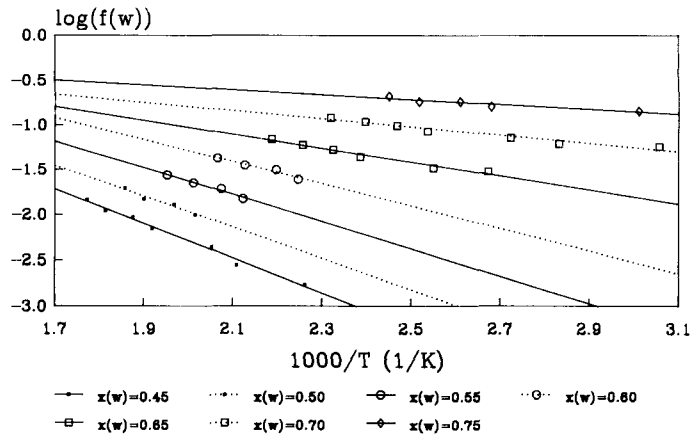


Figure 3.1.3. The activity coefficient of water,  $f_w$ , as function of temperature in a series of CsOH - water mixtures with different mole fractions of water,  $x_w$ .

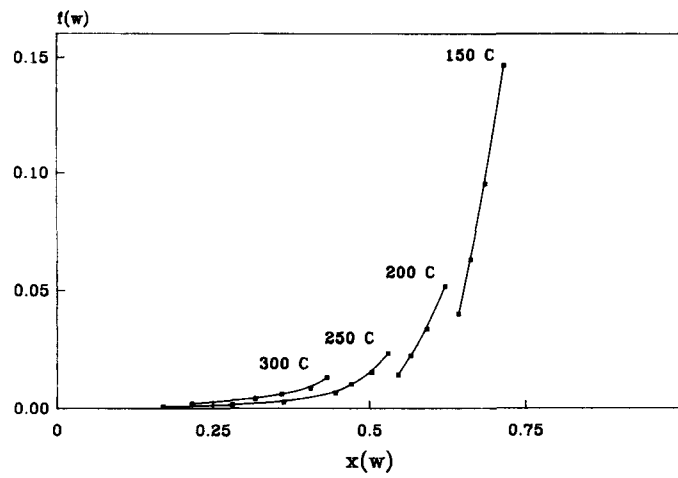


Figure 3.1.4. The activity coefficient of water,  $f_w$ , as a function of composition,  $x_w$ , at a series of temperatures.

Table 3.1.1. Experimental data for the cesium hydroxide/water system.  $P(w)$ ,  $t$ ,  $x(w)$ ,  $a(w)$  and  $f(w)$  are water vapor pressure, temperature, mole fraction of water, activity of water and activity factor for water respectively.

$P(w)$ (mbar)	$t^{\circ}C$	$x(w)$	$a(w)$	$f(w)$	$P(w)$ (mbar)	$t^{\circ}C$	$x(w)$	$a(w)$	$f(w)$
6.1	254	0.158	0.00014	0.00091	41.4	250	0.363	0.00107	0.00295
6.1	233	0.226	0.00021	0.00092	41.4	225	0.424	0.00166	0.00392
6.1	219	0.286	0.00027	0.00094	41.4	198	0.482	0.00285	0.00591
6.1	204	0.323	0.00036	0.00112	41.4	188	0.488	0.00353	0.00723
6.1	195	0.354	0.00044	0.00123	41.4	178	0.493	0.00443	0.00899
6.1	189	0.374	0.00050	0.00133	41.4	160	0.500	0.00686	0.0137
6.1	189	0.390	0.00050	0.00127	41.4	150	0.505	0.00891	0.0176
6.1	189	0.403	0.00050	0.00123	41.4	130	0.594	0.0157	0.0264
6.1	186	0.421	0.00053	0.00127	41.4	130	0.603	0.0157	0.0260
6.1	169	0.448	0.00079	0.00176	41.4	128	0.621	0.0167	0.0269
6.1	158	0.459	0.00104	0.00227	41.4	128	0.628	0.0167	0.0266
6.1	157	0.466	0.00107	0.00230	41.4	126	0.638	0.0177	0.0277
6.1	141	0.478	0.00164	0.00343	41.4	125	0.642	0.0183	0.0285
6.1	140	0.476	0.00169	0.00355	41.4	125	0.637	0.0183	0.0287
6.1	130	0.483	0.00226	0.00468	41.4	120	0.646	0.0214	0.0331
6.1	120	0.491	0.00308	0.00627	41.4	110	0.672	0.0296	0.0441
6.1	100	0.498	0.00603	0.0121	41.4	100	0.686	0.0419	0.0611
6.1	88	0.512	0.00940	0.0184	41.4	90	0.710	0.0605	0.0852
6.1	71	0.543	0.0188	0.0346	123.3	300	0.318	0.00144	0.00453
6.1	73	0.571	0.0172	0.0301	123.3	275	0.385	0.00207	0.00538
6.1	72	0.582	0.0180	0.0309	123.3	250	0.446	0.00310	0.00695
6.1	70	0.598	0.0196	0.0328	123.3	225	0.496	0.00484	0.00976
6.1	71	0.612	0.0188	0.0307	123.3	200	0.546	0.00795	0.0146
6.1	70	0.628	0.0196	0.0312	123.3	175	0.595	0.0138	0.0232
6.1	60	0.683	0.0306	0.0448	123.3	150	0.643	0.0259	0.0403
6.1	50	0.707	0.0495	0.0700	123.3	125	0.691	0.0531	0.0769
6.1	39	0.730	0.0873	0.120	123.3	100	0.749	0.122	0.163
20.6	276	0.193	0.00034	0.00177	199.0	300	0.360	0.00232	0.00644
20.6	250	0.281	0.00052	0.00185	199.0	275	0.414	0.00335	0.00809
20.6	247	0.323	0.00055	0.00169	199.0	250	0.471	0.00501	0.0106
20.6	214	0.386	0.00100	0.00259	199.0	225	0.519	0.00781	0.0151
20.6	201	0.452	0.00130	0.00288	199.0	200	0.566	0.0128	0.0226
20.6	201	0.474	0.00130	0.00274	199.0	175	0.614	0.0223	0.0363
20.6	200	0.477	0.00133	0.00279	199.0	160	0.645	0.0322	0.0499
20.6	197	0.470	0.00141	0.00300	199.0	150	0.662	0.0418	0.0631
20.6	172	0.500	0.00248	0.00496	199.0	140	0.685	0.0551	0.08044
20.6	169	0.500	0.00267	0.00534	199.0	125	0.714	0.0858	0.120
20.6	120	0.513	0.0104	0.0203	199.0	120	0.728	0.100	0.137
20.6	110	0.513	0.0144	0.0281	199.0	110	0.751	0.139	0.185
20.6	101	0.535	0.0197	0.0368	312.0	300	0.406	0.00363	0.00894
20.6	103	0.539	0.0183	0.0340	312.0	275	0.455	0.00524	0.0115
20.6	101	0.544	0.0197	0.0362	312.0	250	0.504	0.00784	0.0156
20.6	100	0.598	0.0204	0.0341	312.0	225	0.547	0.0122	0.0223
20.6	101	0.624	0.0197	0.0316	312.0	200	0.592	0.0200	0.0338
20.6	101	0.656	0.0197	0.0300	312.0	175	0.642	0.0349	0.0544
20.6	100	0.659	0.0204	0.0310	312.0	150	0.686	0.0655	0.0955
20.6	98	0.670	0.0218	0.0325	312.0	125	0.748	0.134	0.179
20.6	97	0.663	0.0227	0.0342	500.0	300	0.432	0.00580	0.0134
20.6	92	0.668	0.0273	0.0409	500.0	275	0.481	0.00840	0.0175
20.6	90	0.679	0.0294	0.0433	500.0	250	0.530	0.0126	0.0238
20.6	87	0.674	0.0330	0.0490	500.0	225	0.576	0.0261	0.0453
20.6	71	0.720	0.0635	0.0882	500.0	200	0.621	0.0429	0.0691
20.6	57	0.754	0.119	0.158	500.0	175	0.665	0.0560	0.0842
20.6	50	0.773	0.167	0.216	500.0	150	0.716	0.105	0.147
41.4	300	0.216	0.00049	0.00227	500.0	125	0.781	0.215	0.275
41.4	275	0.293	0.00071	0.00242					

## 3.2 Studies of hygroscopic aerosols

### 3.2.1 Sedimentation in tubes

This section summarizes work performed in Finland by T. Raunemaa and P. Pasanen of the Laboratory for Atmospheric Physics and Chemistry, Department of Environmental Health, University of Kuopio, by A. Hautojärvi of the Nuclear Engineering Laboratory, Technical Research Center of Finland and by M. Kulmala of the Laboratory for Environmental Physics, Department of Physics, University of Helsinki, on the sedimentation of hygroscopic aerosols in tubes.

3.2.1.1 Introduction. Hygroscopic aerosol particles differ in their growth behavior from non hygroscopic particles especially in near saturated conditions. Most metals and their oxides are insoluble and are in practice non hygroscopic. As examples, zinc metal and zinc oxide were used in this study.

Water soluble compounds, which can be classified as salts (like  $\text{CaCl}_2$ ), acids and bases grow in favorable conditions to much larger sizes.

The crystal structure of salts forces a step like growth in salts. The hygroscopic acids and bases, like sulfuric acid, sodium hydroxide and cesium hydroxide, grow practically continuously.

Some fission products are known to be hygroscopic and soluble in water. Others may behave similarly in the conditions present during a severe accident. The hot alkali metal vapors react with water,  $\text{Cs} + \text{H}_2\text{O} \rightarrow \text{CsOH} + 1/2 \text{H}_2$ , and the hydroxides formed are strongly hygroscopic.

When particles absorb water their settling velocity increases. This affects the amount of suspended particles in the containment area /2/. Resuspension after deposition on containment surfaces also depends on the hygroscopic properties of the deposited material.

Due to chemical and physical processes vapor-to-particle conversion is accelerated when temperature is lowered from high (around  $1000^\circ\text{C}$ ) to moderate ( $200^\circ\text{C}$ ) and to room ( $25^\circ\text{C}$ ) temperatures /3,4/. Below the critical point of water ( $374^\circ\text{C}$ ) hygroscopicity becomes more and more important.

At an early stage of particle transformation, high total surface area means high probability for surface attachment and complex particle compositions. Particle properties at these early stages depend on the mixture of initial substances. The main interest in this study was, however, directed to the bulk aerosol, as that determines the physical behavior in large spaces.

3.2.1.2 Test matrix. Sedimentation was studied in small diameter (5.6 mm) tubes in the test matrix represented in Table 3.2.1.1. The

particle mass concentration varied between 0.4-10 g/m<sup>3</sup>.

Table 3.2.1.1. The test matrix in the small scale sedimentation experiments in 1985-86 at Kuopio.

temperature (°C)		low R.H.		high R.H.		velocity (m/s)
		25	120	25	120	
non hygroscopic	Zn, ZnO	x	x	x	x	0.7-26
hygroscopic	CaCl <sub>2</sub>	x		x		0.7
hygroscopic	CsOH <sup>2</sup>	x	x	x	x	0.7
mixture	CsOH+Zn	x	x	x	x	0.7
resuspension	Zn		x			0.7/0.7-12
	CsOH		x			0.7/0.7-12

In this context we will mainly consider the results with the cesium hydroxide/zinc mixture. Our other results are presented elsewhere /1/.

3.2.1.3 Experimental. Experiments in humid conditions were carried out in an arrangement shown in Figure 3.2.1.1. A similar facility, but with the necessary modifications, was used in dry tests. Analysis of the sedimented material was performed using several techni-

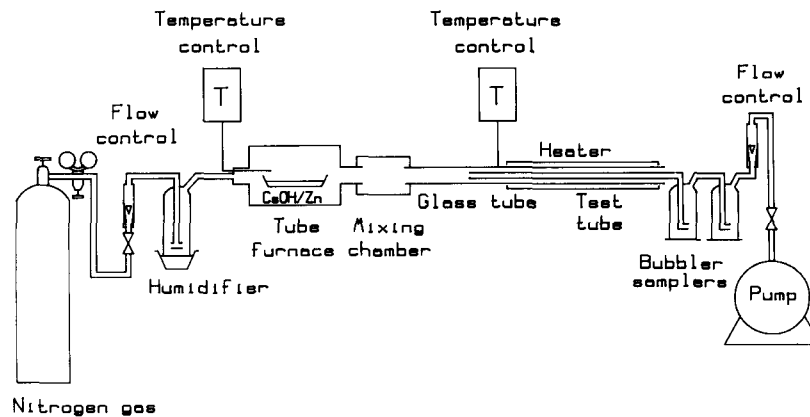


Figure 3.2.1.1. The experimental set-up of the hygroscopicity test in wet conditions.

ques. Determinations were carried out by means of chemical, atomic absorption spectroscopic and conductivity methods. Deposition was successfully determined also by using isotope excited X-ray fluorescence (XRF) developed for the present purpose /1/.

The aerodynamic mass median diameter, AMMD, of the aerosol was estimated from the measured data with the aid of deposition calculations applied to the conditions of each experiment.

3.2.1.4 Deposition characteristics of mixed cesium hydroxide/zinc aerosol. The mixed cesium hydroxide/zinc aerosol was generated by heating cesium hydroxide and zinc in the same furnace. Two crucibles, one containing metallic zinc and the other containing a water solution of cesium hydroxide, were placed in this order in the furnace. The mass ratio of cesium hydroxide to zinc metal was varied from 1:24 to 20:1.

Table 3.2.1.2. Deposition characteristics of cesium hydroxide and zinc aerosol mixture at 25°C.

R.H. %	Deposition		Particle AMMD		CsOH:Zn*
	CsOH %	Zn %	CsOH um	Zn um	
5	10.7	29.0	2.0	4.1	1:24
5	4.6	8.3	1.2	1.7	3:2
5	1.1	16.4	0.2	2.5	2:1
5	15.2	3.1	2.4	1.0	3:1
10	4.6	-	1.2	-	-
100	3.8	3.7	1.1	1.1	3:2
100	8.9	19.0	1.7	3.0	5:3
100	3.6	2.4	1.0	0.8	6:1
100	3.6	8.3	1.0	1.7	8:1
100	5.1	9.6	1.3	1.8	10:1
100	4.9	2.5	1.2	0.8	20:1
100	2.0	-	0.7	-	-

\* The generation ratio.

Tables 3.2.1.2 (25°C) and 3.2.1.3 (120°C) give characteristic results in terms of total deposition at a constant temperature in a, 125 cm long 5.6 mm diameter, steel tube and the estimated mean aerosol sizes of particles for these deposition values.

The deposition characteristics of cesium along the tube were measured by an XRF technique. Atomic absorption spectroscopy was used for zinc, and for comparison also for cesium, analysis. As described elsewhere /1/ the adopted XRF technique uses an Am-241 source for X-ray excitation and performs the analysis from outside the 0.05 mm steel tube. The tube is moved in front of the detector assembly and the deposition observed in one point or at several positions of the tube. This kind of analysis is not possible in larger scale experi-

ments with thick tube walls.

At high temperature the largest relative humidity was estimated to be 25%. This corresponds to 100% R.H. measured at 85°C, which was the upper temperature limit for the instrument used.

Table 3.2.1.3. Deposition characteristics of cesium hydroxide/zinc aerosol mixture at 120°C.

Tube material and diam. (mm)	Flow velocity m/s	R.H. %	Deposition		Particle diam.	
			CsOH %	Zn %	CsOH um	Zn um
Steel	0.7	<0.11	2.5	-	2.1	-
(SIS 2333)	5.6	0.7	<0.1	9.1	1.8	-
		0.7	25*	2.0	0.7	-

\*See text.

The mass concentrations in the low temperature tests varied from 350 to 9200 mg/m<sup>3</sup> for cesium hydroxide and from 100 to 10750 mg/m<sup>3</sup> for zinc. Flow velocity was 0.7 m/s, i.e. a laminar flow pattern can be assumed for all experiments.

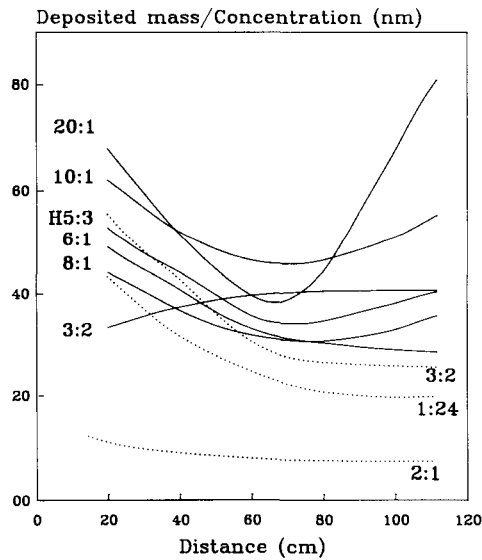


Figure 3.2.1.2. Deposition divided by concentration for settling of cesium hydroxide on the tube wall in mixed aerosol tests. The Cs:Zn concentration ratios are shown on the right. H = very high concentrations. The broken line = dry, the solid line = wet aerosol.

3.2.1.5 Analysis of results and discussion. Tests with mixtures of cesium hydroxide and zinc were carried out with a large variation of mass ratios and concentrations. In dry conditions, deposition along the tube decreased with distance as was observed to occur for non - hygroscopic pure zinc particles and also is expected from theory.

In humid conditions the deposition pattern was seen to change. An abundant settling in both tube ends was obtained. This phenomenon was enhanced when the concentration of cesium hydroxide increased. Deposition characteristics of cesium hydroxide in the mixed aerosol are shown in Figure 3.2.1.2.

There are two explanations for the observed behavior. We may assume that the short delay before the vapor enters into the settling tube caused the observed effect or that resuspension and relocation were responsible for the odd behavior.

When aerosol is produced from the hot furnace its temperature is over the critical point of water. The hygroscopic property of a substance cannot affect its growth at such a high temperature. Only when the temperature decreases, which occurs during the transport, condensation of water on the particle surface becomes possible. It takes about two seconds to travel from the mixing chamber to the test tube. If mixing is not effective, this is too short time for a hygroscopic growth to the equilibrium size. Particle growth then continues in the test tube and increases the deposition in the tube.

The second explanation is based on resuspension and relocation. When a sufficient amount of material is collected on the tube wall this material can be relocated with the flow. This is more probable at high concentrations. Based on preliminary tests two processes are possible. The amount of particles weakly bound onto the wall was found to be about 20% of the total mass. These particles can be suspended with the same flow velocity as from which they settled. Sticky aerosols cannot be suspended with this flow velocity. Resuspension of loose particles takes a long time, the time depending on layer formation rate. This in turn depends on aerosol concentration.

Cesium deposition at various concentrations is shown in Figure 3.2.1.3. Obviously, high concentration results in high deposition. Sedimentation of, originally, smaller cesium hydroxide particles is increased with concentration due to particle growth.

The growth rate of pure cesium hydroxide particles was, however, found to be larger by a factor of 2 as compared to the mixed cesium hydroxide/zinc aerosol. The growth in the mixture was found to be independent of CsOH:Zn ratio. This result includes a certain uncertainty. It seems reasonable to assume, that zinc aerosol behaves as a growth inhibitor in cesium hydroxide/zinc mixture. Final AMMD particle size of the hygroscopic material seems to be rather equal for pure cesium hydroxide (2.3  $\mu\text{m}$ ) and for the mixture of cesium hydroxide and zinc (1.3  $\mu\text{m}$ ).

The effect of coagulation can be seen as increased deposition yields at high concentrations, see the two uppermost curves in Figure

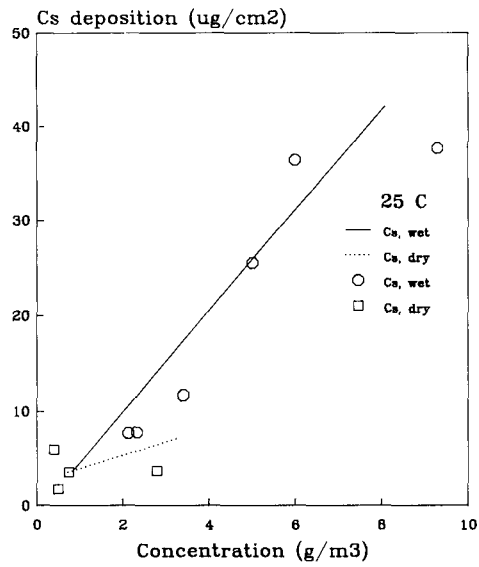


Figure 3.2.1.3. The amount of cesium in a deposited cesium hydroxide/zinc mixture as a function of concentration.

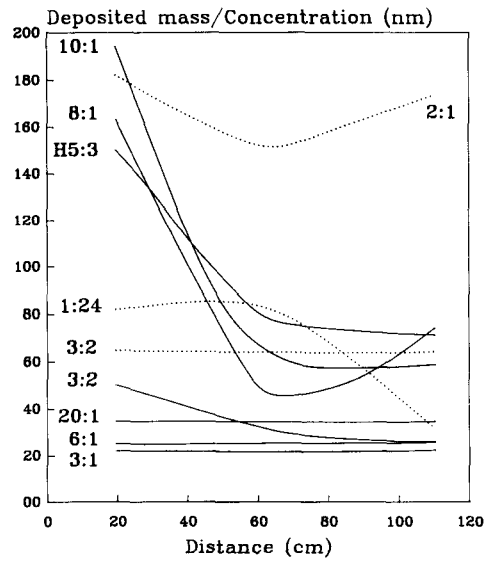


Figure 3.2.1.4. Deposition divided by concentration for settling of zinc in the tests with mixed cesium hydroxide/zinc aerosol. The Cs:Zn concentration ratios are shown near the curves. H = very high concentration. The broken line = dry and the solid line = wet aerosol.

3.2.1.2. The hygroscopic behavior of cesium hydroxide seems to be dominant for the aerosol at high Cs:Zn ratios, which is plausible.

Settling of non hygroscopic zinc aerosol as a function of distance is shown in Figure 3.2.1.4. Settling differs from the cesium deposition which suggests that zinc and cesium hydroxide are not present in the same particles.

#### 3.2.1.6 References

- /1/ P. Pasanen, T. Raunemaa, A. Hautojärvi and M. Kulmala, Behavior of Hygroscopic Aerosols: Test Results on Sedimentation in Tubes (1987).
- /2/ J. Jokiniemi and R. Sher, Modeling the Growth of Water Soluble Particles in the NAUA Code, EPRI, To be published (1986).
- /3/ M. Kulmala, M. Olin and T. Raunemaa, Gas to Particle Conversion at High Temperature. Report Series In Physics HU-P-238, University of Helsinki, Helsinki (1985).
- /4/ M. Kulmala, Nucleation, Internal Report, Department of Physics, University of Helsinki, Helsinki (1986).
- /5/ F. Rahn, LACE TR-012, Summary of the LWR Aerosol Containment Experiments (LACE) Program, EPRI, Palo Alto, California (1987).

#### 3.2.2 Condensational growth of hygroscopic aerosols in moist air

This section summarizes work performed in Finland by K. Koistinen, P. Pasanen and T. Raunemaa of the Laboratory for Atmospheric Physics and Chemistry, Department of Environmental Health, University of Kuopio and by Jorma Jokiniemi of the Nuclear Engineering Laboratory, Technical Research Center of Finland, on growth by condensation of some hygroscopic aerosols in moist air.

3.2.2.1 Introduction. A soluble particle near saturated conditions picks up a considerable quantity of water and, consequently, grows up manifold. This phenomenon has an important role in situations where hygroscopic aerosols and sufficient amount of water vapor are present /1/.

Physical and chemical properties of particles determine the final diameter of growing particles. There are several groups of chemicals (acids, salts and bases) which are hygroscopic. These can collect water up to the point where the pressure and temperature of water vapor is the same far from the droplet and at the droplet surface.

In some accident situations fission products can be released from the reactor coolant system to the surrounding containment and form very hygroscopic aerosol. Hot alkaline metal vapors react easily

with water vapor, e.g. cesium is rapidly transformed to cesium hydroxide and the reaction product is strongly hygroscopic /2/.

If enough water vapor is available the particle size increases. The effect is enhanced when the temperature is lowered and the saturation ratio is increased /2/. In still environment the settling of particles will then be the most important way for particle removal.

At early stage of particle formation the large total surface area of particles means high probability for adsorption of gaseous substances and very complex particle compositions may result. At length, however, it is the physical sedimentation process, which removes particle mass from the air. Experimental results for the growth of hygroscopic aerosol particles are required to assess this sedimentation rate of fission products and consequently the Source Term in release estimations to the environment.

Hygroscopicity plays an important role also in the dispersion of radioactivity to the environment after containment failure. Rainout of hygroscopic aerosols in close vicinity to the containment building has been studied theoretically /3/ and experimentally /4/. Hygroscopicity will affect the lung deposition during inhalation of water soluble radioactive particles /5/.

3.2.2.2 Behavior of hygroscopic aerosols. Formation and presence of water soluble compounds will affect on the behavior of fission products in the primary system and in the containment during nuclear power plant core melt accidents. In the primary circuit translocation of deposited material may occur due to material hygroscopicity, and in the containment area, steam will condense on the hygroscopic particles even at subsaturated conditions. This affects the residence time in the containment.

3.2.2.2.1 Water activity. The saturation ratio at the particle surface ( $S_r$ ) can be determined through minimization of the Gibbs free energy. Including the effect of surface tension this leads to /6/:

$$S_r = \frac{p_{v,r}}{p_s(T_r)} = A_w \exp\left(-\frac{2 s_l(T_r) M_w}{r R_g d_l T_r}\right) \quad (1)$$

Here  $s_l$  denotes the surface tension,  $d_l$  the density of the liquid droplet,  $M_w$  is the molecular weight of water and  $T_r$  the temperature at the particle surface.  $p_{v,r}$  is the water vapor pressure at the droplet surface and  $p_s(T_r)$  is the saturation water vapor pressure at the temperature  $T_r$ .  $A_w$  is the chemical activity of water,  $r$  the particle radius and  $R_g$  the universal gas constant.

The chemical activity in water for a solution can be expressed according to the modified Raoult's law /7/:

$$A_{w,j} = \frac{1}{1 + f_i M_w m_i} \quad (2)$$

where  $f_i$  is the van't Hoff factor and  $m_i$  is the molality of salt  $j$ . For very dilute solutions  $f_i$  is constant and the saturation ratio can be calculated from equations (1) and (2) using experimental values for  $f_i$ .

For concentrated solutions one must use experimental data to calculate the water activity, if available. Meissner (1980) introduced a correlation to calculate the reduced activity coefficient ( $G$ ) from an extended Debye-Huckel equation. Now the water activity ( $A_w$ ) is obtained by integrating the Gibbs-Duhem equation /8/:

$$-55.5 \ln(A_{w,j}) = \frac{2 I_j}{z_1 z_2} + 2 \int_1^{G_j} I_j d(\ln G_j) \quad (3)$$

where  $z_1$  and  $z_2$  are the charge of the cations and anions, respectively, of electrolyte  $j$ .  $I_j$  is the ionic strength of a solution. This method gives a fair agreement with the experimental data at different electrolyte concentrations and temperatures from 25 to 120°C. Other methods are more complex and they need at least two adjustable parameters /9/.

Several methods to calculate the water activity of mixed solutions have been compared in the literature /10/. A relation developed by Robinson and Bower is recommended, because it gives predictions for the water activity within 1 to 2% accuracy, and is less complicated than the other methods.

3.2.2.2.2 Mass and heat transfer. If simultaneous mass and heat transfer to aerosol particles is considered, one can find relations for the droplet temperature and growth rate in steady state /11/. Clausius-Clapeyron equation can be used to obtain the saturation vapor pressure  $p_{s,T}$  when the difference between the particle surface temperature ( $T_r$ ) and the gas temperature ( $T_o$ ) is less than few K and a zeroth-order approximation for the mass flux can be used. Thus we get the well known Mason equation for the droplet growth rate /14/:

$$r \frac{dr}{dt} = \frac{(S_a - S_r)}{(N_M + N_T)} \quad (4)$$

where  $N_M$  describes the mass transfer effect,  $N_T$  the heat transfer effect and  $S_a$  is the atmosphere relative humidity, R.H.

3.2.2.2.3 The equilibrium radius. When the behavior of hygroscopic aerosol particles in a nuclear power plant containment atmosphere is considered, an equilibrium between the atmospheric R.H. and satura-

tion ratio at the particle surface can be applied in certain conditions.

If some part of the particle is composed from an insoluble compound, the equation for the equilibrium radius ( $r_e$ ) according to eqs. (1) and (2) is /2/:

$$(S-1)r_e^4 - \left(\frac{2 s_1 M_w}{d_l R_g T}\right)r_e^3 + \left(\frac{d_{po} r_o^3}{d_p}\right)\left(\frac{i S M_w f_m}{M_s} + 1 - S\right)r_e + \frac{2 d_l M_w d_{po} r_o^3}{R_g T d_p d_l} = 0 \quad (5)$$

where  $r_o$  is the initial radius of the seed particle,  $d_{po}$  the initial density of the seed particle,  $d_p$  the actual density of the particle,  $d_l$  the solution density,  $m_{is}$  the mass of the insoluble component,  $m_s$  the mass of the soluble component,  $M_s$  the molecular weight of the soluble component and  $f_m$  is the mass fraction of the soluble compound ( $= m_s / (m_s + m_{is})$ ).

At equilibrium  $S_s = S_r = S$ ,  $r = r_e$  and  $T_r = T_s = T$ . To be accurate one should notice that  $d_p$  is a function of  $r$ . An iterative solution for this equation is possible by reproducing the calculation with

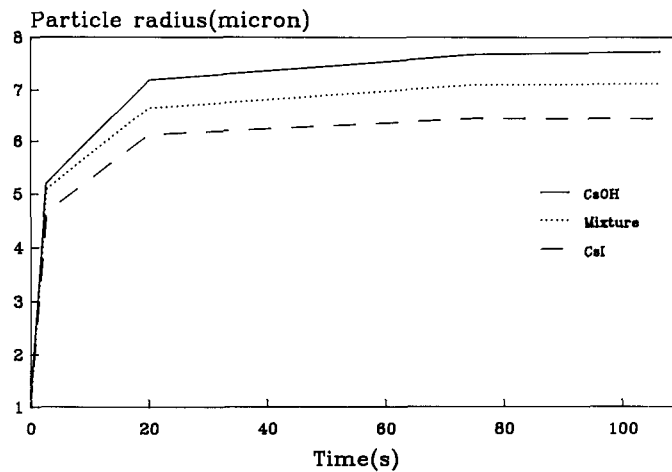


Figure 3.2.2.1. Growth rates for initially 1 um particles of different chemical composition at 99.8% R.H. and at gas temperature of 373 K.

new values for  $d_p$ . For concentrated aqueous solutions  $i$  is a function of  $r$  and  $T_p$ .

Figure 3.2.2.1 shows the calculated growth rates for initially 1  $\mu\text{m}$  dry particles of different chemical composition at 99.8% relative humidity.

**3.2.2.3 Experimental.** In studying the effect of hygroscopic properties of aerosols formed during reactor accidents, the same kinds of compounds must be used as expected in actual accident situations. Cesium is one of the most abundant species released in these accidents. Cesium as cesium hydroxide should therefore suite well for the simulated composition. Cesium hydroxide is the strongest base known and very hygroscopic. In the pretests, sodium chloride was chosen as hygroscopic material. It is not so chemically aggressive as cesium hydroxide. The sodium chloride aerosol was used to check the functioning of the test facility.

The scheme of the test chamber is shown in Figure 3.2.2.2. The 1.03  $\text{m}^3$  cylindrical chamber is made from stainless steel. The walls of the chamber have to be heated in order to prevent steam condensation on the cold wall surfaces.

A constant output atomizer was used for generation of the aerosol. The generated aerosol was led to a tube furnace, which was set up at 500°C. The temperature inside the aluminium oxide furnace tube

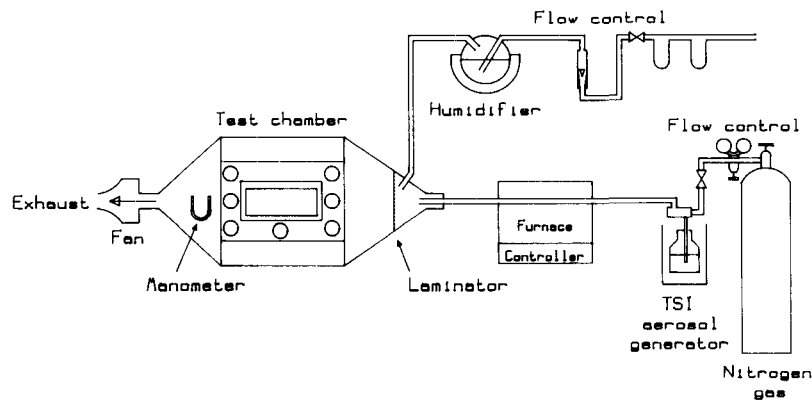


Figure 3.2.2.2. The schematic of the facility.

(inner diameter 18 mm and outer diameter 24 mm) was found to be very stable, only a few degrees variation from the set temperature was observed.

The dry aerosol flow was led from the furnace to the chamber through a stainless steel tube (length 50 cm) to cool the aerosol. The cooling was necessary to avoid problems connected to heat flow into the chamber. The extra heating would disturb the stabilized thermodynamic conditions in the chamber.

The water vapor was mixed with the dry aerosol at the chamber inlet, just prior to entering the study volume (see Figure 3.2.2.2). This set up was necessary to precisely mark the moment of aerosol to water vapor mixing. In the experiments the vaporization of water by using boiling technique was found to be good enough to produce the required water vapor.

The flow rate of the purified air through the water bottles was 35 l/min. It appeared to be an efficient way to humidify the air in the chamber to the required humidity. The relative humidity is shown in Figure 3.2.2.3 as a function of time in one experiment.

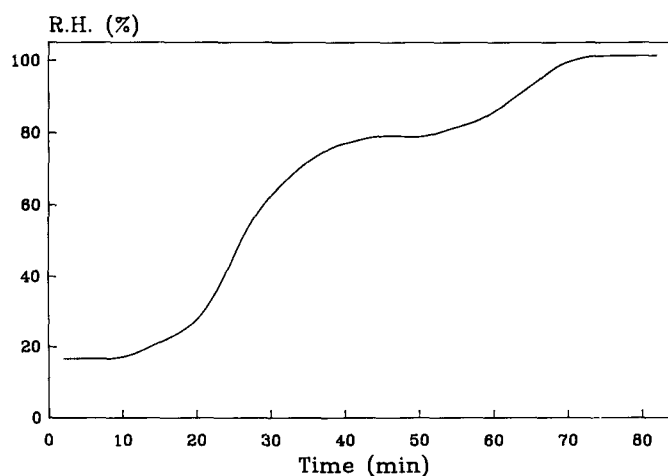


Figure 3.2.2.3. The relative humidity in the middle of the chamber as a function of time in one of the tests.

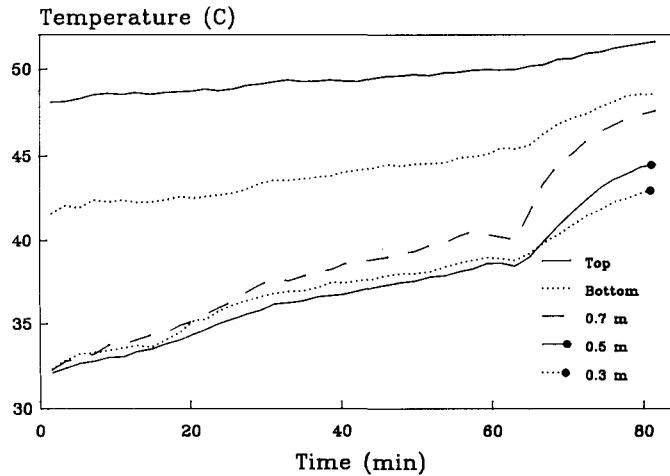


Figure 3.2.2.4. The temperature gradient in the chamber (0.3 m, 0.5 m, and 0.7 m are the heights from the bottom of the measurement locations in the gas. The gas and the chamber bottom and top surface temperatures are measured in the middle of the chamber).

3.2.2.4 Measurements. The requirements on the measuring instruments were high because of the conditions needed in the tests. Very high relative humidity at high temperature is difficult to measure properly. Only a few suitable methods are available for continuous recording of the size and concentration of aerosol particles containing much water. In on line measurements the detection time should also be short enough to observe the changes in size distribution.

The generation rate and size of the generated aerosol should be known. Scanning electron microscopy was used to check the size distribution of the aerosol in the inlet and after growth. This could, however, only be performed with precision for the test aerosol, sodium chloride. Cesium hydroxide is difficult to handle in the sample processing for the SEM analysis. The particle size in the chamber atmosphere were measured by means of optical particle counter, OPC, (Royco analyzer 4100 with sensor 1200) and electrical aerosol analyzer EAA (TSI 3030).

In studying the hygroscopic growth of particles and the changes in the size distribution the prevailing conditions should be known. The physical characteristics, relative humidity and temperature, should be measured on line at all times.

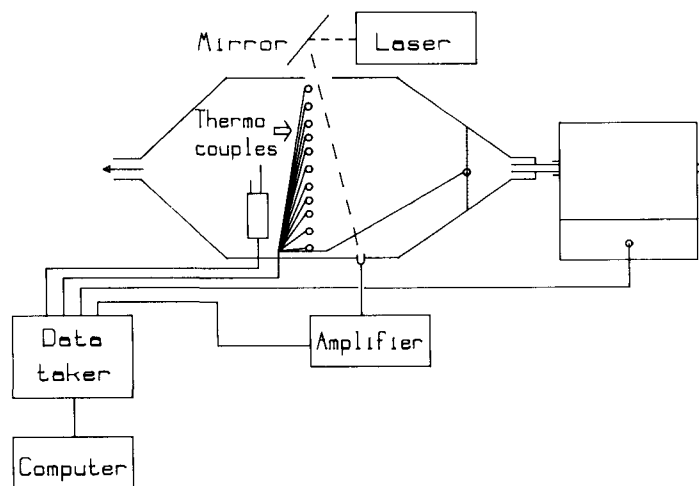


Figure 3.2.2.5. The set up of control instrumentation.

A layout of the system necessary to fulfill the requirement for on line measurements is shown in Figure 3.2.2.5. The temperature was measured with thirteen NiCr-Ni thermocouples (type K). The couples were calibrated before use. Nine of the couples were placed in the gas atmosphere in the middle of the chamber at 10 cm distance from each other. Two of the thermocouples were attached onto the surface of the chamber. One thermocouple was situated on the inlet laminator plate and one inside the tube furnace.

The relative humidity was measured with a digital psychrometer (Therm 2246-2). It works best at moderate and high levels of relative humidity. The output values are accurate to  $< \pm 1\%$  relative humidity.

The particle number distribution was measured by means of an optical particle counter, OPC (Royco 4100). The size ranges were set from 0.7  $\mu\text{m}$  to 13.5  $\mu\text{m}$  in six channels. Because of the used particle concentrations, dilution was necessary during the measurements. The total dilution ratio was about 1:50. The OPC uses the optical size of the aerosol particle for size selection.

The sub-micron particles were measured by means of electrical aerosol analyzer, EAA (TSI 3030). The size range of EAA is from 0.01 to 1.0  $\mu\text{m}$ .

The detection system is shown in Figure 3.2.2.6. Measuring lines were kept as short as possible to prevent condensation on the tube

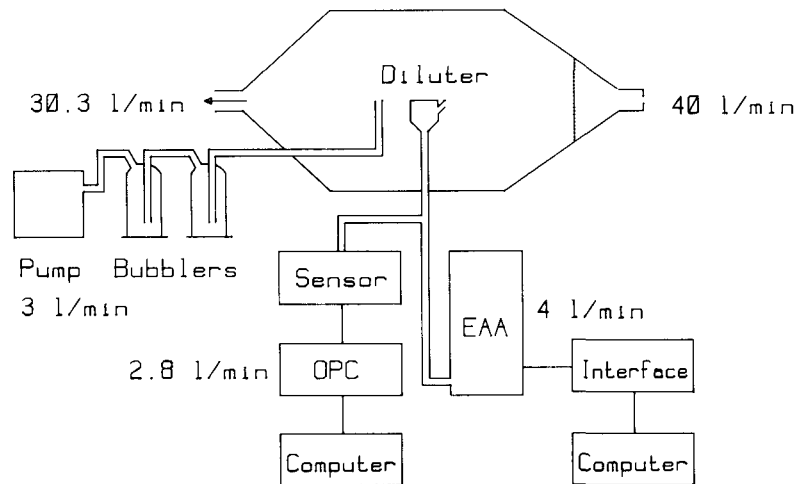


Figure 3.2.2.6. The schematic of the measurement system for the particles.

wall.

### 3.2.2.5 Results

3.2.2.5.1 Facility testing. Pretests were necessary to finalize the test facility for the hygroscopicity studies. The concentration span for the EAA and OPC measurements, water vapor production system and aerosol mass concentration measurements had to be tested. Sodium chloride aerosol was adopted as a test material in these various pretests.

The background aerosol concentration in the chamber was measured without aerosol generation. Only the nitrogen flow from the generator, 2.7 l/min, and the purified air flow, 35 l/min, were introduced into the chamber. The furnace was always on.

The background aerosol measurements were carried out at dry, and at saturated conditions, respectively (Figures 3.2.2.7 and 3.2.2.8). The aerosol concentrations were in these measurements found to be three orders of magnitude lower than with the aerosol under the same conditions.

3.2.2.5.2 Theoretical calculations. The calculations were carried out with the NAUA-HYGROS computer code /2/. This model has a capabi-

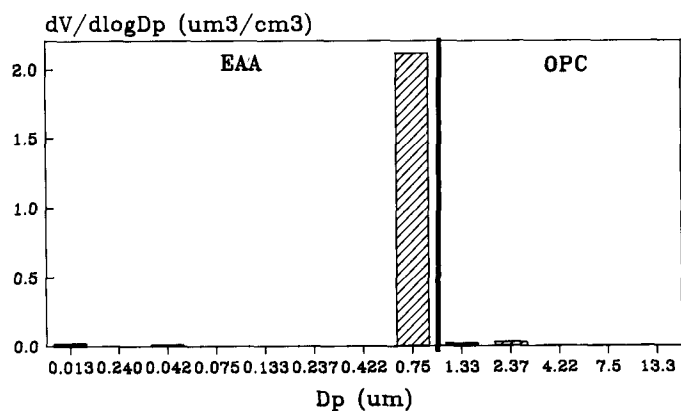


Figure 3.2.2.7. The volume distribution of the aerosol background at R.H. 24%.

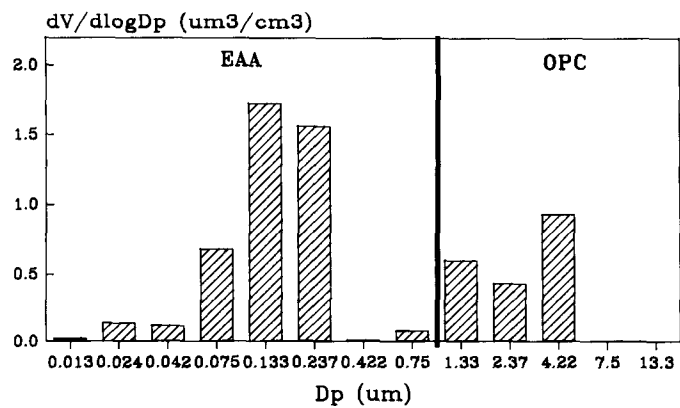


Figure 3.2.2.8. The volume distribution of the aerosol background at R.H. 100%.

lity to analyze aerosol dynamics in a well mixed volume /17/. The process considered in the present calculations include: a) particle growth by condensation and coagulation, b) particle deposition and c) convection (aerosol source or leakage). The growth due to hygroscopicity is modeled according to the theory presented in section 3.2.2.2.

In the calculations presented here only the behavior of larger particle size mode (measured by the OPC) is analyzed. Because of the steady state conditions throughout the experiments, aerosol behavior can be simulated with a small volume travelling from the chamber inlet to the location of measurements. This well mixed volume had the same volume/surface and volume/sedimentation areas as the actual chamber. The measured input particle size distribution was used in the model input. During calculations, the particle size distribution was discretized into 80 size intervals from 0.1  $\mu\text{m}$  to 50  $\mu\text{m}$ . For sodium hydroxide and cesium hydroxide the input particle concentrations and gas temperatures were taken from the measurements.

3.2.2.5.3 Experiments with hygroscopic CsOH. Cesium represents one of the most abundant fission products released in core melt accidents. Cesium is proposed to react readily with water to form cesium hydroxide.

Cesium hydroxide was generated from a solution of 0.02 g cesium hydroxide in one  $\text{cm}^3$  of deionized water. The aerosol flow rate into the chamber was 2.70 mg/min to yield a mass concentration of 67  $\text{mg}/\text{m}^3$  in the chamber. The measurements were carried out at different locations in the chamber: after 10 minutes travel in the chamber, after 5 minutes and after 2 minutes at closer distances from the inlet.

SEM analysis of the cesium hydroxide aerosol was not successful because of the strong solubility of cesium hydroxide already at low R.H. levels. Handling of highly soluble aerosols for SEM characterization became difficult. Cesium hydroxide also penetrated easily through the sampling filter.

Table 3.2.2.2. The volume mean diameters (VMD) and geometric standard deviations (SGV) values of cesium hydroxide aerosol at different R.H. levels after 10 minutes travel time at 40°C.

R.H. (%)	SGV <sub>EAA</sub> /SGV <sub>OPC</sub>	VMD <sub>EAA</sub> /VMD <sub>OPC</sub> ( $\mu\text{m}$ )	VMD <sub>Calc</sub> ( $\mu\text{m}$ )
24	1.8 / 1.4	0.18 / 1.78	1.73
60	1.8 / 1.4	0.15 / 1.90	2.17
82	(1.4)/ 1.4	(0.09)/ 1.97	2.78
92	(1.4)/ 1.4	(0.09)/ 2.17	3.55
98	(1.4)/ 1.6	(0.10)/ 2.65	5.22
100	(1.3)/ 1.5	(0.10)/ 3.44	12.51

3.2.2.5.3.1 After 10 minutes travel time. The VMD values obtained for the cesium hydroxide aerosol were 0.18  $\mu\text{m}$  (EAA) and 1.78  $\mu\text{m}$  (OPC) at dry conditions (Table 3.2.2.2). The median size measured by the EAA decreased from the 0.18  $\mu\text{m}$  to around 0.10  $\mu\text{m}$  at saturated conditions. The volume of this 0.2  $\mu\text{m}$  peak stayed almost constant.

The total volume of the dry 1.78  $\mu\text{m}$  sized aerosol increased by a factor of 20 at 100% R.H. The volume increase is twofold as compared to the size increase to 3.44  $\mu\text{m}$  at saturation. The volume ratio between the 0.2  $\mu\text{m}$  and 1.8  $\mu\text{m}$  peaks changed from 1:1 at dry atmosphere to 1:25 at 100% R.H.

3.2.2.5.3.2 After 5 minutes and 2 minutes travel time. Further tests were carried out at closer positions to the inlet to get more information on cesium hydroxide aerosol. Size distributions were measured after five and two minutes travel and growth.

It should be noted that observable aerosol size distribution depends on the studied location in the chamber. When measurements are performed at shorter travel time locations aerosol concentration increases and causes saturation of the instrument. The input concentrations have to be decreased for the analysis to be correct or dilution is necessary. Dilution is, however, problematic when working with a highly hygroscopic aerosol at elevated temperatures and high humidity.

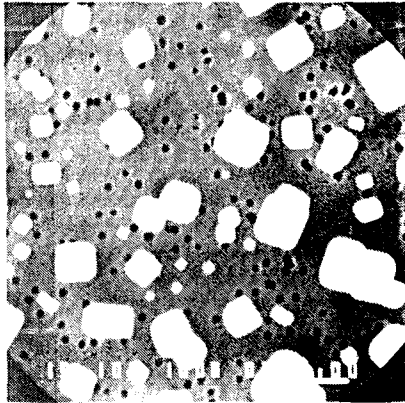


Figure 3.2.2.9. Micrograph of the sodium chloride aerosol. The enlargement of the micrograph is 10000 X.

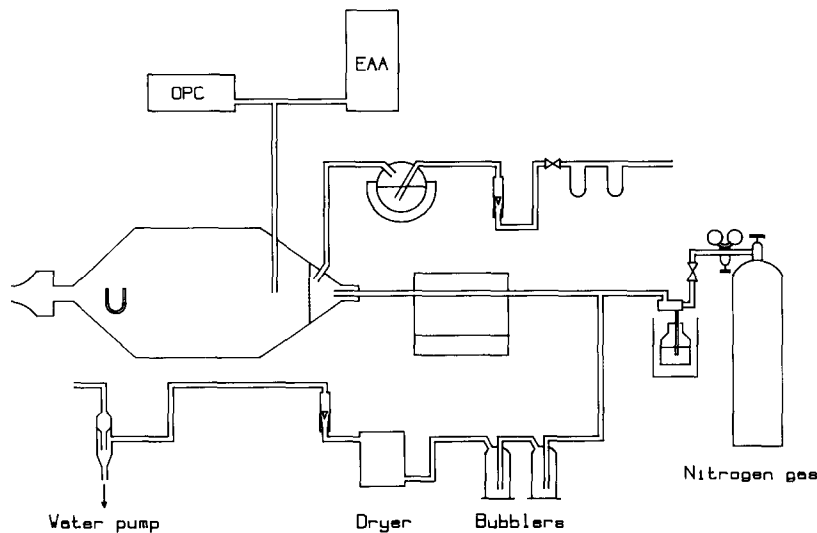


Figure 3.2.2.10. The schematic of the modified facility.

In the present studies both ways to get tolerable readings were employed. Aerosol flow to the chamber was decreased by taking a partial flow from the aerosol generator, Figure 3.2.2.10. A dilution ratio of 1:50 was used in all size directed analyses.

When the aerosol size was measured after 5 minutes growth time the aerosol mass flow was set to 0.34 mg/min, which yielded a mass concentration of 8 mg/m<sup>3</sup> in the chamber.

Table 3.2.2.3. The volume mean diameters (VMD) and geometric standard deviations (SGV) values of cesium hydroxide aerosol at different R.H. levels after 5 minutes travel time at 40°C.

R.H. (%)	SGV <sub>EAA</sub> /SGV <sub>OPC</sub>	VMD <sub>EAA</sub> /VMD <sub>OPC</sub> ( $\mu\text{m}$ )	VMD <sub>calc</sub> ( $\mu\text{m}$ )
20	2.0 / 1.7	0.31 / 1.72	1.77
62	1.6 / 2.2	0.15 / 2.16	2.23
93	(1.7)/ 2.0	(0.10)/ 2.34	3.85
98	-	-	5.58
99	(1.5)/ 1.3	(0.10)/ 5.30	6.74
100	-	-	15.75

The VMD of dry sub-micron particles detected by EAA was 0.31  $\mu\text{m}$  and decreased to about 0.10  $\mu\text{m}$  at 99% R.H. (Table 3.2.2.3). The volume

of the peak changed by a factor of 0.3.

The VMD of the dry aerosol measured by OPC was 1.72  $\mu\text{m}$ . The median size increased up to 5.30  $\mu\text{m}$  at R.H. 99%. The volume of the peak increased by a factor of 1000. The volume increase is 30 times larger than the size increase.

When the measurements were carried out at the location corresponding two minutes travel time the aerosol mass flow was set<sub>3</sub> to 0.32 mg/min, which yielded a mass concentration of 8 mg/m<sup>3</sup> in the chamber.

The VMD values of dry aerosol were 0.25  $\mu\text{m}$  (EAA) and 1.78  $\mu\text{m}$  (OPC). The median size of the sub-micron peak decreased from the dry value 0.25  $\mu\text{m}$  to about 0.09  $\mu\text{m}$  at 98% R.H. (Table 3.2.2.4). The volume of the peak changed by a factor of 0.6.

The 1.78  $\mu\text{m}$  peak increased to 6.34  $\mu\text{m}$  in volume size at 98% R.H. The volume of the peak increased by a factor of 250. The volume increase is tenfold as compared to size increase.

Table 3.2.2.4. The volume mean diameters (VMD) and geometric standard deviations (SGV) values of cesium hydroxide aerosol at different R.H. levels after 2 minutes travel time at 40°C.

R.H. (%)	SGV <sub>EAA</sub> /SGV <sub>OPC</sub>	VMD <sub>EAA</sub> ( $\mu\text{m}$ )/VMD <sub>OPC</sub> ( $\mu\text{m}$ )	VMD <sub>calc</sub> ( $\mu\text{m}$ )
19	2.2 / 1.8	0.25 / 1.78	1.80
69	1.7 / 1.9	0.10 / 2.28	2.45
90	(1.7)/ 1.4	(0.09)/ 2.84	3.54
98	(1.7)/ 1.9	(0.09)/ 6.34	5.88
99	-	-	7.25
100	-	-	16.71

3.2.2.6 Discussion. The measurements were carried out by combining the detection with the EAA and OPC, i.e. different kind of instruments. This means that the size measurement based on dynamical property (EAA) is compared with the measured value based on the optical property (OPC). With hygroscopic aerosols where water content varies this introduces inaccuracy.

The EAA has a long (about 80 cm) sampling line inside the instrument. There exist problems in trying to avoid water condensation on this line at high R.H. levels. Therefore the inner sampling line had to be heated during the measurements.

The results obtained by the OPC correspond to optical sizes. They depend on the index of refraction of the particle. The OPC is calibrated with latex particles. In the case of rapid condensational growth the refractive index is varying from that of bulk material (cesium hydroxide) to the refractive index of water (dilute cesium hydroxide aerosol at high R.H.). The indices of refraction for latex

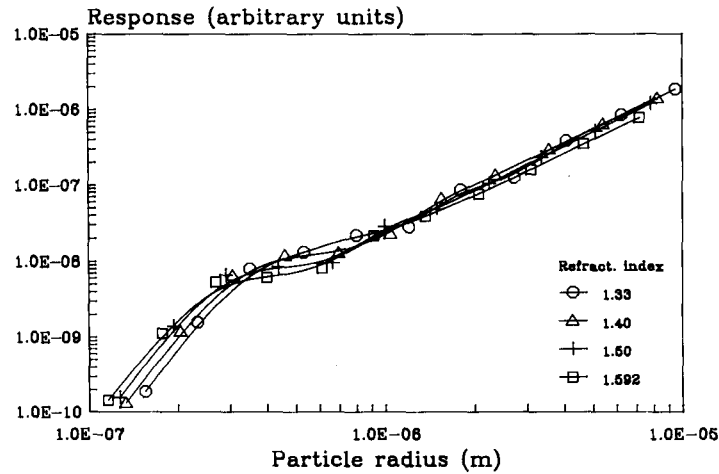


Figure 3.2.2.11. Response curves of the OPC for latex particles and water.

particles, cesium hydroxide (80% solution) and water are 1.592, 1.460 and 1.334, respectively. The response curves of the instrument for latex particles and water are given in Figure 3.2.2.11. The response curve of cesium hydroxide lies between these two curves.

The response of the OPC to the latex particles and to the materials used in this work is nearly equal when  $D_p > 1.4 \mu\text{m}$  (Figure 3.2.2.11). The response between  $0.7 \mu\text{m}$  to  $1.4 \mu\text{m}$  differs, however. The uncertainties in this size region were avoided by selecting the lower and upper limits for the first channel in the OPC to correspond to these values.

The results are presented in the form of volume parameters because these describe the growth phenomenon better than number values. In a condensation process the volume increase is interesting. The mass parameters were avoided, because the density of the particles at different R.H. levels is not exactly known.

The most important processes changing the airborne particle composition in the chamber are condensational growth and sedimentation. The experimental results represent the changes in the particle size and volume due to these two processes.

3.2.2.6.1 Cesium hydroxide aerosol. The hygroscopic growth of cesium hydroxide starts with very small amounts of water. The deliquescence point for the  $\text{CsOH-H}_2\text{O}$  system in the temperature range  $20 - 100^\circ\text{C}$  is about 2% R.H. At low R.H. levels the growth is slow and does not

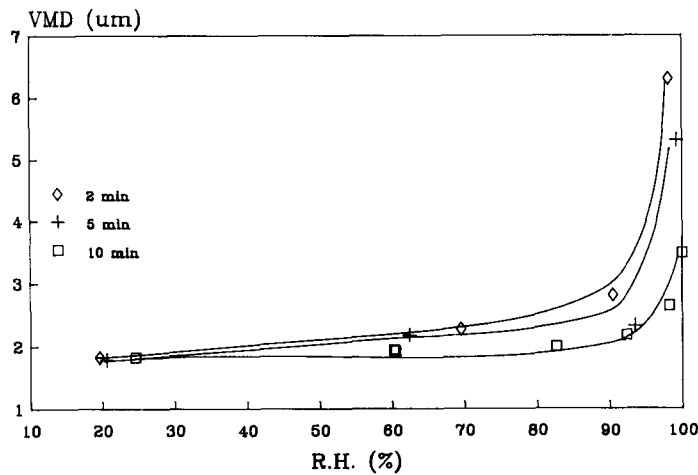


Figure 3.2.2.12. The relative growth of the cesium hydroxide aerosol after different growth times as a function of R.H.

remarkably affect the airborne size distribution. The growth increases rapidly at high R.H. which was observed in the experiments. As by sodium hydroxide, sedimentation becomes important for particle removal and changes the airborne size distribution.

The volume distribution at dry conditions was found to be bimodal with a small peak at around 0.3 um. The origin of the sub-micron peak stays unclarified, but it is of minor importance due its weakness.

When comparing the size distributions of cesium hydroxide aerosol after different growth times the median size after two minutes growth is the largest of the three (Figure 3.2.2.12). After 5 minutes growth the VMD of the distribution is about 30% smaller and after 10 minutes growth 45 % smaller than the value after two minutes growth.

Because of low concentrations and relatively large initial particle sizes (>1 um), coagulation was not important in the chamber processes. For large particles Brownian coagulation is slow and gravitational coagulation starts to affect the results if mass concentration exceeds  $1.0 \text{ g/m}^3$ . In the experiments mass concentrations was less than  $0.1 \text{ g/m}^3$  for the original dry particles, and thus the results from different experiments are not sensitive to coagulation growth.

The effect of sub-micron particles on the size growth might be

important at least in principle. This was estimated by assuming the input mass fraction of the fine mode to be between 1 and the  $d$  in Tables 3.2.2.2, 3.2.2.3 and 3.2.2.4.

In the present model a constant particle size distribution in vertical direction is assumed. However, flow patterns could differ during the experiments and could have an effect on particle concentration and sedimentation. The calculated and measured results should then be best comparable after 2 minutes growth, when sedimentation has not yet taken place. This was also the case, when the measurements and calculations were compared after different travel times.

At high R.H. care must be taken when the measured and calculated values are compared, because of high sensitivity on the R.H. of hygroscopic aerosols. Only a 1% error in the measured R.H. can cause dramatic change in the results. This is referred in Tables 3.2.2.1 - 3.2.2.4 where the effect of R.H. on the particle size (VMD) is visible.

### 3.2.2.7 Conclusions

The experiments carried out in a flow type reactor chamber showed that the growth of hygroscopic CsOH and NaOH particles is significant at high relative humidities (R.H. > 96 %). The results of theoretical calculations indicate that this growth will greatly increase the deposition rates of the particles by gravitational settling. Thus, the measured changes in the particle size distribution as a function of R.H. can be explained by hygroscopic growth and sedimentation. At relative humidities less than 90 % the growth was moderate and did not affect much the aerosol deposition rates. The measured and calculated volume median particle size distributions agreed reasonably within the estimated error limits. The most critical parameters affecting the aerosol size distributions were found to be the R.H. and the residence time in the chamber before sampling.

It is concluded that, during severe LWR accidents, the emissions and dispersion of radioactive particles to the environment are reduced due to hygroscopic properties of the materials in the particles. The source term is thus reduced by the increased gravitational settling at high humidity conditions. This happens in various processes, e.g. when gas is bubbling through water pools or flowing through filtered venting systems and especially when airborne radioactive matter settles in the containment atmosphere. Hygroscopicity will also increase the rainout of aerosol near the plant and affect the lung deposition of radioactive particles.

### 3.2.2.8 Nomenclature

$D_p$  is the diameter of the particle, R.H. relative humidity,  $VMD_{EAA}$  volume median diameter measured by EAA,  $VMD_{OPC}$  volume median diameter measured by OPC,  $VMD_{calc}$  volume median diameter calculated with the NAUA code,  $SGV_{EAA}$  standard deviation of the volume distri-

bution measured by EAA and  $SGV_{OPC}$  is the standard deviation of the volume distribution measured by OPC. EAA means electrical aerosol size analyzer and OPC optical particle counter.

### 3.2.2.9 References

- /1/ F. F. Cinkotai, The Behaviour of Sodium Mist particles in Moist Air. *J. Aerosol Sci.* 2 (1970) 325.
- /2/ J. Jokiniemi, The Growth of Hygroscopic Particles during Severe Core Melt Accidents, *Nucl. Tech.* 83, 1 (1988) 16 - 23.
- /3/ C. D. Leigh, Analyses of Plume Formation, Aerosol Agglomeration and Rainout Following Containment Failure, NUREG/CR-4222 (1986).
- /4/ W. Schöck et al., Large-Scale Experiments on Aerosol Behaviour in Light Water Reactor Containments, *Nucl. Tech.* 81, 2 (1988) 139-157.
- /5/ G. A. Ferron, Inhalation of Salt Aerosol Particles-II. Growth and Deposition in the Human Respiratory Tract, *J. Aerosol Sci.*, Vol 19, No 5 (1988) 611-631.
- /6/ I. N. Tang, *J. Aerosol Sci.*, (1986) 361.
- /7/ R. A. Robinson and R. H. Stokes, *Electrolyte Solutions*, 2nd Ed. London, Butterworths (1970).
- /8/ H. P. Meissner, Prediction of Activity Coefficients of Strong Electrolytes in Aqueous Systems, *ACS Series* 133 (1980) 495-511.
- /9/ F. X. Ball, W. Furst and H. Renon, An NRTL Model for Representation and Prediction of Deviation from Ideality in Electrolyte Solutions Compared to the Models of Chen (1982) and Pitzer (1973), *AIChE J.* 31(3) (1985) 392-399.
- /10/ J. Sangster and F. Lenzi, On the Choice of Methods for the Prediction of the Water Activity and Activity Coefficient for Multicomponent Aqueous Solutions, *The Canadian J. of Chem. Eng.*, 52 (1974) 392-396.
- /11/ S. M. Kreidenweis, R. C. Flagan and J. H. Seinfeld, Evaporation and Growth of Multicomponent Aerosols Laboratory Applications, *Aerosol Sci. and Tech.*, 6 (1987) 1-14.
- /12/ P. E. Wagner, Aerosol Growth by Condensation. In *Topics in current Physics, Aerosol Microphysics II* (W. H. Marlow ed.), Springer-Verlag Berlin, Heidelberg (1982) 129-177.
- /13/ J. C. Barrett and C. F. Clement, Growth Rates for Liquid Drops, *J. Aerosol. Sci.*, 19(2) (1988) 223-242.

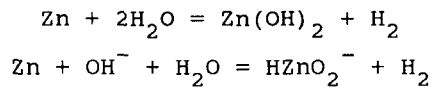
- /14/ B. J. Mason, The Physics of Clouds. 1st Ed. Clarendon Press, Oxford (1957).
- /15/ Instruction Manual Model 3075/3076 Constant Output Atomizer, TSI Inc., Minnesota (1978).
- /16/ P. Pasanen et al., Behavior of Hygroscopic Aerosols: test results on sedimentation in tubes, Proceedings on the OECD/NEA Workshop on Water Cooled Reactor Aerosol Code Evaluation and Uncertainty Assessment. Held in Brussels, Belgium 9th -11th September 1987, CEC, Luxembourg (1988) 280 - 290.
- /17/ H. Bunz, M. Koyro and W. Schöck, NAUA Mod4, A Code for Calculating Aerosol Behaviour in LWR Core Melt Accidents; Code Description and Users Manual, Report KfK 3554, Kernforschungszentrum Karlsruhe, Karlsruhe (1983).
- /18/ R. C. Weast (ed.), Handbook of Chemistry and Physics, CRC Press Inc., Florida (1987).
- /19/ J. Krey, Dampfdruck und Dichte des Systems NaOH-H<sub>2</sub>O, Zeitschrift für Physikalische Chemie Neue Folge, 81 (1972) 252-273.

### 3.2.3 Conclusions

The experiments on aerosol growth and sedimentation in tubes clearly demonstrate the importance of hygroscopicity and relative humidity on the growth of the nuclear aerosols expected during LWR accidents. Comparisons between measured deposition and observed particle sizes and results from calculations with the NAUA-HYGROS code show a reasonable agreement.

The results for dry conditions also indicate that about 20% of the deposit on the tube walls was resuspendable at the flow velocity where the the deposition took place. However, resuspension seems to be a slow process.

The detailed interpretation of the experiments with zinc aerosol, or mixed CsOH/Zn aerosol, in humid conditions is complicated by the following two chemical reactions.



The first reaction is known to occur at high temperature in the presence of steam. It could be important in the furnace region of the apparatus.

The second reaction is known to proceed when zinc metal comes in contact with strongly alkaline solutions, e.g. solutions formed when water is taken up by cesium hydroxide. Formation of cesium zincate will have an important effect on the hygroscopicity. The escaping hydrogen gas probably also affects particle growth, agglomeration

and deposition.

None of these reactions were considered in the experiments nor in their interpretation.

### 3.3 Reactions of boron carbide with steam and stainless steel

This section summarizes work performed by J. O. Liljenzin and J. P. Omtvedt of the Department of Chemistry, University of Oslo, Norway, on the interaction between boron carbide and steam or stainless steel.

#### 3.3.1 Introduction

Boron is used as neutron absorber in both BWR and PWR reactors. In pressurized water reactors it is used as a solution of lithium borate in the coolant, in boiling water reactors as solid boron carbide,  $B_4C$ , in the control blades and as an emergency shut down solution of sodium borate. We will concentrate on the solid boron carbide used in the BWR control blades. The blades are made from stainless steel of cruciform cross section. The boron carbide is present as a powder filled into horizontal drilled holes in the wings of the control blade. These holes are filled with boron carbide powder, sealed with plugs and welded tight.

During core overheating in a severe nuclear accident, the stainless steel in the control blades will melt at a lower temperature, 1370-1510°C, than unoxidized zircaloy in the fuel boxes and fuel pins, 1820°C. The melting of the stainless steel can have two effects; firstly the boron carbide with its high melting point, 2350°C, might be exposed to the steam/hydrogen atmosphere and react with it to more volatile boron/carbon compounds, secondly the boron carbide might react with the components in the stainless steel to form metal carbides and metal borides of lower melting point. In a practical situation both processes compete for the boron carbide. The metal borides formed may later react with hydrogen, steam and water to produce various boranes and different forms of boric acid.

This work should be seen in this context as it aims at a determination of the rates of these competing reactions and a formulation of equations which can be used to interpolate and extrapolate the measured rates to the conditions encountered in a severe core-melt accident.

#### 3.3.2 Experimental

All experiments were performed in the apparatus shown in Figure 3.3.1. The water cooled vacuum tight chamber made it possible to operate the furnace tube at prescribed temperature and pressure in an reasonably well defined atmosphere.

Due to convective heat losses at higher pressures the furnace had to

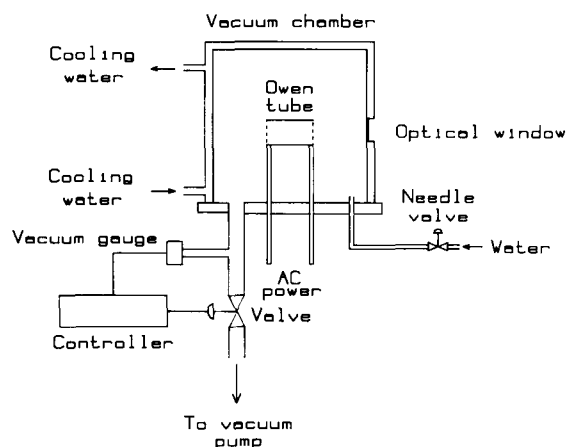


Figure 3.3.1. Schematic diagram of the equipment used for boron carbide oxidation/reaction studies at reduced pressures.

be operated at pressures below 100 millibar in order to reach the higher of the temperatures of interest. In the steam oxidation experiments, a pure steam atmosphere was generated by a continuous bleeding of liquid distilled water through a needle valve into the chamber. The steam generated was continuously removed through the pressure regulating valve by a rotary vacuum pump. Any reaction products will thus be removed rapidly, preventing the system to reach equilibrium.

Pressure in the furnace chamber was measured by a pressure transducer of membrane type, Baratron type 222B from MKS instruments. The output signal from the pressure transducer was fed to an analog pressure controller, VAT. The controller operated the pressure regulating valve, VAT, by means of a pneumatic system to maintain a constant preselected pressure in the outlet of the furnace chamber. At 10 millibar, the pressure fluctuated normally by about 3 millibar around the setpoint.

The furnace tube was made of 311 high temperature resistant stainless steel. The steel surface was rapidly covered with a dull dark brown oxide film the first time the tube was heated in a steam atmosphere to high temperature. A thin shiny black deposit was formed in the ceiling of the tube. No further corrosion of the furnace tube was observed in any of the experiments.

The furnace could be observed through an optical window in the water cooled wall. Temperatures were measured manually by use of an optical pyrometer and regulated by hand. A subjective error estimate of

the temperature readings is  $\pm 3^{\circ}\text{C}$ . The average temperature in each experiment was calculated as a mean value of a series of temperature readings taken about 15 minutes apart. The temperature variation in one experiments was usually within  $\pm 15^{\circ}\text{C}$ . The optically measured brightness temperatures were corrected to true temperatures using standard Tables assuming a spectral emissivity of 0.85 at  $0.65\ \mu\text{m}$  corresponding to oxidized stainless steel (18-8 type).

The test specimens of solid pieces of boron carbide, obtained from O. Lindquist, University of Göteborg, or cut boron carbide cubes placed on small stainless steel slabs were placed in the furnace tube. The vacuum pump started with a closed water inlet. When the prescribed pressure was reached, the water flow was turned on in the oxidation experiments and the heating current to the furnace tube was switched on. The operating temperature was normally reached in about one minutes time. The temperature and pressure were then kept constant during a reaction period of about 3 to 5 hours. At the end of an experiment, the current was turned off and the furnace tube left to cool at constant pressure. When the furnace was near room temperature, the connection to the vacuum pump was closed and air bled into the chamber.

A white crystalline condensed material could be found on the cool chamber surfaces after all oxidation experiments. The deposit looked like boric acid.

### 3.3.3 Kinetics of boron carbide oxidation in steam

The amount reacted was determined by weighing the piece of boron carbide used before and after the experiment on an analytical balance. No deposit of reaction products were found on the surface of the piece of boron carbide, nor on the furnace tube. A change in the surface of the boron carbide could be seen after oxidation experiments at the highest temperatures. The surface became slightly pitted and covered with a thin layer of a dull black material, presumably carbon.

Table 3.3.1 gives the weight losses observed after various times and temperatures in a 10 millibar steam atmosphere. These results can only be approximately translated to reacted amount per time and unit area as the pieces used in this series of experiments had a highly irregular surface on all but one side. Larger chunks of boron carbide were cut into thin slices by the Institute of Geology at the University of Oslo and these slices, having reasonably plane surfaces, were used in the later experiments. The reaction rates measured at  $950^{\circ}\text{C}$  and 10 millibar water vapor pressure using cut pieces of boron carbide with well defined geometric surface area were used to normalize the data from experiments with irregular boron carbide pieces. However, the actual surface area is of minor importance in the determination of the activation energy as each piece was used for several temperatures and the different pieces used were chosen to be of similar outlook. The main reason for the irregular surface is the presence of many large and small crystal facets protruding from the, reasonably flat, main surface on one side.

Table 3.3.1. Oxidation of boron carbide in a 10 millibar steam atmosphere. Approximate size of the boron carbide was 3x11x15 mm. The surface, about 11 cm<sup>2</sup>, was irregular. Data are normalized to the rate measured with cut boron carbide pieces.

Temperature (°C)	Reaction time	Weight loss rate (%/h)	Specific loss rate (umole/m <sup>2</sup> s)
854	4h 15m	0.303	15
860	5h 25m	0.325	16
910	3h 30m	0.531	25
961	5h 55m	1.12	61
1002	3h 55m	3.24	156
1055	3h 35m	5.81	243

The reaction rate fits fairly well to an Arrhenius type equation, see Figure 3.3.2.

$$-\frac{dn}{A dt} = f \exp\left(-\frac{E}{R T}\right) \quad (1)$$

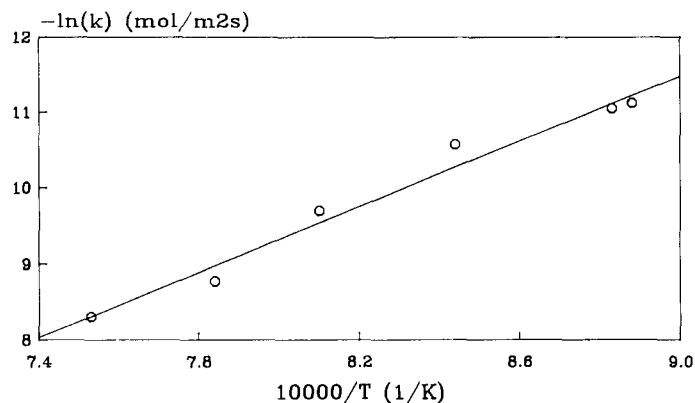


Figure 3.3.2. Temperature dependence of the reaction rate of boron carbide in a 10 millibar steam atmosphere.

where  $-dn/dt$  is the mass loss rate (moles/s),  $A$  the geometric surface area,  $f$  the "frequency factor",  $E$  the activation energy,  $R$  the general gas constant and  $T$  the absolute temperature. The activation energy was found to be  $(181 \pm 14)$  kJ/mole and the frequency factor was  $\exp(8.1 \pm 1.4)$  mole/m<sup>2</sup>s in an atmosphere of 10 millibar water vapor.

The effect of water vapor pressure was studied in a second series of experiments using cut slices of boron carbide. The results are given in Table 3.3.2. As can be seen from the Table there is very little, if any, change in reaction rate with water vapor pressure. This effect can be understood if vaporization of boron oxide or boric acid from the surface is rate limiting.

Table 3.3.2. Oxidation of cut pieces of boron carbide at 961°C in a steam atmosphere. The data given are averages of duplicate experiments.

Pressure (millibar)	Time	Weight loss rate (%/h)	Specific loss rate (umole/m <sup>2</sup> s)
3.19	3h 50m	0.300±0.004	60.9± 5.9
5.30	3h 50m	0.315±0.003	64.8± 6.5
7.70	4h 15m	0.291±0.073	59.3±21.2
9.66	3h 45m	0.322±0.010	67.0± 5.3
9.74	3h 40m	0.403±0.001	78.3± 8.0
12.5	3h 50m	0.199±0.078	40.4±19.8
14.5	4h 45m	0.297±0.038	58.1± 1.5

#### 3.3.4 Kinetics of reaction between boron carbide and steel

The rate of reaction between boron carbide and stainless steel was studied in the same apparatus as used for the steam oxidation experiments. The water supply was shut off and the furnace chamber was operated at low pressure.

Cubic pieces of boron carbide were put on top of small slabs of machined stainless steel plates. The sample was then heated to the desired temperature.

Below 1000°C no reaction could be observed at all. When heated up to approximately 1150°C a very rapid reaction started between boron carbide and stainless steel. In one of the first experiments the sample could be quenched. Figure 3.3.3 shows a photograph of the quenched sample. The low-melting reaction product can be seen surrounding the base of what was left of the boron carbide chunk. The melt had also penetrated through the steel slab in a small spot near the center of the boron carbide.

In a later experiment the melt almost completely dissolved both the boron carbide and the stainless steel slab. Thereafter the melt broke rapidly through the wall of the oven tube and solidified on the baseplate of the vacuum chamber. It seemed then meaningless to continue these experiments as originally planned. It is clear that

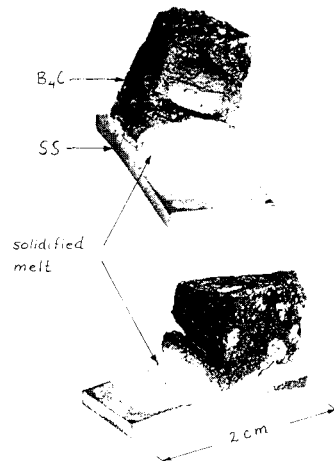


Figure 3.3.3. Photograph of a quenched sample showing the solidified reaction product surrounding the base of the boron carbide piece. Maximum temperature was about 1150°C for a short time.

the reaction begins very suddenly and then proceeds fast because the melt formed is of low viscosity, highly aggressive towards both boron carbide and stainless steel and has a lower melting point than that at which the rapid reaction begins.

### 3.3.5 Results and discussion

Several studies of the rate of reaction between boron carbide and steam have been published. Litz and Mercuri /1/ studied the oxidation rate of boron carbide powder placed in a platinum dish between 470 and 1020K. They computed the specific reaction rate from the measured area (BET) and the weight loss rate and interpreted the results in terms of the equation:

$$-\frac{dn}{p_w A dt} = f \exp\left(-\frac{E}{RT}\right) \quad (2)$$

where  $p_w$  is the water vapor pressure. The results are given in Table 3.3.3. Woodley /2/ measured the weight loss rate and rate of hydrogen evolution from a small block of boronated graphite in a steam atmosphere. Woodley also found the reaction rate was proportional to the 0.48 power of the water vapor pressure and suggested the following equation:

$$-\frac{dn}{(p_w)^{0.48} A dt} = f \exp\left(-\frac{E}{RT}\right) \quad (3)$$

Numeric values for the parameters are given in Table 3.3.3. Elrick et al. also studied the steam oxidation of boron carbide coupons at 1270K and 620 torr H<sub>2</sub>O pressure, see also Table 3.3.3. In this case the coupons became covered with a deposit of boron oxide during the experiment.

Table 3.3.3. Intercomparison of steam pressure exponents and activation energies for steam oxidation of boron carbide.

Eqn. used	steam pressure exponent found	E (kJ/mole)	Ref.
1	0	181±14	this work
2	1	46	/1/
3	0.48	74.5	/2/

Elrick et al. /3/ found that equation 2 with the parameter values given by Litz et al. underpredicted their observed rate of oxidation by a factor of seven and equation 3 with parameter values given by Woodley underpredicted the rate by a factor of ten. One problem when comparing the results from these experiments is uncertainty about the effectively exposed surface area. In our experiments, this should be of less importance as we used solid pieces of boron carbide with all surfaces exposed to the steam atmosphere and pressures low enough to evaporate the reaction products.

The rapid melting of stainless steel in contact with boron carbide has also been observed in the DF-4 experiments /4/ between 1520 and 1570K. Furthermore, melting experiments at KfK, Karlsruhe, /5/ also shows an early melting of stainless steel in contact with boron carbide. Even if the phase diagrams are complex, this can be explained by the formation of low-melting eutectica in the B-Fe, C-Fe and B-Ni systems.

It would therefore be interesting in the near future to prepare solidified melts from various mixtures of boron carbide and stainless steel. The remelting points of these could then be measured, giving information on the melting/solidification point as function of the ratio between boron carbide and stainless steel.

### 3.3.6 References

- /1/ L. M. Litz and R. A. Mercuri, Oxidation of Boron Carbide by Air, Water, and Air-Water Mixtures at Elevated Temperatures, J. of the Electrochemical Society, 110 (1963) 8.

- /2/ R. E. Woodley, The Reaction of Boronated Graphite with Water Vapor, Carbon, 7 (1969) 5.
- /3/ R. M. Elrick, R. A. Sallach, A. L. Ouellette and S. C. Douglas, Boron Carbide - Steam Reactions with Cesium Hydroxide and with Cesium Iodide at 1270K in an Inconel 600 System, NUREG/CR-4963, SAND87-1491, September 1987.
- /4/ R. O. Gauntt, Information given in letter to S. A. Hodge, Sandia National Laboratories, ACRR Reactor-Safety Experiments, December 16, 1988.
- /5/ S. Hagen and P. Hofmann, Behavior of B<sub>4</sub>C Absorber Rods under SFD Conditions, SFD Program-Review Meeting, Rockville, Maryland, USA, October 21 - 24, 1986.

#### 3.4 Stickiness and flow properties of a deposited wet slurry

A liquid aerosol mixed with an insoluble component has an affinity to stick on surfaces. A relocation of a deposited aerosol may occur depending on the mole fraction of the solid component and on the viscosity of the liquid component. These phenomena have been studied experimentally in the LACE program and in the small scale tests carried out at the University of Kuopio.

In the scoping tests of the LACE program, the mole fraction of the insoluble component, Al(OH)<sub>3</sub>, was varied between 0 and 1 and in the LACE tests, the insoluble material, MnO, mole fraction was varied between 0.62 and 0.91. The mole fraction of the insoluble component depends on the amount of aqueous solution (hygroscopic matter + water) in the aerosol. In the LACE tests, the chemical analyses showed that the hygroscopic material used (NaOH and CsOH) did not react chemically with the insoluble material. The flow was turbulent in these tests, corresponding to Reynolds numbers between 30,000 and 100,000. The results showed that if the mole fraction of the insoluble component is low the deposited material will move along the pipe as a liquid film and does not stick to the surfaces. If the mole fraction of the insoluble component is high the deposited dry aerosol will be resuspended. An aerosol characterized by an intermediate mole fraction of the insoluble component, 0.6 and 0.7, seemed to be very sticky and can cause a plugging of a pipe /1/.

The results of the small scale experiments at the University of Kuopio show, that when the aerosol contains only hygroscopic matter (CsOH) the deposited material will move along the tube even at flow conditions corresponding to natural convection (Reinolds number 630). These experiments also showed that deposition of pure hygroscopic matter in pipe bends is significant at relatively low Reynolds number (1000 - 3000) /2/. However, the LACE scoping tests showed that with high Reynolds numbers (100,000) there is a translocation of hygroscopic matter and dry aerosols from pipe bends and a high penetration through the whole piping system was revealed. In the LACE tests significant deposition of sticky aerosol in pipe bends was observed even with high Reynolds numbers (100,000).

Currently, the models used in reactor accident analyses can not handle the translocation or resuspension phenomena in pipes. The deposition of sticky aerosol is, however, better treated and the results of the latest versions of TRAP-MELT /3,4/ and RAFT /5,6/ codes compare reasonable with the values obtained in the LACE tests LA1 and LA3 where sticky aerosol was used.

#### 3.4.1 References

- /1/ R. Hesbøl, Some Notes on the Resuspension and Relocation of Wet Aerosols in Pipe Systems Obtained in the LACE Tests.
- /2/ T. Raunemaa, Personal Communication, 1989.
- /3/ A. L. Wright et al., Summary of Posttest Aerosol Containment Experiments (LACE) LA1, LACE TR-022, 1987.
- /4/ A. L. Wright et al., Summary of Posttest Aerosol Containment Experiments (LACE) LA3, LACE TR-024, 1988.
- /5/ K. H. Im and R. K. Ahluwalia, Turbulent eddy deposition of particles on smooth and rough surfaces, J. of Aerosol Sci., Vol 20(4), 1989.
- /6/ R. K. Ahluwalia, Personal communications, 1987.

#### 3.5 Acidity/basicity of water solutions in the containment during some selected accident sequences

Besides the materials normally considered in ex-vessel phenomena in core melt accidents, several other important materials are also present in a real nuclear power station. In a typical Swedish BWR containment there are large amounts of aluminium, copper, zinc and various synthetic rubbers around and below the vessel. The atmosphere in the containments of these reactors is inerted during operation and consists of nitrogen and steam. When a core melt situation arises with molten corium exiting through the bottom of the pressure vessel much of these secondary materials are subjected to high temperatures by direct contact with the melt or by thermal radiation from the melt during its downward flow into the pedestal. This will pyrolyse the organic materials and may even melt and vaporize some of the aluminium, copper, iron and zinc present near the melt passage.

Such processes and their effect on the source term have seldom been considered. It is therefore important to point out the possible effects these materials may have on the chemical environment in the containment and indicate the possible effects on iodine chemistry. A quantitative evaluation is at present very uncertain as basic data, especially gas volumes and flow rates, on accident progression in presence of these materials are not available. This is largely due to the lack of models for these effects in most codes for severe

accident modeling known to us and especially in MAAP.

### 3.5.1 Pyrolysis of insulating materials

The amounts of organic polymer materials present in a typical modern swedish PWR containment has been determined by ABB ATOM AB on behalf of the RAMA and NKA/AKTI-150 projects /1/. Some of their results are given in Table 3.5.1. It is known from experiments /2/ that the synthetic rubbers used, mainly as electrical insulation, begin to give off considerable amounts of condensable and non-condensable gases and acidic substances already at 400°C in a nitrogen/steam atmosphere, see Table 3.5.2. The gases evolved are of such amount that they can influence the pressures and streaming pattern in the containment significantly. Thus a calculation of their transport and ultimate fate in the containment based on the output from a normal MAAP calculation will be very approximate and mostly of a qualitative nature.

The acidic substances, mainly hydrochloric acid, sulfur dioxide and carbon dioxide, will change the acidity of condensates and water pools and thereby influence the iodine chemistry, especially in the radiation fields present.

Table 3.5.1. Inventory in a typical BWR containment of some materials important in severe core melt accidents. All amounts are in metric tons and areas in square meters. Amounts given are accurate to about 10% /1/.

Material	Lower drywell		Upper drywell		Wetwell	
	Amount	Area	Amount	Area	Amount	Area
Rubber insulation	2.8	-	1.6	-	0.0	-
Copper wires	1.0	-	0.5	-	0.0	-
Aluminium	0.7	40	8.3	4500	0.0	-
Zinc plating	0.6	>1200	17.2	>35000	0.0	-

Table 3.5.2. Amount, volume and acid equivalents of pyrolysis products produced in a nitrogen/steam atmosphere from typical rubber insulation in the amounts used in swedish BWR containments /2/.

Temperature (°C)	Non-condensable gas (Nm <sup>3</sup> )	Condensable gas (kg)	Acidic compounds (moles of H <sup>+</sup> )
400	68	270	1600
600	120	150	13000
800	350	250	12000
1000	480	70	11000

The non-condensable gases comprise various amounts of several unsaturated organic compounds like ethene, acetylene and propene, depending on the pyrolysis temperature, see Figure 3.5.1. These

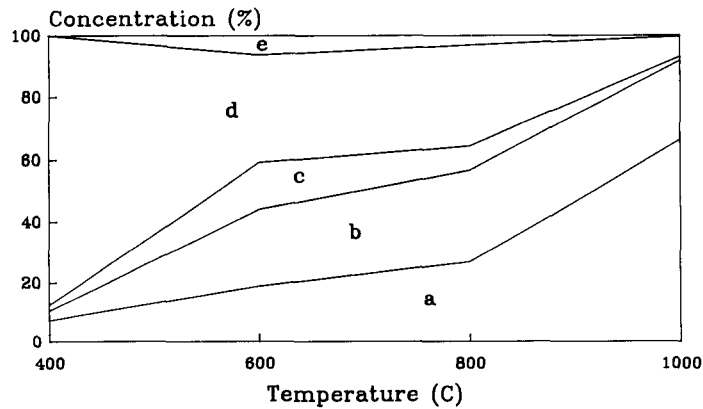


Figure 3.5.1. Composition of non-condensable gas produced by pyrolysis in a nitrogen/steam atmosphere of a typical insulation rubber used in swedish/finnish BWR containments. Data are given as percent by volume at room temperature measured by gas chromatography /2/.

a = sum of hydrogen and methane, b = sum of ethene and acetylene, c = ethane, d = propene, e = propane.

substances are prone to add hydrogen iodide to their double or triple carbon-carbon bonds forming organic iodides. From Figure 3.5.1 it is evident that a high pyrolysis temperature, as expected, yields more of low molecular weight products than a low temperature.

The pH-values expected in the lower drywell, upper drywell and wetwell of a swedish BWR containment, based on the results from two MAAP calculations /3, 4/, are illustrated in Figure 3.5.2, for two accident sequences, TB and AB, by assuming that the pyrolysis gases produced corresponds to a pyrolysis at 800°C of the organic material present below the vessel. Furthermore, it was assumed that the amount pyrolysed increased from zero to half of the maximum amount possible as a linear function of the amount of core melt leaving the vessel. To compute the distribution of pyrolysis gas in the different compartments the transport of the gases produced were assumed to be similar to the movement of nitrogen between the compartments. An acid-base balance was then made in each compartment for a series of times. All effects from corrosion were neglected when making these balances. The excess/deficit of acid, in hydrogen ion equivalents, was then divided by the volume of liquid water in respective compartment to obtain a nominal hydrogen concentration in each compartment as a function of time. Values for time periods

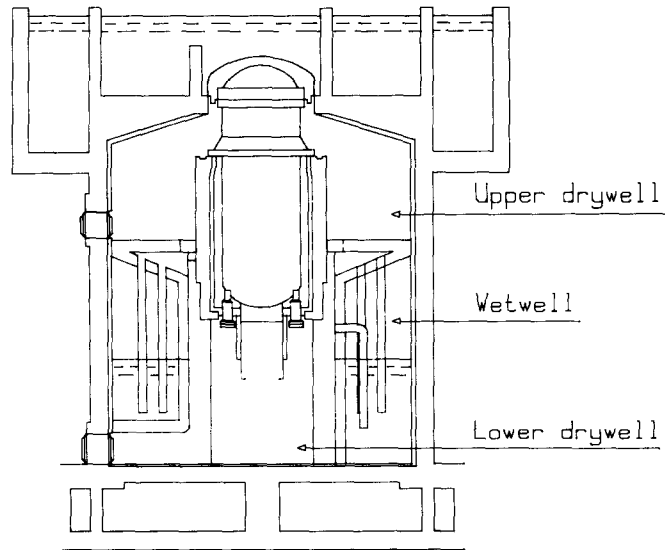


Figure 3.5.2. A schematic drawing of an ASEA-ATOM BWR containment showing the interconnections and names used in this report for the various compartments.

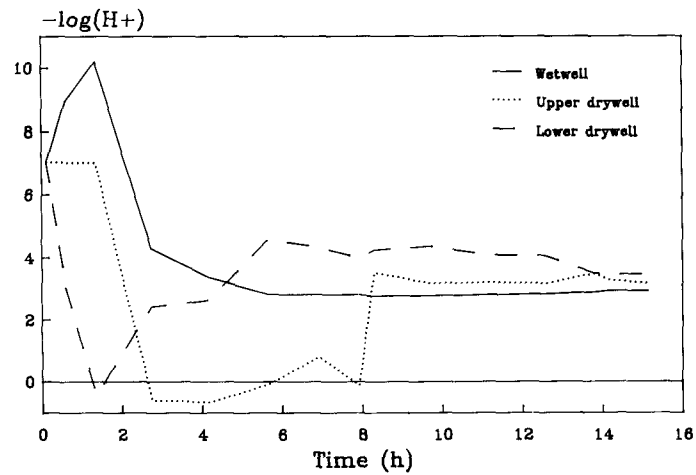


Figure 3.5.3. Approximate calculation of the acidity in the three compartments in a BWR containment as a function of time during a TB sequence based on thermal-hydraulics modeled by MAAP 3.0 /3/. The logarithm of the free hydrogen ion concentration was arbitrarily set to 7.0 at any time when either no liquid water was present or no acidic/alkaline substances were present in a compartment.

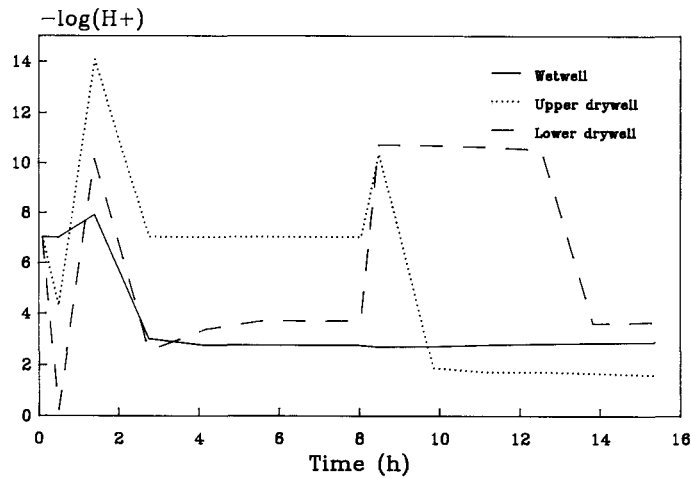


Figure 3.5.4. Approximate calculation of the acidity in the three compartments in a BWR containment as a function of time during a AB sequence based on thermal-hydraulics modeled by MAAP 3.0 /4/. The negative logarithm of the free hydrogen ion concentration was arbitrarily set to 7.0 at any time when either no liquid water was present or no acidic/alkaline substances were present in a compartment.

without any liquid water present were arbitrarily set to  $10^{-7}$ . The results are shown in Figures 3.5.3 and 3.5.4 as function of time into the accident.

As can be seen from the Figures, the water in all compartments becomes acid at one time or the other. The final state is always acidic. This will favor the evolution of hydrogen iodide and elementary iodine by radiolysis of the aqueous solutions. However, as corrosion phenomena were neglected, especially on zinc plated surfaces, the final state may in reality be less acidic than that shown in these Figures.

### 3.5.2 Corrosion of aluminium and zinc

Aluminium and zinc are present in swedish BWR containments in considerable quantities, mostly as thin plates and surface coating respectively. Table 3.5.1 gives some typical data.

A high local pH caused by an initial deposition of a hygroscopic cesium hydroxide containing aerosol will lead to rapid corrosion with hydrogen evolution. The corrosion will stop or decrease strong-

ly once the alkali metal hydroxide, mainly cesium hydroxide, has been used up in the process. Alkaline corrosion at high pH is important and rapid for both aluminium and zinc. The alkaline corrosion will bind some cesium in the corrosion products.

When the acidic gases from the pyrolysis of insulating materials spread in the containment the situation will be reversed. Most wet surfaces will then soon reach a low pH. At low pH, corrosion of zinc is more pronounced than corrosion of aluminium. Also acid corrosion will produce hydrogen and some of the acidic substances will become neutralized in the process. At the same time some cesium may be leached from earlier formed corrosion products.

The large areas covered with aluminium and zinc and the large amounts of these materials give them the potential to be the major source of hydrogen in the containment. Catastrophic corrosion of these metals could produce 2 500 kg of hydrogen, should it occur. However, there seems to be several factors limiting the amount of corroded material. The major limitation will be a limited supply of the alkaline and acidic substances necessary for large scale corrosion as these are consumed by the corrosion process. The situation would be much worse if there was any source of mercury or mercury salts in the containment because mercury and its salts acts as catalysts for corrosion of aluminium by water even at neutral pH.

Because of the incomplete information available from the MAAP calculations on the deposition of fission products onto various surfaces in the compartments it is presently not possible to make any quantitative estimation of the amount of corroded aluminium and zinc. We can only point out the importance of corrosion as it will produce hydrogen, consume hydroxide at high pH and consume acid at low pH. The fact that very large surfaces are covered with these metals indicates that the effects from corrosion will be seen fairly rapidly. The net effect of metal corrosion will be a reduction in the span of pH-values and an extra production of hydrogen which also increases pressure and changes gas flows in the system.

### 3.5.3 Copper

When electric wiring below the vessel comes into direct contact with the exiting very hot core melt it is likely that some copper will melt and even vaporize. The copper vapor will condense onto cooler surfaces. The effects from the presence of finely divided copper can be manifold.

Copper condensed on zinc plated surfaces will give galvanic corrosion at low pH. This will accelerate corrosion of zinc. It is not clear at present if copper also will have any large effect on the corrosion rate of aluminium.

It is known from experiments, e.g. /2/, that metallic copper acts as a good getter for elementary iodine. Hence, the vaporized and condensed copper will react with and bind any elementary iodine present in the same compartment as the copper. This action is similar to

that of silver from PWR control rods. Even if we assume that only 2% of the copper present immediately below the vessel is vaporized and available as iodine getter this corresponds to about 20 kg copper which could bind up to 40 kg of elementary iodine as CuI. However, there is only about 21 kg of iodine normally assumed present in the fuel. This makes us believe that no elementary iodine could exist as such for any length of time in the pedestal atmosphere after the core melt has penetrated the vessel bottom. Hence, we believe that any radiolytic production of elementary iodine in the finally acidic water of the lower drywell is of no concern.

#### 3.5.4 Conclusions

There are three possibly important effects on iodine chemistry from the presence and reactions of secondary materials.

1. Acidic compounds from the pyrolysis of organic polymers sooner or later causes low pH-values in all water pools inside the containment. Low pH-values will lead to radiolytic production of elementary iodine and secondary formation of hydroiodic acid.
2. Hydrogen iodide is known to add to unsaturated organic compounds such as those found in the pyrolysis gases forming organic iodides of various kinds.
3. Elementary iodine is, at least in the lower drywell, probably captured by finely divided copper from vaporized electric wiring.

Corrosion of aluminium and zinc will produce hydrogen, but will at the same time consume alkaline and acidic substances thereby reducing the possible swing in pH-values. Catastrophic corrosion could possibly make aluminium and zinc the major source of hydrogen in the containment.

This section has mainly concentrated on the effects of secondary materials present in a BWR containment, but similar questions must exist also for PWR containments even if they could be of smaller importance because of a larger containment and a smaller amount of materials immediately below the pressure vessel.

As seen from the discussion above, the secondary materials can have large effects on the iodine source term by changing the iodine speciation, by binding cesium in corrosion products and they can even have some important effects on the thermal-hydraulic processes during a severe core melt accident. Hence, there should be a need to include such materials and phenomena in future nuclear accident analysis codes.

### 3.5.5 References

- /1/ Kelen, T., RAMA III - Kompletterande materialinventering inom inneslutningen för bedömning av pH och redoxpotential vid svåra haverier, ABB ATOM AB, Report RM 88-1099, rev. 1., 1988.
- /2/ Fridemo, L., Liljenzin, J.O., Produkter från kabelpyrolys, Department of Nuclear Chemistry, Chalmers University of Technology, Report KKR 841108, Göteborg 1988.
- /3/ Enerholm, A., FRISK - FORSMARK 3 - MAAP-beräkning för totalt elbortfall, designsekvens (Fall 1), Swedish State Power Board, Report PK-93/87, 1988.
- /4/ Enerholm, A., FRISK - FORSMARK 3 - MAAP-beräkning för stort ångledningsbrott och totalt elbortfall (Fall 3), Swedish State Power Board, Report PK-93/87, 1988.

### 3.6 Assessment of the contribution to formation of hydrogen to be expected in the primary system under core melt accident conditions due to corrosion of steels

Iron from steels can react with steam at high steam/hydrogen ratios forming hydrogen and iron oxides. However, the heat of reaction is much smaller than for zirconium, about 0.24 MJ/kg iron as compared

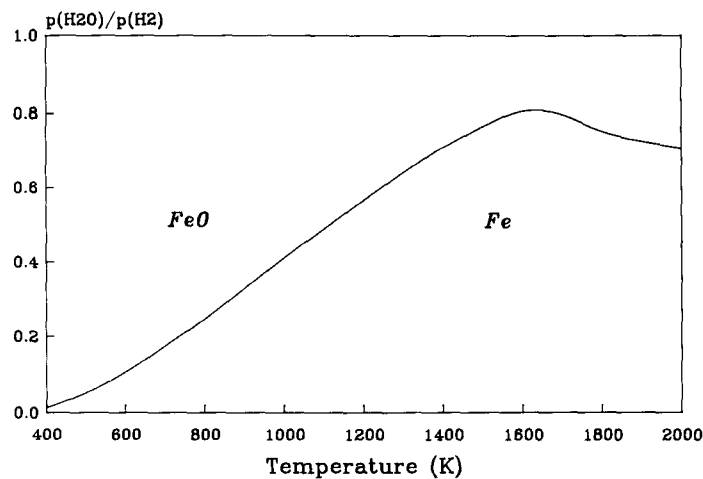


Figure 3.6.1. The redox state of iron as function of steam/hydrogen partial pressure ratio computed from published thermodynamic data. The line corresponds to a 1:1 oxide/metal equilibrium ratio.

to about 6.4 MJ/kg zirconium at 1500 K. In those parts of the system where steam/hydrogen ratios below 1 occur, the reaction will instead lead to a reduction of iron oxides by hydrogen, see Figure 3.6.1.

The amount of hydrogen formed by oxidation of steel in the primary system is a complicated function of temperature, steam/hydrogen ratio, corrodant concentrations and time. An upper boundary can be set by assuming that all iron in internal steel structures in the vessel have been oxidized by steam to iron oxide. Hence, no more than 2400 kg of hydrogen can possibly be formed this way for a BWR 3000 reactor. However, the probable value is very much smaller due to the reducing action of the hydrogen produced by both iron and zirconium oxidation. The amount of iron oxidized may even be zero in scenarios where low steam/hydrogen ratios persist during the high temperature phase of the accident.

#### 4 DISCUSSION OF POSSIBLE INFLUENCES OF CHEMICAL BEHAVIOR ON SPECIFIC PROCESSES AFFECTING THE COURSE OF EVENTS IN CORE MELT ACCIDENTS

Chemical reactions are of major importance for the development of a core melt accident. Perhaps most important is the reaction between zirconium and steam which releases a major part of the energy needed to melt the core. However, many other chemical reactions also proceed and can have a large impact on the release, transport and deposition of various materials and fission products as they will evolve or absorb heat and change the transport properties of the materials involved.

##### 4.1 Melt progression

As the temperature of the core increases it will start to melt. In a BWR reactor the more low-melting materials include the control rods and other stainless steel components with a melting point below or around 1500°C. Predicting the melting of the core is complicated by the occurrence of low-melting eutectica. Thus the Zr-Fe and Zr-Ni systems have melting points down to below 1000°C while the B-Fe system has melting points below 1100°C, see section 4.3. Since e.g. zircaloy and stainless steel is not intimately mixed it is, however, not probable that such eutectica will form unless the melting point of either metal, e.g. stainless steel, is exceeded.

Molten stainless steel will probably attack the zircaloy cladding producing some of the low-melting eutectica mentioned above. This will also increase the rate of hydrogen evolution from zirconium. The stainless steel in the control blades will also react with the boron carbide in the blades. Boron and carbon will dissolve in the melt and chromium may possibly form carbides and borides. The resulting melt has a melting point below 1150°C.

##### 4.2 Hydrogen formation

Hydrogen formation in the hot or molten core comes mainly from oxidation of zirconium:



Zirconia forms a passivating layer on top of the metal at low temperatures. At temperatures exceeding 1200°C the reaction rate increases rapidly. Hydrogen evolution from a zirconium rich melt would be limited by the transport of water vapor through the porous product layer or by the transport of oxide ions through a thin barrier-type zirconia layer on the surface of the melt. The formation of zirconium containing low-melting eutectica would decrease the temperature for the onset of rapid hydrogen evolution.

Hydrogen production from stainless steel should also be considered. As in the case of zirconium, the reaction rate increases as tempera-

ture rises. The formation of melts increases the hydrogen production rate.

Starting at a high steam/hydrogen molar ratio, iron and chromium will both oxidize. When the ratio has decreased to 1, only chromium will continue to contribute to the hydrogen evolution. The iron oxides formed initially may then be reduced to the metal as the gas becomes more and more reducing.

The presence of compounds such as boron oxide which are corrosive towards stainless steel will increase the rate of hydrogen production in the vessel and in the containment.

Boron from the control blades will contribute to hydrogen production. From a thermodynamic viewpoint boron will react with water whether it is in the form of carbide, boride or dissolved in stainless steel. However, the kinetics of this reaction remains to be studied.

#### 4.3 Evaporation and nucleation

When the core starts to melt most of the volatile fission products, cesium, iodine, krypton and xenon, will already have left the hot fuel. The vaporization of less volatile fission products, tellurium, selenium, barium, strontium, molybdenum, ruthenium and rhodium, is more difficult to predict. Evaporation of these elements from the molten core depends on transport phenomena and on the equilibrium vapor pressure of the different chemical species involved.

The chemical state of the fission products will change during an accident sequence. Such reactions needs to be considered since they determine the equilibrium vapor pressure of the element over the hot or molten core.

The most important factors are oxidation of the metallic elements in the core by steam and reactions of fission products with other materials in the hot or molten core.

From the start two melts, one oxidic the other metallic, will tend to separate. Due to steam oxidation more metal will be converted to oxide with time. Strontium and barium will only be stable in their more volatile elemental form in extremely reducing conditions, e.g. in a Zr rich melt. As soon as they leave this environment they will be oxidized by steam or by other oxides. Other fission products may have low volatility because they dissolve in the metallic melt. As the metallic part of the melt is oxidized, these fission products will become more volatile.

Dissolution of fission products in the melts and reactions with substances in the melts are important. When a substance dissolves in a melt its vapor pressure is generally decreased. In some melts where the chemical bonding between two different atoms in the melt is similar to the forces in the pure substance the equilibrium pressure may be predicted from:

$$p_{i,T} = p_{i,t}^{\circ} X_i$$

where  $p_{i,T}$  is the equilibrium vapor pressure of substance  $i$  at temperature  $T$  over the melt,  $p_{i,t}^{\circ}$  the equilibrium vapor pressure of pure substance  $i$  at the same temperature and  $X_i$  its mole fraction in the melt. This expression holds fairly well for many melts e.g. molten stainless steel. A more general expression is given by:

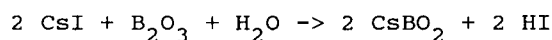
$$p_{i,T} = p_{i,t}^{\circ} f_i X_i$$

where  $f_i$  is the activity coefficient of substance  $i$  in the melt at the actual temperature and melt composition. Where strong chemical interactions or compound formation occurs activity coefficients may become quite low. The first, simpler, expression would be expected to work for e.g. molybdenum, rhodium, palladium, technetium and ruthenium in the metallic part of the melt.

Tellurium and selenium may be vaporized from the fuel at a relatively low temperature. It is likely that they would react with the solid or melting zircaloy cladding so that little tellurium and selenium escapes from the core. As the core melts these elements will stay associated with metallic zirconium as long as this is present, leading to lower vapor pressures.

#### 4.4 Reactions in the reactor coolant system

Chemical reactions may occur that changes the chemical state of the released fission products in the RCS. These changes include oxidation or reduction by the steam-hydrogen atmosphere and various reactions with other materials vaporized from the core. Thus cesium iodide that would be expected to contain most of the released iodine after vaporization may react with boron oxide formed by oxidation of boron carbide in the control blades by steam:



Tellurium in vapor form may react with tin to form tin telluride, SnTe.

#### 4.5 Aerosol nucleation

As the vaporized material moves away from the melt it will cool down and some material will start to condense. Condensation may occur on surfaces and on particles already present. It may also occur by nucleation. Nucleation of particles need some supersaturation of the gas with respect to the condensing substance. Condensation on pre-existing particles is the thermodynamically favored process.

The concentration and area of preexisting aerosol particles, the rate of cooling, the degree of supersaturation of the gas and the diffusivity of the condensing species will together determine the rate of nucleation.

Nucleation can proceed through two somewhat different mechanisms called homogeneous and heterogeneous nucleation.

Homogeneous nucleation is the direct unassisted formation of nuclei consisting of a single substance, sometimes called self-nucleation. Homogeneous nucleation is uncommon in nature but can readily be obtained under controlled conditions in the laboratory. It is opposed by the Kelvin effect given by

$$p/p_s = \exp((4sM)/(dRTD)) \quad (4.5.1)$$

where  $p$  is the actual vapor pressure,  $p_s$  the saturation vapor pressure,  $s$  the surface tension,  $M$  the molecular weight,  $d$  the density,  $R$  the gas constant,  $T$  absolute temperature and  $D$  the "Kelvin diameter". The ratio  $p/p_s$  is usually called the saturation ratio. The Kelvin diameter is the diameter of a drop in equilibrium with the gas phase. An examination of equation 4.5.1 shows that a saturation ratio of 220 is required in theory for growth to start from an individual water molecule ( $D = 0.0004 \mu\text{m}$ ). Experience shows that condensation to particles begins at much lower supersaturation values /5/. This can be understood if the condensation starts from a temporary aggregate of molecules formed by statistical collision processes between molecules. For a given vapor, gas and temperature the supersaturation required for homogeneous nucleation is called the critical saturation ratio. The measured critical saturation ratio for pure water vapor is 3.5 at  $20^\circ\text{C}$  and increases to 4.3 at  $0^\circ\text{C}$ . When the saturation ratio exceeds the critical saturation ratio a high number concentration of sub-micron particles is suddenly formed having a narrow but not monodisperse size distribution.

In heterogeneous nucleation, the formation of nuclei are promoted by preexisting "condensation centers". These can be ions or very small particles of other substances. Hence heterogeneous nucleation is often also called nucleated condensation. Heterogeneous nucleation is the most common nucleation process in natural systems, e.g. cloud formation in the atmosphere. Whereas homogeneous nucleation usually requires saturation ratios in the range 2 to 10, heterogeneous nucleation can even occur in unsaturated conditions forming size stable droplets. Three kinds of primary nuclei have been recognized: insoluble nuclei, ions and soluble nuclei.

The effect of insoluble nuclei depends on size, shape, chemical composition, surface structure and surface charge. They are in general less effective than soluble nuclei in decreasing the critical saturation ratio.

Ions are formed continuously in a gas irradiated by high energy radiation. The effect of ions as primary condensation centers is well known and used in e.g. cloud chambers for visualization of charged particle tracks. The needed supersaturation ratio for water vapor at room temperature is about 2.

Soluble nuclei decreases the chemical potential of the condensing substance and hence reduces the supersaturation needed for nuclea-

tion. This is especially important for water vapor nucleation where hygroscopy plays an important role. The opposite phenomenon where tiny water droplets decreases the critical pressure for condensation of a soluble substance may also have importance in some conditions that occur during a severe accident. The critical saturation ratio for water in the presence of soluble nuclei is given by

$$p/p_s = (1 + (6imM)/(M_s d D_p^3))^{-1} \exp((4sM)/(dRTD)) \quad (4.5.2)$$

where  $m$  is the mass of the soluble salt having molecular weight  $M_s$ ,  $i$  the number of ions formed when the salt dissolves in water. The remaining symbols refer to water and have the same definitions as in equation 4.5.1. The presence of a soluble substance introduces hysteresis in the saturation ratio/droplet size dependence, see Figure 4.5.1.

The gas containing the hot vapors from the core will contain particles. This is because particles of substances with low vapor pressure, e.g.  $ZrO_2$  and  $UO_2$ , will become suspended in the flowing gas, forming an aerosol together with the vaporized material. The concentration and area of these particles, the number of ions per volume unit, the composition and degree of supersaturation of the gas and the diffusivity of the condensing species will together determine the type and rate of nucleation.

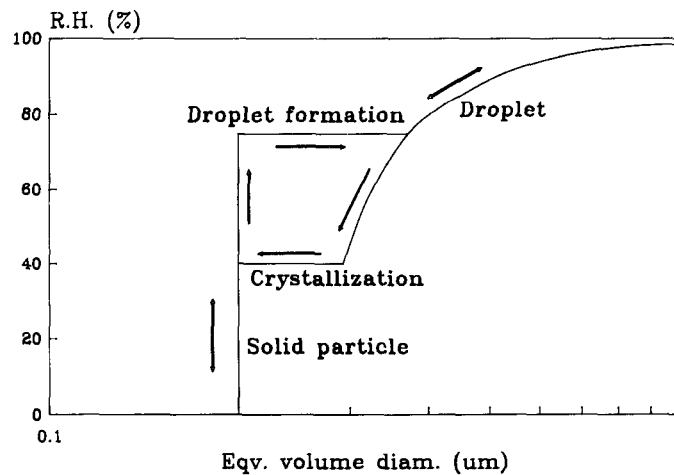


Figure 4.5.1. Drop size for a NaCl aerosol as function of relative humidity /5/.

Speciation is obviously important to the condensation of fission products as it determines their equilibrium vapor pressure. Thus molybdenum has a low vapor pressure in the form of Mo and  $\text{MoO}_2$ . At high steam/hydrogen ratios and lower temperatures  $\text{MoO}_3$  and  $\text{Cs}_2\text{MoO}_4$  may form that are more difficult to condense. In the reducing conditions that will occur in the vessel after melt-through  $\text{CsOH}$ ,  $\text{CsI}$  and Cs-borates may be reduced to elemental cesium that has considerably higher vapor pressure than other cesium species. This may cause much of the cesium left in the vessel to revaporize and enter the containment.

A relatively large part of the material vaporized from the molten core will consist of iron, chromium and nickel from stainless steel. Nickel and iron are both stable in elemental form at steam/hydrogen ratios less than one. Particles containing metallic iron and nickel may react with and dissolve some fission products, notably tellurium, causing them to convert to particulate form at temperatures well above the saturation point.

As can be seen from the discussion above it is important to know a comprehensive set of critical saturation ratios for relevant substances and conditions. It is also important to know water activities in concentrated solutions of soluble substances and the mixtures of them that can appear during the course of a severe accident.

#### 4.6 Condensation and chemisorption on aerosol particles

The general theory for condensation on aerosol particles without specific chemical reactions is given in section 4.5 above.

All water soluble chemical compounds present in aerosols tend to reduce the partial pressure of water in equilibrium due to a lowering of the water activity. This is most pronounced for cesium hydroxide and its water solutions. Hence, dry aerosols containing soluble compounds will try to pick up water until they form a solution which is in equilibrium at the actual temperature with the steam partial pressure in the surrounding gas. The tendency to pick up water from the atmosphere is called hygroscopicity. Its effects are largest when the relative humidity of the gas is near 100%.

The equilibrium water vapor partial pressure above cesium hydroxide solutions has been measured as a function of temperature and concentration within the NKA/AKTI-150, see section 3.1 above. The results from these experiments have also been compared with theoretically calculated data from Knights /8/.

Aerosol growth and the increased sedimentation caused by the presence of hygroscopic materials in the aerosols have also been studied. A general overview of these results and the calculation methods developed for hygroscopic aerosols is given by Jokiniemi. His model has also been included in a special version of the NAUA code, NAUA-HYGROS /6/.

Cesium hydroxide, silver and copper containing aerosol particles will be very effective getters for elementary iodine, hydroiodic acid and organic iodides because of their large area and effective contact with the surrounding gas.

#### 4.7 Agglomeration of aerosol particles

As is well known, the particles in an aerosol will collide and agglomerate with each other because of their motion. This is caused by four basic mechanisms:

- Brownian motion
- Gravitational settling
- Turbulent gas motion
- Inertial gas motion

Brownian agglomeration is due to collisions caused by the random motion of particles imposed by collisions with gas molecules, Brownian motion. It is only important for particles of sub-micron size.

Gravitational agglomeration arises when slowly settling particles collide with and are captured by more rapidly settling particles. It is under certain circumstances, e.g. large particles in a slowly flowing situation, a dominant agglomeration process.

Turbulent agglomeration is a process where the collision frequency between particles is considerably increased by the turbulent motion of the gas carrying the particles. It is important for large particles and when there are small eddies of the gas (fluid) motion.

Inertial agglomeration arises because of differences in density between the particles and the gas. Particles of different sizes will therefore respond differently to acceleration/retardation forces which will lead to an increased collision frequency. This is especially important in pipe bends and valves.

The models for aerosol agglomeration are based on experiments, correlations and classical physics. Extensive literature is available in for example references /1/, /2/, /3/, /4/ and /7/.

It is known from experiments that not all collisions between particles will leave them stuck together. In fact bouncing has been observed, especially between particles of substances with different surface wetting properties /3/. However, to simplify the calculations a sticking probability of unity is assumed in all codes studied. This can to some extent be compensated for by the selection of a suitable shape factor for the aerosol particles, differing from the factor that might be computed from the geometrical shape of the particles. However, complete compensation can only be achieved at a single value of temperature, turbulence etc, as the sticking probability varies with the relative collision velocity. In nuclear accidents it is probable that the sticking probability will change with time due to water uptake by initially dry aerosol particles,

and a time dependent shape factor might be needed.

It can be expected that the condensation of vapor will result in very small particles, less than 1 micron. These primary particles will grow in size due to agglomeration, which is a particle growth mechanism decreasing the number concentration of particles in a gas, but not the mass concentration.

Formation of inactive aerosols or addition of inactive material to suspended radioactive aerosols increases the removal rate of the active material. Addition of fresh aerosol increases agglomeration rate and suspended aerosol mass. The condensation of inactive material on preexisting aerosol particles increases their mass and removal rate. Hence, the release of condensing inactive material to the gas phase thus "washes" out any active aerosol material from the gas. This is especially effective when the addition of inactive material occurs over an extended time period.

Saturated or near saturated steam can in this context be considered as an inactive material. When steam condensation occurs and the relative humidity is near 100%, it is more probable that the steam will condense onto the existing aerosol particles rather than by selfnucleation and fog formation. This effect is further enhanced if the aerosol particles contain water soluble substances, see 4.5 above. Condensation of steam onto an aerosol leads not only to an increase in mass but also to a contraction of the aerosol agglomerates to spherical shape due to the surface tension of water. This will decrease the shape factors. Both mass addition and shape factor decrease will cooperate to enhance settling.

The hygroscopic behavior of most aerosol materials appearing during a severe accident makes it important to compute the steam saturation accurately at all times as small variations in steam saturation have large effects on aerosol growth. At present this is not possible with the available thermal hydraulic modeling.

Occurrence of dense aerosols in the primary system can influence the gross vapor phase density and hence change density gradients and streaming patterns. In such cases the aerosol moves as a cloud. Somewhat similar phenomena are utilized in the mining industry where minerals heavier than water float in water containing a high proportion of suspended solids. Such effects are very little investigated in nuclear accident analysis and may need further attention.

Finally, turbulence and gas jet formation can both lead to formation and removal of aerosols by inertial impaction, resuspension of deposited material, disintegration of agglomerated aerosol particles and gas velocity driven film transport along surfaces. Such phenomena are probably of importance for aerosol behavior in pipes, pipe bends, narrow openings and valves, especially at high flow rates. Several of these phenomena were observed in the LACE pretests and tests.

#### 4.8 Condensation and reactions on surfaces in the reactor cooling system

Part of the material released from the hot core will condense on the stainless steel surfaces of the pressure vessel. In addition to physical condensation, chemical reactions between the fission products and stainless steel may be important. Thus cesium hydroxide has been shown to be enriched in the oxide scales on stainless steel, probably in the form of silicate. Tellurium is known to penetrate the oxide on stainless steel and dissolve in the metal. These effects may cause some fission products to be retained in the RCS also after melt-through. Fission products in particulate form may also react on the steel surface, especially if they are molten.

#### 4.9 Reevaporation

The formation of large radioactive deposits on surfaces, as observed in the Marviken V and LACE tests, can lead to local heating of the deposit and also of the supporting surface. The increasing temperature will sooner or later lead to a beginning evaporation of the more volatile parts of the deposited material. If the deposit contains e.g. cesium hydroxide and cesium iodide, the cesium hydroxide will evaporate more rapidly than the cesium iodide. This changes the composition of the deposit with time and the vapor produced is enriched with respect to cesium hydroxide.

Reevaporation processes are probably most important for thick deposits in the primary system and in pipes. It is most likely unimportant when the deposit contains a large mass of water as steam production will keep the temperature down until much of the decay heat is gone. However, shallow pools of water may evaporate quickly enough to leave a residue still able to generate the heat needed to cause reevaporation of volatile fission products.

The major impact of reevaporation is in such scenarios where the reevaporation has led to the presence of a considerable amount of hot fission product gas at the time when containment venting occurs. The escape of the hot gas from the primary system into the cooler containment atmosphere will lead to instantaneous production of a fine aerosol.

#### 4.10 Resuspension

Resuspension can occur from solid or liquid deposits. A prerequisite for a large resuspension is a high gas velocity over the deposit.

The presence of hygroscopic materials and a steam atmosphere will give most solid aerosol deposits a sticky appearance. Such deposits can not easily be resuspended.

Liquid deposits can form surface waves where the crests blow off forming a fairly coarse aerosol. If such liquid aerosol enters a hotter region, the drop size will decrease due to evaporation of

water. Formation of a coarse aerosol by resuspension of liquid films at high gas flow rates in tubes were observed in the LACE pretests.

Some reentrainment may also occur during fast dryout of small puddles of water after depressurization of the containment.

#### 4.11 Fission product release from melt - concrete reaction

When the molten core material comes in contact with concrete, the concrete will decompose thermally, it will also react chemically with the melt.

The thermal decomposition of concrete will release steam, carbon dioxide and refractory oxides e.g. CaO and SiO<sub>2</sub>. In addition sulfur dioxide, SO<sub>2</sub>, and potassium hydroxide, KOH, may be released. The gaseous decomposition products will partly bubble through the melt pool and may react chemically with the melt on their way. Steam would liberate hydrogen while carbon dioxide would be converted to carbon monoxide and elementary carbon. As the gas bubbles break at the surface of the molten pool, droplets will be generated that will contribute to the total suspended radioactive material in the containment. Carbon dioxide and sulfur dioxides will influence the chemistry in the containment by their acidity while calcium oxide will tend to increase the pH in containment water.

The melt may also attack the concrete chemically. The oxidic melt will probably dissolve the components of concrete to some extent with the possible formation of silicates. The metallic part will on the other hand tend to reduce some components in the concrete, e.g. sulfate may be reduced to sulfide and potassium hydroxide may be reduced to potassium metal. It is also conceivable that SiO<sub>2</sub> will be reduced to elemental silicon. The melt - concrete interaction thus leads to direct release of fission products from the melt. The chemistry of the melt will change due to the melt - concrete interaction. The metallic part of the melt will oxidize further due to water vapor and reducible compounds in the concrete. The oxidic part of the melt will also change its composition due to reactions with concrete before it solidifies. The melt - concrete reaction will however also influence the fate of fission products more indirectly due to the release of substances that alter the chemistry in the containment.

#### 4.12 Acid-base balance (pH) in the containment

The pH in the aqueous phase in the containment is important to iodine chemistry. Compounds that influence the pH in the aqueous phase include some of the fission products themselves e.g. cesium hydroxide. However, the fission products make up only a small fraction of all material that will be released to the containment. This means that the acid - base properties on non-radioactive aerosols and gases must be considered. The origin and properties of some compounds that may influence pH in the containment pool are mentioned below.

#### Carbon dioxide:

Generated in several ways i.e. by combustion of organic matter and by thermal decomposition of carbonate containing concrete. Boron carbide may also be a potential source of carbon dioxide. Depending on the steam/hydrogen ratio part of the carbon present will instead form CO. Carbonic acid forms when carbon dioxide dissolves in water. The apparent acidity constant is about  $10^{-7}$  M.

#### Boron, boranes and boron oxide:

Much boron is present in the control blades in a BWR in the form of  $B_4C$  and early in the fuel cycle of a PWR as lithium borate dissolved in the primary coolant. The boron carbide is encapsulated in stainless steel. As the steel alloys with the boron carbide and melts some of the boron carbide may become exposed to steam. The reaction will produce boron oxide and hydrogen. The extent of this reaction is difficult to predict, partly because of the lack of experimental data on the boron carbide - water reaction and partly because it is hard to tell for how long bare boron carbide will be exposed before it alloys and melts, disintegrates or form part of the core melt. When the control blades become engulfed in the melt the hydrogen evolution from them will be greatly reduced. The reaction rate of boron carbide is expected to be great at temperatures around and above the boiling point of  $B_2O_3$  ( $2124^\circ C$ ). Boron oxide will be converted to boric acid in the aqueous phase ( $pK_a=9$ ) or to oligomers with slightly lower  $pK_a$  if the concentration is high. Melting experiments with boron carbide - stainless steel - simulated fuel have shown that reducing conditions lead to the formation of a large number of boron compounds ( $>100$ ), but little boron oxide and boric acid. However, these compounds will convert to boric acid with time.

#### Sulfur, sulfides and sulfur oxides:

The sulfur oxides of interest are sulfur dioxide ( $SO_2$ ) and sulfur trioxide ( $SO_3$ ). Concrete based on Portland cement may contain up to 1% by weight of sulfate. During thermal decomposition above about  $800^\circ C$  this sulfur will be released, at least partly, and mainly in the form of sulfur dioxide. Reducing conditions would instead tend to give hydrogen sulfide ( $H_2S$ ), sulfide or sulfur. The sulfur oxides form acids of greater strength than the ones mentioned above and may influence pH.

#### Oxides of nitrogen, ammonia:

If there is any oxygen present in the containment together with nitrogen, the radiation field would probably give rise to  $NO_x$  which in turn forms nitrous or nitric acid in water. The containment pool water with large amounts of suspended particles with elements in low oxidation states would be expected to react with these oxidizing acids to liberate  $NO$ ,  $N_2O$  and  $N_2$ . If the reducing milieu is alkaline the reduction may proceed all the way to ammonia. This may e.g. occur on wet zinc plated surfaces. Ammonia dissolves in water to form ammonium hydroxide, a moderately strong base ( $pK_b=5$ ).

#### Silicon and silicon dioxide:

Silicon dioxide ( $SiO_2$ ) will be released in aerosol form during the core - concrete reaction. It will not by itself influence the pH in

the aqueous phase but may neutralize basic compounds at high temperatures e.g. CsOH. Very strong reducing conditions may form elementary silicon instead.

Hydrogen chloride:

Hydrogen chloride (hydrochloric acid, HCl) is formed during pyrolysis of chlorine containing rubbers and plastics e.g. lipalon used as insulator in electric cables contains both chlorine and sulfur. Hydrochloric acid is a very strong acid. It will contribute considerably to containment pool acidity and may in addition react in the gas phase e.g. with cesium hydroxide or with cesium iodide, liberating hydrogen iodide. It is very corrosive.

Cesium hydroxide:

Cesium hydroxide will be the dominant cesium species at least during the early stages of vaporization from the hot core. The possibly important reaction with boron oxide in the vessel may convert much of it into borate before melt-through. Cesium hydroxide has also a number of possible reaction partners in the containment. Thus carbon dioxide will form hydrogen carbonate or carbonate, silicon dioxide may form silicate and hydrochloric acid will form chloride.

Calcium oxide:

Calcium oxide is released in particulate form during core - concrete reaction. It may react with acid compounds in the gas phase (e.g. boron oxide, carbon dioxide, sulfur oxides, hydrogen sulfide, hydrochloric acid). It also reacts with water forming the hydroxide which will tend to increase pH in the pool water.

Potassium hydroxide:

Potassium hydroxide (KOH) may be evolved from the heated concrete. Its properties are similar to those of cesium hydroxide. Natural potassium is slightly radioactive (contains a small amount of the longlived isotope K-40).

It seems probable that the balance between acidic and basic substances in the containment would tend towards the acidic side, at least if boron carbide or boron containing melts are oxidized to a large extent. This means that the containment pool water probably will be acidic sooner or later with important consequences for iodine behavior.

#### 4.13 Speciation of iodine in the primary system

Iodine is one of the most easily evaporating elements in a core melt-down sequence. When the temperature is starting to increase, noble gases, iodine and cesium are considered as those elements which would leave the fuel elements first. The chemical form of iodine in the fuel elements before release would be partly as gaseous  $I_2$  but to a greater extent CsI. This is based on the fact that both cesium and iodine are produced to a relatively high extent with a Cs/I ratio of 10. In a humid atmosphere, thermodynamic calculations show that the completely dominating iodine specie is CsI. Even if other forms may exist temporary within the fuel, the reac-

tion rates occurring at the initial phases of a core melt down sequence are so fast that one can assume that iodine after release is present exclusively as CsI. This fact has also been demonstrated in several laboratory studies and in large scale experiments like LOFT and MARVIKEN. Data from LOFT and TMI-2 indicate a slightly smaller release factor for Cs than for I, but this does not influence the picture of CsI being the dominating iodine specie.

#### 4.13.1 Possible iodine chemical forms following an accident.

In a reducing atmosphere containing  $N_2$ ,  $H_2O$  and  $H_2$  as dominating gases in the primary system we may consider five different iodine species as possible /1/, thus excluding the oxidized forms  $HIO$ ,  $HIO_2$  and  $HIO_3$ . These five compounds are characterized in Table 4.13.1 with respect to the possible phases in which they could be accommodated.

Table 4.13.1 Iodine chemical forms under reducing conditions

Specie	Phase considered
CsI or $I^-$	Gas, aerosol, solution, surfaces, deposited aerosol
$I_2$	Gas, solution
HI	Gas, solution
$CH_3I$	Gas, solution
AgI	Aerosol, surfaces, deposited aerosol, precipitate

If liquid water is present, CsI and HI would be dissolved, while  $I_2$  and  $CH_3I$  would be present mainly in the gaseous phase. When no water is present, and at elevated temperatures, CsI and AgI may be transported as aerosols and deposited on surfaces, while  $I_2$ , HI and  $CH_3I$  will be transported and possibly released as gases. The gas/liquid partitioning,  $P = C(aq)/C(g)$ , for  $I_2$  and  $CH_3I$  is given as /2/:

$$^{10}\log(P(I_2)) = 6.29 - 0.0149T$$

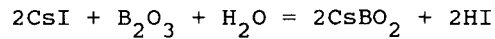
$$^{10}\log(P(CH_3I)) = -4.82 + 1597/T, \text{ where } T \text{ is in K.}$$

The possible formation of species other than CsI within the primary system will be discussed and evaluated in the following paragraphs.

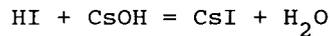
#### 4.13.2 Formation of hydrogen iodide

When the released fission products are transported between different compartments of the primary system the atomic ratio Cs/I may be changed by selective retention of specifically stable Cs compounds. One very important factor is the possible formation of  $B_2O_3$ , and to what extent  $B_2O_3$  could be formed from  $B_4C$  under conditions<sup>3</sup> possible in a core melt down sequence. The reaction between CsI and  $B_2O_3$  has been demonstrated in different laboratory investigations<sup>2,3</sup> and especially studies at Winfrith /3/ have shown that the following

reaction is going:



HI will be destroyed if it again meets active Cs, e.g. in the form of CsOH:



HI will also be retained by liquid water, and if silver ions are present in solution the iodine will be precipitated and retained as AgI.

The conclusion is that it is very important to model the formation of  $\text{B}_2\text{O}_3$  in a correct manner, since the formation of this compound in large amounts would change the transport mechanism of iodine completely within the primary system.

#### 4.13.3 Radiolytic reactions in the primary system.

At a core melt down sequence the strong radiation field that occurs within the primary system will break all kinds of chemical bonds. The resulting fragments are often radicals that reacts readily among themselves or with other molecules in the system. In principle, the radiation field will help the chemical system to come to chemical equilibrium, that means that if CsI is decomposed radiolytically the most probable pathway is that CsI is reformed. Of course, metastable compounds as  $\text{I}_2$  or  $\text{CH}_3\text{I}$  may form by radiolytic processes, but if they have a relatively long residence time in the radiation field, they would also be decomposed radiolytically and CsI would be the most probable product. However, if the transport out from the strong radiation field is fast, then one must consider a fraction of the total iodine present as  $\text{I}_2$  or as  $\text{CH}_3\text{I}$  if there is any source of carbon available.

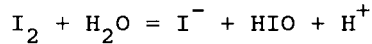
In conclusion, the radiolytic activity tends to keep the chemical system at equilibrium, but under transient conditions one must take into account the formation of other species than CsI in the primary system. The fraction of CsI that is transformed is difficult to estimate, but could be modeled as 5% of the total iodine as  $\text{I}_2$  and/or  $\text{CH}_3\text{I}$ . The formation of HI as a radiolytic product is also possible, but could due to this mechanism only affect the iodine transport in the primary system in a marginal way.

#### 4.14 Speciation of iodine in the aqueous phase

The aqueous chemistry of iodine was penetrated in great detail at the second CSNI workshop on iodine chemistry in reactor safety, Toronto, 1988, June 2-3. The proceedings were published in March 1989 /4/.

The main difference when the fission products leave the primary system out into the containment building or to some scrubber system,

is that liquid water is available in large amounts. For iodine, it is thus important to understand and describe the hydrolytic reactions. Under oxidizing conditions it will now be possible to form  $\text{IO}^-$ ,  $\text{IO}_2^-$  and  $\text{IO}_3^-$  from gaseous  $\text{I}_2$ . This means that  $\text{CsI}$ , the most probable iodine specie,  $\text{HI}$  and  $\text{I}_2$  will be retained in the water pool or in a scrubber system.  $\text{I}_2$  will be retained through its hydrolysis according to



This reaction is strongly dependent on the pH value of the solution.

Hydrogen iodide is easily dissolved in liquid water and its vapor pressure above water is drastically reduced, more than four orders of magnitude at  $25^\circ\text{C}$ , compared to that of pure hydrogen iodide in the absence of water.

From these introductory remarks, it is evident that the partitioning factor,  $P$ , is of great importance for the possibilities to retain most of the iodine in the reactor containment building. The formation of  $\text{CH}_3\text{I}$  is also crucial, since this is the only form that is not easily dissolved or hydrolysed in the water phase.

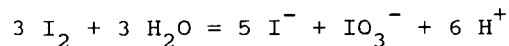
#### 4.14.1 Transport of iodine from the primary system to the containment

An excess of  $\text{CsOH}$  is predicted in the primary system for almost all accident sequences. This makes it highly probable that transport of iodine from the primary system to the containment generally is in the form of  $\text{CsI}$ .

#### 4.14.2 Hydrolysis of $\text{I}_2$

The fate of elementary iodine in the containment is strongly dependent on acidity and on the prevailing redox conditions. It is dominated by the aqueous chemistry of iodine and iodine compounds.

The solubility of elementary iodine in pure water is known to increase with temperature by an order of magnitude in the range  $0 - 110^\circ\text{C}$  /9/. The dissolved iodine disproportionates slowly in water according to the gross reaction



The rate of reaction depends on temperature. As mentioned above, hypoiodous acid,  $\text{HIO}$ , is an intermediate which, however, never occurs in large concentrations. The gross reaction equation shows that the equilibrium is shifted towards iodide and iodate at high pH and towards iodine at low pH. Furthermore, reducing conditions will convert iodate back to iodine, hence giving iodide as the main end product, whereas strongly oxidizing conditions will result in the formation of iodate as the end product.

#### 4.14.3 Formation of CH<sub>3</sub>I

Methyl iodide is not a thermodynamically favoured substance in the conditions prevailing during a severe accident and its formation is thus only a transient phenomena. The detailed mechanism for formation of methyl iodide under the conditions expected during severe accidents is not completely known. However, it is clear that radiation plays an important role and that methane is an important source material. The formation of methyl iodide is predominantly in the aqueous phase /10/. However, it has even been postulated that methyl iodide can be formed from iodine and inorganic carbon, e.g. carbonate, in an intense radiation field in order to explain the result from some early experiments. It has been found that the presence of some organic materials leads to an increased formation of methyl iodide by ionizing radiation /10/. Most of the present estimates of methyl iodide formation are in the region 0.03 - 1% of the total amount of iodine present.

#### 4.14.4 Conditions under which iodine may be released to the environment

A substantial concentrated release of iodine to the environment can only be expected when several phenomena coincide in time, which seems rather unlikely. First of all, a substantial part of the iodine must be present in the gas phase either as aerosol or as vapor when a containment break occur. A large amount of iodine bearing aerosol, e.g. CsI, is most probable in the rather early stages of the accident and hence the containment break must occur early. Oxidizing conditions together with acidic water pools in the containment could also lead to a certain amount of elementary iodine as vapor in the containment atmosphere during a limited time. The containment must then be open to the environment at the same time.

It is more likely that a very limited slow release of iodine may occur over a length of time, as observed during the TMI accident.

The presence of filtered venting systems containing a water solution designed to capture iodine compounds should reduce the risk for any substantial release of radioactive iodine to the environment to a very small level.

#### 4.15 References

- /1/ C. N. Davies (Ed.), Aerosol Science, Academic Press (1966).
- /2/ S. K. Fridlander, Smoke, Dust and Haze, Wiley & Sons, New York 1977.
- /3/ N. A. Fuchs, The Mechanics of Aerosols, Pergamon Press 1964.
- /4/ G. M. Hidy, J. R. Brock, Topics in Aerosol Research, Vol. I, II, and III, Pergamon Press, New York 1971 - 1973.

- /5/ W. C. Hinds, *Aerosol Technology; Properties, Behavior, and Measurement of Airborne Particles*, Wiley 1982.
- /6/ J. Jokiniemi, *The Growth of Hygroscopic Particles during Severe Core Melt Accidents*, *Nucl. Technol.*, 83 (1988) 16.
- /7/ J. R. Pruppacher, J. D. Klett, *Microphysics of Clouds and Precipitation*, Reidel, New York 1978.
- /8/ C. F. Knights, *The Caesium Hydroxide - Water System*, LACE TR-037.
- /9/ H. Stephen, T. Stephen, Eds, *Solubilities of Inorganic and Organic Compounds, Vol 1, Binary systems*, Pergamon Press 1963.
- /10/ E. C. Beam, Y.-M. Wang, S. J. Wisbey, W. E. Shockley, *Organic Iodide Formation During Severe Accidents in Light Water Nuclear Reactors*, *Nuclear Technology*, 78 (1987) 34.



## 5 THE MODELING OF CHEMICAL BEHAVIOR IN ACCIDENT ANALYSIS CODES

It is well known that chemical interaction of released fission products, control materials, structural materials and steam can influence the physical properties of important radionuclides and hence influence the size of the source term resulting from a severe nuclear accident.

The small release of iodine compounds to the environment during the accident at TMI emphasized this and gave rise to discussions and to development concerning the importance of chemistry for the size of the source term.

The importance of chemistry has been increasingly recognised since TMI and it is now clear that also computer code modeling of the chemical behavior of the released elements as a function of time during a severe reactor accident must be a part of severe reactor accident analyses.

The code development has - when it comes to chemistry - especially concentrated on 4 areas of importance:

1. Release from reactor fuel and structural materials.
2. Chemical reactions in the primary system.
3. Core concrete interaction.
4. Chemical reactions in the containment.

The objectives of the developed codes are different. Some codes are developed for risk assessment studies while others are special codes developed for more detailed studies e.g. chemical analysis.

A survey (not complete) of the existing computer codes and the associated modeling dealing with chemical behavior important radionuclides during severe reactor accidents is given in this chapter of the report.

### 5.1 Release from fuel and structural materials

The release of fission products from reactor fuel and the release of structural materials are modeled in a number of computer codes.

The following codes will be described shortly: GRASS codes, VICTORIA, CORSOR and FAEREL.

#### 5.1.1 GRASS codes

The GRASS codes (GRASS-SST, PARAGRASS, FASTGRASS, FASTGRASS-VFP) have been developed at Argonne National Laboratory.

The GRASS codes are mechanistic codes developed for predicting the behavior of fission gas and volatile fission products in  $UO_2$  fuel during steady-state and transient conditions.

The phenomena modeled in the GRASS codes depend primarily on the formation and interaction of fission gas bubbles with fuel. This affects fuel morphology and leads to transport of fission product bubbles through the altered fuel and finally to fission product release.

The level of detail in the modeling is very high. The treatment is probably the most mechanistic of all existing codes. This level of detail causes the element set in the codes to be limited. Noble gases, Cs, I, Te, Ba and Sr are handled at present.

The chemical modeling in the GRASS codes are limited. It is possible to perform a chemical equilibrium calculation with the PARA-GRASS/FASTGRASS-VFP/FASTGRASS codes but on a limited species set.

The latest version of FASTGRASS /1/ handles the chemical interactions between I, Cs, Ba, Sr and the fuel matrix.

Comparisons between FASTGRASS predictions of fission product release and experiments are in good agreement.

FASTGRASS analyses /1/ underline 4 conclusions about fission product behavior and release during severe fuel damage conditions:

1. Fission product behavior in solid fuel is strongly dependent on fuel microstructure and irradiation history as well as fuel temperatures.
2. Fission product behavior is strongly dependent on fission product/fuel chemistry. Cs, Ba and Sr for example become sequestered within the  $UO_2$  as oxides, uranates or molybdates.
3. Fuel liquefaction/dissolution, fracturing, oxidation and relocation strongly affects fission product behavior during severe fuel damage types of accidents.
4. The FASTGRASS predictions are in good agreement with data from recent release experiments.

The fission product release models in the GRASS family of codes are included in the SCDAP /2/ reactor analysis code developed at EG&G Idaho.

#### 5.1.2 VICTORIA

VICTORIA /3//4/ is a computer code modeling fission product behavior in the reactor coolant system of a LWR reactor during a severe accident.

The VICTORIA work was initiated at Sandia National Laboratories.

VICTORIA was originally planned as a sub-module of the MELPROG/TRAC /2/ computer code.

The MELPROG/TRAC code was developed at Sandia National Laboratories for the Nuclear Regulatory Commission to obtain more accurate estimates of the in-vessel source term. The code is a detailed mechanistic system code which analyzes severe accident progression in the reactor coolant system of a nuclear power plant.

The effect of chemistry on fission product release is primarily a consideration of the effect of chemical speciation on mass transport within the fuel region.

Mass transport is largely controlled by concentration gradients. Chemical reactions of fission products and clad material can change the concentration of the migrating species and hence change the transport and release of these species.

Therefore it is necessary to determine the speciation of fission products within the fuel in order to calculate transport and release properly.

The fission product release/transport models in VICTORIA take this into account by treating fuel grains, open porosity, the fuel/clad gap and the bulk coolant as ideal solutions and performing equilibrium chemistry calculations by minimizing the free energy in each of these regions.

Currently only fuel release models for intact and disrupted fuel are working in VICTORIA. Release from rubble beds, liquifying rods, melting debris, molten fuel pools and release under quenching and/or oxidation conditions are goals for future developments of VICTORIA.

Comparisons of release rates calculated with VICTORIA and observed release rates in the ST-2 experiment performed in the ACRR reactor at Sandia show a fairly good agreement. Fig. 5.1 show the experimental results /5/ for Cs and the release rates calculated with VICTORIA and with CORSOR-M.

### 5.1.3 CORSOR (STCP)

The fission product release model in the NRC Source Term Code Package (STCP) /6/ is called CORSOR or CORSOR-M. The SCTP is a group of 4 codes (MARCH 3.0, VANESA, TRAP-MELT3 and NAUA/SPARC/ICEDF).

The methodology in CORSOR treats fission product release as a phenomenon that is dependent only on temperature. The model is empirical and based on 3 sets of experiments 2 sets from Oak Ridge National Laboratory and 1 set from KfK in Karlsruhe.

The CORSOR/CORSOR-M model are used in several of the integrated suit of codes such as the SCTP, the EPRI code CORMLT and the MELCOR code developed by NRC.

Fuel chemistry is not treated in any of the CORSOR-based release models.

In general CORSOR calculations have been overestimating the release of fission products during severe accidents conditions compared to experiments. See e.g. fig. 5.1.

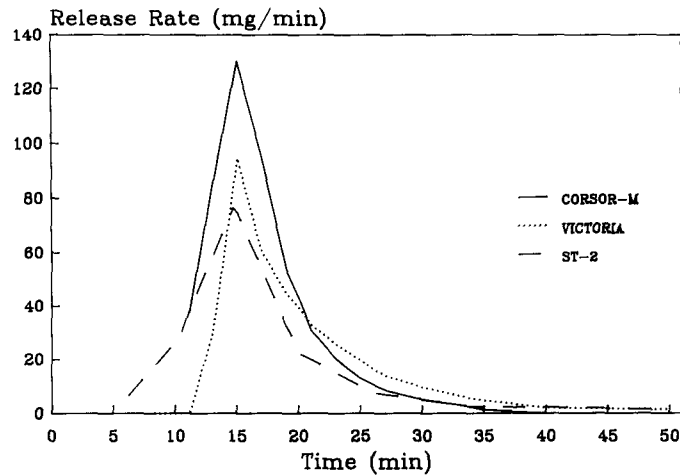


Figure 5.1. Comparison of calculated (CORSOR-M/VICTORIA) and observed absolute release rates as a function of time for cesium release in the ST-2 experiment.

#### 5.1.4 FAEREL

The FAEREL (Fission Product and Aerosol Release) code has been developed in the UK /7/. The code is mechanistic and incorporates models for vaporisation and gas phase mass transport of fission products and fuel, control and structural materials to calculate release rates from severely overheated reactor cores. Further FAEREL includes a limited treatment of the chemistry of the released species.

The code has primarily been used to study the effect of gas phase mass transport limitations on the size of the releases of control and structural materials.

The predicted FAEREL releases /7/ are generally lower than similar results predicted with e.g. CORSOR.

It is seen also from the FAEREL analyses, that chemical interaction can influence the size of the released masses of non radioactive aerosols.

## 5.2 Chemical reactions within the primary system

Many computer codes /8/ treat chemical phenomena as a part of the analysis of what happens in the primary system of a LWR reactor during a severe accident.

The modeling of chemical phenomena differs a lot from one code to another. Typically the integrated codes - used for risk assesment studies - like MAAP, STCP /6/ or MELCOR /4/ use simple chemical models, while a few special codes used for detailed analysis of in-vessel phenomena during a core melt accident use much more detailed modeling.

Three of the more detailed codes (VICTORIA, RAFT and HORN) will be shortly described.

### 5.2.1 VICTORIA

The VICTORIA code /4//8//9/ and the ongoing development of the code is very detailed and ambitious.

Models within the following areas of importance for the behavior of released material within the reactor coolant system are implemented in the code or are under consideration:

Table 5.1 Chemical species treated within VICTORIA

BaO(g)	SrI <sub>2</sub> (c)	TeO(g)	FeTe(c)
BaO(c)	Sr(g)	TeO <sub>2</sub> (g)	FeTe <sub>2</sub> (c)
BaI(g)	Sr(c)	TeO <sub>2</sub> (c)	Mo(c)
BaI <sub>2</sub> (g)	SrUO <sub>4</sub> (c)	Te <sub>2</sub> O <sub>2</sub>	Mo(g)
BaI <sub>2</sub> (c)	SrZrO <sub>3</sub> (c)	H <sub>2</sub> Te(g)	MoO(g)
Ba(g)	SrMoO <sub>4</sub> (c)	UO <sub>2</sub> (c)	MoO <sub>2</sub> (c)
Ba(c)	ZrO(g)	UO <sub>2</sub> (g)	MoO <sub>2</sub> (g)
BaTe(c)	ZrO <sub>2</sub> (g)	U(c)	MoO <sub>3</sub> (c)
BaTe(g)	ZrO <sub>2</sub> (c)	U(g)	MoO <sub>3</sub> (g)
BaZrO <sub>3</sub> (c)	Zr(g)	U <sub>4</sub> O <sub>9</sub>	

### Transport and Deposition

1. Non-radioactive Sources
2. Aerosol Physics
3. Vapor - Surface Interactions
4. Vapor - Aerosol Interactions

Table 5.2 Chemical species treated within VICTORIA

---

CsI(c)	BaUO <sub>4</sub> (c)	Zr(c)	U <sub>3</sub> O <sub>8</sub> (c)
CsI(g)	BaMoO <sub>4</sub> (c)	Sn(c)	UO <sub>3</sub> (c)
CsOH(c)	I(g)	Sn(g)	Kr(g)
CsOH(g)	I <sub>2</sub> (g)	SnO(g)	Xe(g)
Cs(g)	HI(g)	SnO(c)	O <sub>2</sub> (g)
Cs <sub>2</sub> O(g)	H(g)	SnO <sub>2</sub> (c)	O(g)
Cs <sub>2</sub> (OH) <sub>2</sub> (g)	H <sub>2</sub> (g)	SnO <sub>2</sub> (g)	Fe(c)
Cs(c)	H <sub>2</sub> O(g)	SnI <sub>2</sub> (g)	Fe(g)
Cs <sub>2</sub> O(c)	SrOH(g)	SnI <sub>2</sub> (c)	FeO(c)
Cs <sub>2</sub> UO <sub>4</sub> (c)	Sr(OH) <sub>2</sub> (c)	SnTe(g)	FeO(g)
Cs <sub>2</sub> U <sub>2</sub> O <sub>7</sub> (c)	Sr(OH) <sub>2</sub> (g)	SnTe(c)	Fe <sub>2</sub> O <sub>3</sub> (c)
Cs <sub>2</sub> MoO <sub>4</sub> (c)	SrO(c)	SnH <sub>4</sub> (g)	Fe <sub>3</sub> O <sub>4</sub> (c)
BaOH(g)	SrO(g)	Te(g)	FeI <sub>2</sub> (c)
Ba(OH) <sub>2</sub> (g)	SrI(g)	Te(c)	FeI <sub>2</sub> (g)
Ba(OH) <sub>2</sub> (c)	SrI <sub>2</sub> (g)	Te <sub>2</sub> (g)	Fe <sub>2</sub> I <sub>4</sub> (g)

---

### Revaporization

1. Evolution of Chemical Forms
2. Re-Entrainment

VICTORIA handles 14 different elements or more and approximately 100 different species as can be seen from tables 5.1 and 5.2. Chemical reactions are treated by assuming that all reactions reach equilibrium.

The calculations done in VICTORIA at each time step can be summarized as follows:

1. Interface with the thermal-hydraulic calculations or data.
2. Calculation of chemical compositions in the fuel region (grains, open porosity, gap/clad region), in the gas regions and on structure surfaces.
3. Calculation of aerosol growth in the gas regions due to condensation/evaporation and nucleation.
4. Calculation of fission product transport in the fuel regions.
5. Calculation of transport of the gaseous fission products between the gas cells and to and from surfaces.
6. Calculation of aerosol agglomeration and surface deposition in each vessel cell. Calculation of aerosol transport between the gas cells.
7. Calculation of aerosol transport between the gas cells.
8. Calculation of radioactive decay heat sources in the fuel region, in the gas cells and on structure surfaces.

The development and testing of the models in VICTORIA is underway and a first releasable version of VICTORIA is planned to be released by the end of 1989. The code is being validated by comparison to a large number of experiments including release tests and transport tests. The following laboratories and organisations are involved in the development of the code: NRC, SNL (NRC), Winfrith (UKAEA), Chalk River (AECL), Argonne (NRC) and ORNL (NRC).

#### 5.2.2 RAFT (Reactor Aerosol Formation and Transport Code)

The RAFT code was developed at Argonne National Laboratory with support of the Electric Power Research Institute to analyze fission product behavior during severe core melt accidents in the reactor coolant system /10/.

This code calculates the concentration of gaseous species by minimizing the Gibbs free energy of the gas phase system, when the elemental (gaseous) concentration, system pressure and temperature are known.

Changes in elemental concentration result from vapor condensation in the gas phase or on boundary surfaces. For the high-temperature condensation process, the time constant of the gaseous reactions is assumed to be smaller than that of vapor condensation. This means that the gas phase species are essentially in a local chemical equilibrium but may be in non-equilibrium with respect to the condensed phase (nucleation). The rate of condensation is described by the dynamic equations that model the nucleation process (for

details of nucleation processes see AKTI-160 final report).

The transportation of aerosols (condensed phase) is then modeled by agglomeration and deposition processes. Re-evaporation of deposited vapor and aerosol particles is then modeled as a physical process. Changes in vapor pressures (activity coefficients) due to formation of solutions in the deposited material are not taken into account, but can easily be included in the model if their values are known. Also possible chemical reactions in the condensed phase are not taken into account.

The RAFT analyses carried out at VTT for the Loviisa power plant showed that at the nucleation front (the point where particle formation starts) the predominant chemical forms of cesium and iodine are always cesium hydroxide and cesium iodide.

Possible effects of boron were not taken into account.

The potential of condensed phase chemical reactions is not considered in RAFT and the chemical forms of cesium and iodine in aerosol particles were accordingly cesium hydroxide and cesium iodide.

Several sensitivity studies carried out with the RAFT code /11//12/ indicate that the final particle size after condensation depends linearly on the gas cooling rate during the condensation process, e.g. if the particle radius at a cooling rate of 1000 K/s is 0.1 micrometer, then at a cooling rate of 10 K/s it is 10.0 micrometer.

The final particle radius depends also on the chemical form of the nucleating species and on their partial and vapor pressures.

### 5.2.3 HORN

The HORN computer code /13/ has been developed to calculate the transport of volatile fission products in dry primary cooling circuits under severe reactor accidents conditions.

The most fundamental assumptions, restrictions and simplifications in the code are:

1. Flow path is composed of tube segments and tanks connected in series
2. Volatile fission products are minor components of the gas flowing in the path, and hence their behavior does not affect the bulk flow situation
3. Condensed water does not exist in the flow path
4. Chemical forms of fission products including the nucleation of particles are determined assuming an equilibrium composition

5. Heat and mass transfer processes to the wall are described as analogous diffusional processes across the boundary layer
6. Within each time step, steady flow conditions are assumed

The input data required for the code are inlet temperature, pressure distribution, wall temperatures, and flow rates of fission products and carrier gases.

The number of different chemical species handled in the HORN code are around 150 taking into account the following elements:

Fission Products: Kr, Sb, Te, I, Xe, Cs and Ba  
Structural materials: H, O, B, Ag and Cd  
A fictitious element: Fi

The fictitious element (Fi) represent all less-volatile fission products, actinides, and structural elements. Fi is neglected in the chemical equilibrium calculation but is taken into account in the calculations of aerosol transport and decay heat build-up in the circuit walls. Fi is assumed to behave as an aerosol in the reactor circuit.

When the code was developed in 1986 it was tested against transport experiments conducted in the LOFT facility. Further testing might have taken place since.

### 5.3 Core - concrete interaction

Melted fuel, which penetrates the reactor vessel during a core melt accident, will flow into the reactor cavity, and core-concrete interaction will take place.

The VANESA code /14/ predicts the release of radionuclides and the generation of aerosols associated with core-concrete interaction.

The chemistry handled in the code is complicated. The species recognized in the code are shown in table 5.3 to give an impression.

Comparisons of VANESA predictions with experiments show a good agreement.

Further VANESA predictions show protracted releases of Tellurium during nearly all accident sequences and higher releases of refractory radionuclides (Ba, Sr, La, Ce) during some accident sequences compared to earlier predictions. Primarily the VANESA analyses have shown that the core-concrete releases depend on the accident type and the plant in question.

The VANESA code also considers the effect of water pool attenuation. The calculations show, that 1 - 2 meters of water above the melt will attenuate the aerosol release by a factor of 2 - 50 depending on the specific core-concrete interaction.

Table 5.3 Species recognized in the VANESA code

ELEMENT	CONDENSED SPECIES	VAPOR PHASE SPECIES
H	---	H, H <sub>2</sub> , OH, H <sub>2</sub> O
C	C(gr)	CO, CO <sub>2</sub>
O	---	O, O <sub>2</sub>
Na	Na <sub>2</sub> O(l)	Na, NaOH, NaO, (NaOH) <sub>2</sub> , NaH, Na <sub>2</sub>
Al	Al <sub>2</sub> O <sub>3</sub> (l)	Al, AlO, Al <sub>2</sub> O, AlO <sub>2</sub> , Al <sub>2</sub> O <sub>2</sub> , AlOH, Al(OH) <sub>2</sub> , AlO(OH)
Si	SiO <sub>2</sub> (l)	Si, SiO, SiO <sub>2</sub> , SiOH, Si(OH) <sub>2</sub> , SiH, SiH <sub>4</sub> , Si <sub>2</sub>
K	K <sub>2</sub> O(l)	K, KOH, KO, (KOH) <sub>2</sub> , KH, K <sub>2</sub>
Ca	CaO(l)	Ca, CaO, CaOH, Ca(OH) <sub>2</sub> , CaH, Ca <sub>2</sub> COOH,
Cr	Cr(l), Cr <sub>2</sub> O <sub>3</sub> (l)	Cr, CrO, CrO <sub>2</sub> , CrO <sub>3</sub> , CrO <sub>2</sub> (OH) <sub>2</sub> , Cr(OH) <sub>2</sub>
Mn	Mn(l), MnO(l)	Mn, MnO, MnOH, Mn(OH) <sub>2</sub> , MnH
Fe	Fe(l), FeO(l)	Fe, FeO, FeOH, Fe(OH) <sub>2</sub>
Ni	Ni(l), NiO(l)	Ni, NiO, NiOH, Ni(OH) <sub>2</sub> , NiH
Sr	SrO(l)	Sr, SrO, SrOH, Sr(OH) <sub>2</sub> , SrH
Zr	Zr(l), ZrO <sub>2</sub> (l)	Zr, ZrO, ZrO <sub>2</sub> , ZrOH, Zr(OH) <sub>2</sub> , ZrH
Nb	NbO(l)	Nb, NbO, NbO <sub>2</sub> , NbOH, Nb(OH) <sub>2</sub>
Mo	Mo(l)	Mo, MoO, MoO <sub>2</sub> , MoO <sub>3</sub> , H <sub>2</sub> MoO <sub>4</sub> , (MoO <sub>3</sub> ) <sub>2</sub> , (MoO <sub>3</sub> ) <sub>3</sub> , Mo(OH) <sub>2</sub>
Ru	Ru(l)	Ru, RuO, RuO <sub>2</sub> , RuO <sub>3</sub> , RuO <sub>4</sub> , RuOH, Ru(OH) <sub>2</sub>
Ag	Ag(l)	Ag, AgO, AgOH, Ag(OH) <sub>2</sub> , Ag <sub>2</sub> , Ag <sub>3</sub> , AgH, AgTe
Sn	Sn(l)	Sn, SnO, SnOH, Sn(OH) <sub>2</sub> , SnH, SnH <sub>4</sub> , Sn <sub>2</sub> , SnTe
Sb	Sb(l)	Sb, SbO, SbOH, Sb(OH) <sub>2</sub> , Sb <sub>2</sub> , Sb <sub>4</sub> , SbH <sub>3</sub> , SbTe
Te	Te(l)	Te, TeO, TeOH, TeO(OH) <sub>2</sub> , Te <sub>2</sub> , TeO <sub>2</sub> , (TeO) <sub>2</sub> , H <sub>2</sub> Te
I	CsI(l)	CsI, I, HI, IO, I <sub>2</sub> , (CsI) <sub>2</sub>
Cs	Cs <sub>2</sub> O(l), CsI(l)	Cs, CsOH, CsO, Cs(OH) <sub>2</sub> , Cs <sub>2</sub> O, Cs <sub>2</sub> , CsO <sub>2</sub> , CsH
Ba	BaO(l)	Ba, BaO, BaOH, Ba(OH) <sub>2</sub> , BaH
La	La <sub>2</sub> O <sub>3</sub> (l)	La, LaO, LaOH, La(OH) <sub>2</sub> , La <sub>2</sub> O, (LaO) <sub>2</sub>
Ce	CeO <sub>2</sub> (l)	Ce, CeO, CeO <sub>2</sub> , CeOH, Ce(OH) <sub>2</sub>
U	UO <sub>2</sub> (l)	U, UO, UO <sub>2</sub> , UO <sub>3</sub> , UOH, U(OH) <sub>2</sub> , UO <sub>2</sub> (OH) <sub>2</sub>

The METOXA code /15/ is also dealing with releases of fission products during core-concrete interaction. The code is integrated with the MAAP code.

The release of fission products and structural materials is assumed to be governed by equilibrium of the metallic and oxidic core debris, concrete slag, and concrete off-gas.

Results indicate that significant fractions of fission products can be released during core-concrete interaction.

#### 5.4 Chemical reactions within the containment

A complicated chemical environment will exist in the containment of a nuclear reactor during a severe accident. A number of codes have been developed to predict the behavior of fission products or other important elements e.g. hydrogen.

Two codes will be described shortly here namely TRENDS /2//16/ and the hydrogen code HECTR /2/.

The TRENDS code treats especially iodine behavior in the containment after release from the reactor vessel. Iodine species modeled in the code are e.g. molecular iodine (in gas phase, liquid phase, aerosol form, or on surfaces), cesium iodide, hydrogen iodide etc.

The code predicts e.g. gaseous conversions between molecular iodine  $I_2$  and  $CH_3I$ , aqueous formation of silver iodide from iodide, molecular iodide and methyl iodide.

The final aim of the modeling of the iodine behavior within the containment is to predict a time-dependent accounting of iodine species released out into the environment.

The HECTR code analyses the hydrogen transport and combustion in the containment and the pressure and temperature response of the containment during a severe reactor accident.

Six gases - steam, nitrogen, oxygen, hydrogen, carbon monoxide and carbon dioxide - are modeled in the code.

The development of HECTR is still going on and so is the testing of the code against experiments.

#### 5.5 Integrated severe reactor accident codes

Several code systems e.g. MAAP, STCP, and MELCOR /4/ have been developed to analyse more or less complete accident sequences from the beginning of the accident until containment failure and the release of fission products out into the environment.

These code systems are all designed for risk assessment studies and they do not handle chemical problems in any detail.

This means that a reasonable procedure for reactor safety analyses dealing also with detailed chemical studies could be carried out with the risk assessment codes combined with special analyses done with e.g. the VICTORIA code.

#### 5.6 Concluding remarks

It is obvious from this chapter of the report, that the state of the art concerning modeling of chemical behavior in accident analyses codes during the last years has experienced a lot of development and

that modern codes seems to have made quite some progress. On the other it is obviously that the problem we are dealing with is so complex that a lot of development still has to come.

#### 5.7 References

- /1/ J. Rest, Kinetics of Fission Product Release Prior to Fuel Slumping, Argonne National Laboratory, Argonne, Illinois 60439, October 1987.
- /2/ Reactor Risk Reference Document, NUREG-1150, App. N, Vol.3, U.S. Nuclear Regulatory Commission, February 1987.
- /3/ A. J. Grimley, III, Chemistry Models in the Victoria Code, Sand87-2757c, Sandia National Laboratories, Albuquerque, NM, 87185-5800, December 1987.
- /4/ Transactions of the Seventh Water Reactor Safety Information Meeting, NUREG/CP-0104, Rockville, Maryland, October 23 - 25, 1989.
- /5/ M. D. Allen et al., ACRR Fission Product Release Tests: ST-1 and ST-2, Sandia National Laboratories, Albuquerque, NM, 87185-5800, October 1988.
- /6/ J. A. Giseke et al., Source Term Code Package, Users Guide, Mod 1, NUREG/CR-4587, BMI-2138, Batelle Columbus Division, 505 King Avenue, Columbus, OH 43201-2693, July 1986.
- /7/ P. N. Clough, H. C. Starkie and A. R. Taig, Mechanistic Modelling of Whole-Core Releases of Fission Products and Structural Materials from LWRs during Severe Accidents - The FAEREL Code, Safety and Reliability Directorate, SRD R 416, UKAEA, August 1987.
- /8/ A. J. Grimley, III, C. J. Wheatley and P. N. Clough, An Overview of In-vessel Release and Chemical Modelling in Severe Accident Analysis Codes, Toronto, Canada, June 1988.
- /9/ C. J. Wheatley, and A. J. Grimley, Development of Chemistry, Aerosol & Transport Models in VICTORIA, SFD Partners Meeting, April 25 - 29, 1988.
- /10/ K. H. Im et al., RAFT: A computer Model for Formation and Transport of Fission Product Aerosols in LWR Primary Systems, Aerosol Sci. and Tech., 4 (2) (1985) 125.
- /11/ K. H. Im et al., The RAFT Computer Code for Calculating Aerosol Formation and Transport in Severe LWR Accidents, EPRI Report NP-5287-CCM (1987).
- /12/ Ritzman et al., Recent Improvements and Applications of the RAFT Code, Proceedings of the workshop Water-Cooled Reactor Aerosol Code Evaluation and Uncertainty Assessment held in

Brussels (Belgium) from 9 to 11 September 1987 (1988).

- /13/ Masaaki Uchida and Hiroaki Saito, HORN, A Computer Code to analyse the Gas-Phase Transport of Fission Products in Reactor Cooling System under Severe Accidents, JAERI-M 86-158, November 1986.
- /14/ D. A. Powers and J. E. Brockmann, Radionuclide Release and Aerosol Generation during Core Debris Interactions with Concrete, Workshop on Chemical Processes and Products in Severe Reactor Accidents, Captiva Island, Florida, USA, December 9 - 12, 1987.
- /15/ M. G. Plys, M. A. Kenton and R. E. Henry, Ex-Vessel Fission Product Release Modelling within Integrated Accident Analysis, Proceedings of the Committee on the Safety of Nuclear Installations (CSNI) Specialists' Meeting on Core Debris-Concrete Interactions, EPRI NP-5054-SR, Special Report, February 1987.
- /16/ C. F. Weber, E. C. Beahm, T. S. Kress, S. R. Daish and W. E. Shockley, TRENDS, A Code for Modelling Iodine Behavior in Containment during Severe Accidents, ICHMT International Seminar on Heat and Mass Transfer Aspects of Fission Product Releases, May 22 - 26, 1989, Dubrovnik, Yugoslavia.



### 6.1 Overview

Chemistry cannot be considered alone when a model of the real nature is of interest. It is an integral part of reality and the results of chemical reactions is to a large degree dependent on temperature, pressure and of the transport of reactants and products and thus of which compounds are in molecular or atomic contact.

The set of T,P and amounts of initial compounds is called a chemical system. The formation of chemical systems have to be modeled with the same accuracy as chemical reactions. The formation of such systems is to a large degree dependent on non-chemical factors which, nevertheless, have a large influence on which chemical reactions actually occur. Thus it is necessary to ensure that the formation of chemical systems is understood and accurately modeled.

In order to illustrate the problem of chemical system formation and breakdown, a short discussion of the scientific method versus uncontrolled reality is given below.

The success of science during the last centuries is mainly due to carefully designed experiments, where boundary conditions are deliberately constructed in a very limited part of the universe, with as few uncontrollable phenomena as possible. A fairly smooth change is then expected to follow, and some aspect(s) of reality is (are) measured. The scientific systems are thus man made and well defined.

For our problem of modeling the chemical contribution to the effects of an uncovered core, we do not deliberately choose suitable boundary conditions, and the number of possible influential phenomena are not limited by us.

The problem we have to face is rather the reverse of the experimental ideal: the system of interest (the reactor during a transient) essentially reconstructs itself (in a not man-made way) so we do not know the successive states of the reactor. Furthermore, we do not aim at measuring the state of the reactor, but have to utilize already existing data to predict the successive states of the reactor during the sequence (and hope that all necessary data are available).

An additional problem is the specialization of science. In order to properly understand and model a transient, we have to bridge the gap between the disciplines, since the uncontrolled nature does not bother about man made divisions of reality. We also have to provide a model for the creation of subsystems (where interaction takes place) as a result of the phenomena in the reactor as a whole. That is, we have to model the interactions (quantitatively or perhaps only qualitatively) in each subsystem in order to get the boundary conditions for the next set of subsystems.

From a purely chemical point of view, it is necessary to know what chemical systems are formed and when they are formed in order to model which chemical reactions take place in the reactor.

## 6.2 Overview of what needs to be done

We have first to obtain a fairly clear picture of the dynamics of an uncontrolled reality (a mental model) and thereafter design a working model of sufficient accuracy, e.g. a usable computer code.

A first step may be to divide the dynamics of the accident sequence into four parts.

1. The formation and breakdown of subsystems, due to intrinsic changes and transport effects.
2. The intrinsic changes within a subsystem, mainly nuclear fission, radioactive decay and chemistry (including phase transitions).
3. The transport of matter and energy (heat and radiation)
4. The feedback between 1 and 2 above.

The first and last points are necessary to link transport to chemistry in order to obtain a complete description of the dynamics.

Of course it is impossible to use a model which represents reality to an arbitrary degree of precision. Attempts to produce such a model (mentally and by computer) are, however, valuable in that it gives us a better understanding of nature, everyday and during an imagined nuclear reactor accident.

For a chemistry model this means that the intrinsic changes must be adequately modeled and (via points 1 and 3) taken care of by the transport models.

The chemical contribution to point 3 is the initialization of transport or change of transport properties due to chemical reactions. It is very important to adequately model the formation (and breakdown) of chemical systems since they determine which further interactions may take place, and thus determine the future course of the transient.

Point 4, the feedback between the chemistry and transport parts of the model ensures that the effects of chemical changes upon transport are taken into consideration e.g. in the calculation of heat transport between gas and construction materials.

The feedback modeling must also consider the effects of transport upon chemistry, e.g. changed temperature.

Finally, two examples give excellent illustration of feedback: heat transport is influenced by the change of composition and amount of a

deposited layer and its thickness, which in turn influence the degree of heat transport between gas and wall.

### 6.3 Chemical aspects on the feedback

Since feedback is so important, it merges the purely chemical occurrences with those of thermal hydraulics and fission to form the whole undivided reality, a special discussion of feedback is valuable.

The size of particles in a deposited layer is important because it affects the penetration of gas through the layer and also affects the heat flow between underlying construction material and gas.

Imagine a set of moles  $n(i)$  deposited on a wall surface. These moles may be present either as a few heavy crystals with much fresh construction material still exposed to the gas, or as rather small tiny crystallites, a powder, effectively preventing the gas to penetrate the layer and thus a would-be hydrogen evolution may not occur because  $H_2O$  and steel do not occur in the same chemical system (are not in direct contact). The importance of the size, shape, and amount of particles on the wall may be even more appreciated if one consider that it is the cohesive forces between atoms which keeps matter together (from the chemical point of view). The cohesive forces between the atoms of two particles are of course much less than within each particle. The smaller and flatter a particle is, the stronger the cohesive forces will be due to a larger surface to volume ratio, and vice versa.

The forces acting on a particle on a wall are the cohesive forces (van der Waals etc.), the forces due to convection (most important in the outer part of deposited matter) and gravitation. It is possible to view the cohesive force on a vertical wall as giving rise to a friction force and to regard gravity and convection as the pulling forces. Now, as the layer increases in mass, the cohesive forces close to the construction material surface do not increase, while the gravitational force on the layer increase with increased mass. When (and if) the cohesive forces are weaker than the combined force from convection and gravity, the layer material will follow gravity and/or convection. (How will the abruptly increased convection due to the core slump affect the deposited particles ?)

The phenomena of crystal growth, cohesive forces between various kind of particles, the influence of steam on the cohesive forces, the correct convection force etc. are, taken by themselves, very difficult to model. This must also be true for the combined effect of them. It is, however, valuable to consider the above in order to appreciate the complexity of the real world.

It may be noted that small particles of the same substance tend to form fewer large particles as time pass by, since large particles (crystals) have less molar surface tension than have small particles. This may have some interesting consequences. Particles of a substance which occur in fairly large amounts will merge to larger

ones, thus encapsulating substances of lesser amount which are in direct contact with the more abundant substance. The consequence of this is that the chemical reactions, evaporation and initialization of transport is to a large degree determined by the more abundant substance. This phenomenon will of course occur in the aerosol as well.

We believe it is important to note that it is very uncommon to try to grossly understand all practical aspects of how the real world changes, (which nuclear reactor safety people have to do), so our research is actually a fresh one: connecting many seemingly unrelated phenomena (whose details there is no time to ponder) to form a coherent picture of the world around us, or of a severe nuclear power accident. The ultimate phenomena are very much the same.

#### 6.4 A chemists view of accident analysis codes

Accident analysis codes are developed in order to make it possible to estimate the releases of radioactive nuclides for every sequence of reasonable probability. To understand the necessary degree of sophistication of the chemical model, it is valuable to have a chemists overview of what processes occur during a sequence and what should be modeled by accident analysis codes.

An accident begins when the necessary cooling of the core in one way or another cannot be fulfilled. This leads to a large increase of the core temperature, due to remaining radioactivity. The increase in temperature makes the chemical compounds and phases (construction materials, fission products, fuel, cladding, coolant) in the core change properties and begin to interact chemically with their immediate neighbors. The temperature increase also causes a heavy convection. Chemical phenomena of importance are the formation of eutectica with low melting point (relatively to the reactants), formation of volatile compounds, liquid and solid phases. The change in chemical appearance leads to new transport properties which in their turn influence which compounds and phases might come in direct physical contact. The transport takes the (new or old) materials to places with another temperature, and thus the materials change transport properties as well as chemical properties within the core during their transport.

Volatile compounds with a free path to the rest of the reactor is blown away with the convection.

The radio nuclides are transported, (or are not transported) as part of compounds and materials in the vessel, possibly also in the containment whereafter eventually a fraction is released to the environment.

There are three main kinds of phenomena which govern the location of radio nuclides as a function of location and time: chemical phenomena, transport phenomena and heat transfer. The evolution of heat is responsible for all three of them. The direct formation of new materials from old ones is the domain of chemistry, while the mixing of

existing materials and compounds which comes in direct physical contact is the domain of transport phenomena. The temperature which the materials encounter in the various parts of the reactor is modelled by heat transfer.

It is worth noting that all three phenomena influence the results of the others, and to keep this in mind when constructing a model for chemical reactions during severe accident conditions. The phenomena and their mutual interactions constitutes the dynamics of the whole sequence. This dynamics should be deliberately and systematically modeled, which is not the case in most of the presently existing codes. The transfer of heat from the fuel pins increases the temperature of the surrounding materials, the materials change transport properties and takes heat with it (a kind of heat transfer), chemical reactions adds heat (e.g. cladding burning) and the new materials means new transport properties of matter, fission products are transported to other parts of the reactor and adds heat, deposited heat insulating materials on the wall surface change the rate of heat transfer between gas and wall. Heat insulation may also give rise to unanticipated local large increases in temperature on outer materials, due to slow transfer of heat from chemical reactions between aerosol phase and deposited materials.

The necessity of feedback between chemical change and transport is clearly seen here.

#### 6.5 Chemical phenomena which ought to be modeled

The modeling of chemistry during a nuclear accident might be divided to model chemical phenomena in two main parts of the reactor.

1. Chemical phenomena in the core and corium
2. Chemical phenomena outside the core and corium

The thoughts behind the modeling are very similar, but the application of the thoughts to a computer code differ due to the reasons for the division: temperature, flow properties, substances and geometry.

The formation and disruption of chemical systems demands a possibility to know which substances may come in direct contact with each other as a consequence of earlier occasions. It also means that e.g. the correct temperature is important, especially at the wall layer where a heavy temperature gradient may arise.

The intrinsic changes cannot be accurately modeled since it involves time, and the only chemical theory which provide enough data, chemical thermodynamics, does not consider time. Thus it is only possible to compare the relative stability for the chemical system. Since chemical thermodynamics does not involve time and chemical reactions do indeed take time, it is necessary to take it qualitatively into account. This can be done by a linear combination of start composition and final composition for each chemical system.

There are some practical aspects, such as abundance of data and availability of computer time, which make it necessary to slightly change the four ideal points mentioned above, to four slightly altered points which will constitute a less accurate picture of the real world, but also a model of more practical utility.

The chemical model might be based on the following necessary four conditions.

1. A modeling of which materials can be in direct physical contact, that is, the formation and disruption of chemical systems.
2. For those compounds and materials which are in direct physical contact it is necessary to predict the degree, if any, of chemical change. To this end the only theory possible is chemical thermodynamics since it alone provides enough quantitative data.
3. The time aspect of a macroscopic change, such as a chemical reaction and transport of materials. Such phenomena do not occur with infinite rate. This point is necessary since the use of chemical thermodynamics, a static model, implies an attempt to use a static model for a very dynamic process.
4. The initialization of matter transport.

#### 6.6 Reasons for the chosen considerations

Below follows the reasons for the considerations above and recommendation for a model for each of them.

##### 6.6.1 Formation of chemical systems

Direct contact models the necessity of direct molecular contact for a chemical phenomena to occur. A separation by e.g. a mono atomic oxide layer is not direct molecular contact. The set of substances in direct contact together with temperature and pressure constitute a chemical system.

6.6.1.1. A model for formation of chemical systems. Each node in the reactor is divided into four subsystems.

1. Gas phase.
2. Particles in the aerosol.
3. Wall: condensed + deposited material and oxide layer.
4. Surface: gas + surface layer of deposit.

The reasons for this division are:

1. Not all of the aerosol particles in a node comes into direct physical contact with the wall.
2. The gas phase molecules moves with high speed and the phase is thus both relatively homogenous and most of the molecules have opportunity to come into direct physical contact with the wall.
3. Since there is an oxide layer between the gas phase and the construction material under normal operating conditions the aerosol phase will not be able to interact chemically with the construction material.
4. The underlying construction material will come into contact with the aerosol phase and/or the condensed/deposited material only if the oxide layer is broken.

The modeling is performed by choosing the chemical systems to be one or a combination of substances in direct contact for a combination of two of the above subsystems, the combination being between those which are in physical contact, and by performing chemical modeling in each of the chosen chemical systems.

The book keeping (see the initialization of matter transport below) makes it possible to model which deposited/condensed material are in direct contact, and to (qualitatively) which degree. The formation of liquid in the wall surface material provides a medium for exchange of matter between the materials, provided the exchanged species are stable in the liquid.

6.6.1.2 Chemical change. The decision of whether a chemical change occurs or not models chemical reactions and condensation/evaporation and is the most crucial part. A modeling of condensing/evaporation requires that the temperature difference between wall and aerosol is taken into account.

6.6.1.3 A model for prediction of chemical changes. This must predominantly be modeled with chemical thermodynamics since it is the only theory with a sufficient supply of data for the very complex systems we are interested in. An equilibrium calculation is performed in order to find the thermodynamically most stable state in the system, including the distribution of any compound between various aggregation states.

If there is access to reliable purely empirical knowledge for the situations that arises in the reactor, such knowledge is of great importance since it tells what really happens, independently of the unavoidable limitations which are imposed by any model of practical use. Such knowledge ought to have higher priority than the data of chemical thermodynamics. Examples: Some compounds are very unreactive in spite of being thermodynamically unstable. Such compounds are said to be kinetically stable under the prevailing conditions.

Thermodynamic data for corrosion in complex systems are not plentiful, and the rate of corrosion is not even in the realm of thermodynamics.

6.6.1.4. The time aspect. The time aspect models for example that a compound in gas phase which is thermodynamically stable as a condensate on the wall do not have time to condense in the resident node and are partly transported to the node located downstream. An equilibrium calculation of e.g. the aerosol has as assumption that either have all particles opportunity to combine (by transport) with each other into direct contact so as to reach the thermodynamic equilibrium, or that each particle has a high vapor pressure (and the vapors are thermodynamically stable) and the transport of the vapors in the gas phase (the medium for exchange of matter) occurs with nearly infinite speed. Both of these assumptions follows from neglect of the time aspect.

6.6.1.5. A model for the time aspect of change. It is impossible to make any quantitative modeling with respect to time so one has to be content with a qualitative, that is, that chemical changes and transport take time. This might for chemical changes between compounds and materials which are in physical contact be modeled by a linear combination of the start composition and the equilibrium composition, so that the final composition is somewhere in between. A combination of the time aspect and direct contact gives e.g. that since mass transport in solid state is much slower than in gas phase the atoms in two different solid state phases have difficulty to come in direct atomic or molecular contact. This means that solid state solid state chemical reactions occur only slowly in spite of a possible large decrease in chemical potential for a reaction, and the coefficient are put accordingly. As a follow up to the slow mass transport of atoms in solids it is valuable to consider the effect of a layer of solid material. The inner part of such a layer may not be in direct molecular or atomic contact with the aerosol phase and thus be rather uninfluenced of e.g. a large change in oxidation potential in the gas phase.

For the transport of matter in the layer, the time of transport is modeled by only slowly permitting substances deposited at clearly separated time intervals to interact chemically.

For the transport in the aerosol phase, only those particles which are in direct contact (deposited) may interact chemically, but interaction is also permitted via indirect contact through the gas phase.

6.6.1.6. Initialization of matter transport. Imagine that a substance deep in a layer vaporizes, which means a drastic increase in volume. The materials which lie above the evaporating material will then probably be blown off as aerosols into the aerosol phase irrespective of their respective chemical properties. If another material in the gas phase condenses on a particle that consist of a third

material we end up with a kind of aerosol which consists of two compounds, each with its own chemical properties. What happens if the inner material after being deposited chooses to evaporate? The outer material will go into the aerosol phase as aerosol if the vapor pressure is high enough, otherwise the inner substance will remain in condensed state, although its vapor pressure, when considered alone indicates initialization of transport. The same aspect are valid for the case of encapsulated substances in the deposited layer due to formation of large crystals, see the part overview above.

Finally there is the possibility that another material, present in the middle of a deposited layer on the wall surface in relatively large amount, melts. The liquefied material (abruptly changed transport properties) flows down the wall and carries other material with it as well.

6.6.1.7. A model for initialization of matter transport. To model initialization of matter transport, deposited/condensed material are divided into layers, each layer being e.g. 1 micrometer thick.

In order to know when, and if, some materials located outside one layer where a specific material evaporates, will be blown off as aerosol it is necessary to have a book keeping of the amount of material in the layers that has condensed or deposited on top of the evaporating material. The book keeping must be done for all layers.

For the case of encapsulated substances, the book keeping makes it possible to decide which substances are in direct contact and in which amounts, and facilitates the modeling of the effects of encapsulation.

In the case of melting of a large amount of any material in a given layer the book keeping makes it possible to model which materials (those in the current layer and above) will follow the flow (if any) of the melting material.

#### 6.6.2 Modeling of chemistry in the containment

The crucial event for chemical phenomena in the containment is the corium slump. In order to be able to appreciate the problem of a reliable model of chemical phenomena in the containment, it is valuable to view the slump by considering four points: the time aspect, physical contact, chemical changes and the initialization of matter transport.

The core slump introduces a heavy temperature gradient, a large pressure gradient and brings a lot of material into physical contact. The increased temperature makes ex-vessel materials change aggregation state, some of them will evaporate and be transported away, and thus decreasing the time of physical contact with the corium and released vessel gas and aerosol particles. The time for chemical reactions made possible by the physical contact is very

short. The blown away material will, due to the temperature gradient, condense to aerosol particles, presumably mixed encapsulating ones, the particles being formed by the blown away gas particle phase. The inner materials, if any (the particle may be a "homogeneous mixture"), will not be accessible to further reactions other than with the outer layer. Materials which differ by only a few seconds with respect to evaporation may not form particles together.

Ex-vessel material which undergo liquefaction, or maybe break due to thermal strain (caused by the temperature gradient) may follow the corium and be immersed in it, thus preventing any further reactions with non-corium materials.

As seen, the short period of the corium slump does largely determine the composition of the aerosol phase.

We have a system which is very inhomogeneous, changes very rapidly with time and the time for physical contact is very small. The initialization of matter transport caused by the temperature gradient, such as thermal strains, liquefaction of construction materials etc. is very difficult to predict, and so are which materials/substances do really enter into direct contact and for how long time.

The use of chemical thermodynamics to model the result of chemical reactions during the core slump is dubious, but it is the only means we have.

It is, presently, difficult to make any recommendations for a reliable and useful modeling of this crucial sequence.

6.6.2.1 The containment after the slump. Chemistry in the containment after core slumping amounts very much to water chemistry. The atmosphere is damp even before eventual sprinkling and even more so afterwards.

The temperature in the containment may be fairly low, which makes the use of chemical thermodynamics somewhat risky, due to increased chance that some species or intermediaries will be kinetically stable and thus cause the system to equilibrate in a state not thermodynamically optimal.

The water films on the walls are thin, with large surface/volume ratio and consequently the concentrations of substances, originating from water soluble gases and particles with water soluble coating, are much higher than in the pools. The higher concentrations of the solutions will probably make them of non ideal, which means that theoretical data for water films are not applicable. Empirical data have to suffice. The water films are important to model because of corrosion, especially at higher concentrations.

The modeling of chemistry in the containment will to a large degree be of the same kind as in the vessel, differing (probably) by the use of empirical data for kinetic stability and non-ideality of the

water films.

As understood, the predictions made by any chemical model based on chemical thermodynamics are less reliable in the containment than in the vessel because chemical thermodynamics is a poor model for the physical milieu in the containment and the highly dynamic process of corium slump is difficult to model even with respect to which materials are in direct contact.



## 7 RECOMMENDED MODELING OF AEROSOL BEHAVIOR IN ACCIDENT ANALYSIS CODES WITH REGARD TO HYGROSCOPICITY

### 7.1 Introduction

Aerosol particles formed in severe nuclear power plant core melt accidents include hygroscopic compounds. These particles absorb water and grow in a moist atmosphere, decreasing the partial pressure of water vapor in the gas phase and increasing the gas temperature owing to the release of latent heat. This means that there is a strong coupling between aerosols and thermal-hydraulic conditions in the containment atmosphere.

Most inorganic salts, like cesium iodide (CsI), when exposed to increasing humidity, will dissolve at a certain relative humidity (deliquescent point), which depends on the properties of the salt and system temperature. Particles which contain these compounds, will form saturated droplets and undergo at the same time an abrupt increase in size. As humidity increases further, the droplets will grow and become more dilute. When humidity decreases, the droplets become smaller and the particles recrystallize abruptly at a humidity considerably lower than that at which the particles were initially dissolved /1,2/. In the case where particles also contain insoluble compounds, these two humidities are near each other /3/.

On the other hand, a few electrolytes such as  $H_2SO_4$  (sulfuric acid), NaOH (sodium hydroxide) and CsOH (cesium hydroxide), will form an aqueous solution and start to absorb water at a very low R.H. (< 10%). Thus, particles consisting of these substances grow continuously and smoothly with an increasing relative humidity (R.H.). Phase transformations in mixed solutions are more complex, but mixtures are more common in nature and their growth in humid conditions is also considered here.

At a low R.H. (< 85%) a small growth of hygroscopic particles does not increase particle deposition rates significantly. However, changes in the properties of particulate matter may occur. In the case of a severe nuclear accident the relocation of deposited material depends on the physical and chemical properties of this matter. At a high R.H. (> 90%) the growth of hygroscopic particles will increase their settling rate significantly.

### 7.2 Requirements for modeling hygroscopic particles

On the basis of the work carried out to assess the modeling requirements for the behavior of hygroscopic particles /4,5/, we can conclude that for mass and heat transport a simplified model proposed by Mason /3/ can be used in the very humid conditions expected in containment. In these conditions a modified Raoult's law can be used for calculating the water activity. At a low R.H., expected in the reactor coolant system, the equilibrium between water vapor and hygroscopic particles is reached during a very short period of time. In the coolant system it is recommended to use an immediate equilib-

rium for solution droplets and deposited water soluble material. The equilibrium concentration for concentrated solutions can be then calculated from eqs. proposed by Meissner /6/, which give a reasonable agreement with the measurements /7,8/.

In the case of severe accidents there may be particles composed of many water soluble compounds (e.g. CsOH, CsI, Cs<sub>2</sub>CO<sub>3</sub> and other hydroxides). The calculations performed /5/ indicate<sup>2</sup> that the growth of hygroscopic particles is sensitive to the chemical composition of airborne particles expected to be released in severe accidents.

Condensation on hygroscopic particles plays an important role in very humid conditions in the containment atmosphere. This has been demonstrated in the LACE experiments, where a rapid removal of hygroscopic particles was revealed. On the basis of these experiments and the detailed analyses of hygroscopic aerosol behavior it can be recommended that modeling of aerosol behavior and thermal-hydraulics should be coupled. The decrease in steam partial pressure due to condensation on particles and the increase in gas temperature due to the heat of condensation will decrease the R.H. in containment. Among the accident analyses codes this is done only in the recent version of the CONTAIN code. In the MAAP code these effects are not considered and thus MAAP overpredicts the R.H. and settling rate. The simple correlation method used in MAAP has some limitations for predicting the aerosol size distribution in a condensing atmosphere.

The coupling is necessary for the desired accuracy in core melt accident analyses because small changes in thermal-hydraulic conditions will have a large impact on the radioactive aerosol behavior in the containment if condensation on particles is considered.

### 7.3 References

- /1/ I. N. Tang, Phase Transformations and Growth of Aerosol Particles Composed of Mixed Salts, J. Aerosol Sci., 7 (1976) 361-371.
- /2/ M. D. Cohen, Studies of Concentrated Electrolyte Solutions Using the Electrodynamic Balance, Ph. D. Thesis, California Institute of Technology, Pasadena, California (1986).
- /3/ B. J. Mason, The Physics of Clouds, 1st Ed. Clarendon Press, Oxford (1957).
- /4/ J. Jokiniemi and R. Sher, Modeling the Growth of Water Soluble Particles in the NAUA code, OECD/NEA Workshop on Water-Cooled Reactor Aerosol Code Evaluation and Uncertainty Assessment, Held in Brussels, Belgium 9th-11th September 1987, CEC, Luxembourg (1988) 280-290.

- /5/ J. Jokiniemi, The effect of selected binary solutions on steam condensation and aerosol behavior in containment, The 3rd Chemical Congress of North America, Nuclear Reactor Severe Accident Chemistry Symposium, Held in Toronto, Canada June 5-10 (1988).
- /6/ H. P. Meissner, Prediction of Activity Coefficients of Strong Electrolytes in Aqueous Systems, ACS Series 133 (1980) 495-511.
- /7/ L. G. Johansson and S. Kazikowski, An Experimental Study of Equilibrium Water Vapour Pressures in the CsOH-H<sub>2</sub>O System, The 3rd Chemical Congress of North America, Nuclear<sup>2</sup> Reactor Severe Accident Chemistry Symposium, Held in Toronto, Canada June 5-10, 1988.
- /8/ J. Krey, Dampfdruck und Dichte des Systems NaOH-H<sub>2</sub>O. Zeitschrift für Physikalische Chemie, Neue Folge, 81 (1972) 252-273.



8 DESCRIPTION OF THE MODELING OF CHEMICAL BEHAVIOR USED IN THE  
MAAP CODE. ASSESSMENT OF THE SIGNIFICANCE OF SIMPLIFICATIONS  
AND APPROXIMATIONS

The description of the chemical model in MAAP is according to the documentation with some modifications evident from the available source code, and has been planned so that for each chosen key-event information is given concerning;

1. Which elements is added from the various parts of the reactor.
2. The modeling of chemistry.

Following this description comes a list of crucial shortcomings in MAAP, as well as cases where the documentation do not fit the code.

#### 8.1 The core

1. MAAP models that Cs, I, Ru, Sr, Ne, Ar, Mn, Sn and possibly Te is released from the core as volatiles or aerosols.
2.
  - a. All of I is modeled to react with Cs to CsI.
  - b. The remaining Cs reacts with water to CsOH.
  - c. Ru do not react with anything, but remains in elementary form.
  - d. Sr reacts to SrO.
  - e. Mn and Sn reacts with hydrogen or water, depending on the hydrogen to water ratio.
  - f. Te is modeled not to be dissolved in the zirconia, but to be released from the core, if the user so wishes.

#### 8.2 The rest of the reactor vessel.

The reactor vessel is divided into several nodes during the execution.

1. No elements are added in any node.
2. The transport properties of the fission products are modeled by the following six groups;
  - a. Inerts. Xe, Kr are modeled as an ideal gas. The group also includes Sn and Mn and for PWR:s Ag, In, Cd as well.

The remaining groups are modeled for one of its members, so that the vapor pressure above the condensed phase is empirical, and the vapor pressure of the gas is modeled as

an ideal gas.

- b. CsI. The group models CsI only.
- c. TeO<sub>2</sub>, TeH. The group models TeO<sub>2</sub>.
- d. Sr, SrOH, Sr(OH)<sub>2</sub>, SrO. The group models SrO<sub>2</sub>.
- e. Ru. The group models Ru only.
- f. CsOH. The group models CsOH only.

The modeling of chemistry is calculation of maximal theoretical equilibrium pressure and then compare this value with the starting vapor pressure in the gas phase. The starting vapor pressure is calculated from the ideal gas law and the amount of matter in the flow volume. If the gas is not saturated with vapor, (empirical vapor pressure) any existing condensed material on the wall will evaporate until maximal vapor pressure is reached. If the material on the wall is not sufficient to reach the maximal vapor pressure, evaporation of aerosol particles is then turned on. For the case when the actual vapor pressure is larger than the maximal, vapor is condensed on the aerosol particles. The modeling of chemistry thus assumes that the wall temperature always is higher than the gas temperature. When particles or vapor (excluding the noble gases) come into contact with water pools, the fission products get stuck there.

8.3 The region below the vessel when the corium flows through this region.

- 1. No elements are added.
- 2. No modeling of chemical phenomena occurs.

8.4 The bottom of the containment when the corium is situated there.

- 1. If the bottom consists of concrete, the elements Ba, Si, K, Na are added.
- 2. The added elements are assumed to exist as BaO, Si<sub>2</sub>O, K<sub>2</sub>O and Na<sub>2</sub>O and are modeled only as aerosols. The modeling of the amount that leaves the corium is performed by using thermodynamic formulas with the assumption that the corium behaves as an ideal mixture.

8.5 The containment, excluding the bottom, after the slump.

- 1. No elements are added.
- 2. Chemical modeling as in the vessel.

8.6 Interaction between thermal hydraulics and chemistry.

There are six ways in which MAAP takes the interaction of chemistry and thermal hydraulics into account:

1. Phase transition water/steam.
2. Hydrogen evolution due to cladding oxidation.
3. Mass increase of aerosol due to fission products.
4. Distribution of rest effect from fission products.
5. Heat evolution due to cladding oxidation.
6. Heat absorbed by water to form steam.

#### 8.7 Shortcomings of the chemical model in MAAP.

The fact that there are large amount of boron carbide in the core, which might give rise to volatile boron compounds and possibly also carbon compounds, is not taken into account in the modeling of fission product release from the core.

The construction materials tin and manganese are assumed to be released in the form which is thermodynamically most stable under the release conditions and to retain this form even under conditions totally different from the release conditions. If one considers what effect materials imbedded in a layer on walls might have on the transport of materials in the outer part of the layer when the imbedded materials change aggregation state, or form large crystals with encapsulated substances, see part 7, it is realized that manganese and tin must be treated as reactive species.

Corrosion of structural materials like steel is not modeled in MAAP. Experiments at Chalmers have showed that corrosion under realistic conditions can be as high as 1 mm/h /1/. The elements involved were tellurium, tin and manganese.

During the slump MAAP models that copper wires with insulation, control rod drive motors, including oil, grate and mineral wool do not change appearance or at least have no decisive influence on the final release of fission products into the environment. Admittedly, it is a difficult sequence to model, but necessary. The possibility of having fission products coming out of the vessel in conjunction with the corium cannot be excluded due to the decrease of pressure in the vessel, with aerosol formation together with the material under the vessel. It is of interest to know the possible mixtures an aerosol particle can consist of, see the reason number four for conditions that should be taken into account as a general recommendation for the modeling of chemistry.

The modeling of condensing/evaporation is not reliable for two reasons.

1. The assumption that condensation always takes place on the aerosol and not on the walls implies that the wall temperature always is assumed to be higher than the aerosol temperature. This assumption is not well founded, and the temperature difference is not taken into account.
2. The vapor pressure expressions (no equilibrium calculation) which are used are only valid for one of the compounds in

respective group. This means that the other compounds in the group are not really included in the group.

One reason for the choice of which compound to model might be the conviction that the respective element finally ends up in the chosen compound. Such thought contains two flaws. The first is that the fission products might very well react chemically with any other element and remain so, thermodynamically stable. The second is that even if some of the fission products actually do end up as the chosen compound it may not be transported according to its purely chemical (i.e. vapor pressure) properties, see the reasoning behind the initialization of matter transport above. Also, the complicated water chemistry in the containment will certainly influence the transport of the fission products.

MAAP does take the time for evaporation/condensing into account, a process which is claimed to be very fast. Since MAAP takes no account of chemical reactions, the conditions number one and two in part 7 are of no concern here, neither is the time for chemical reactions.

Since the distribution of fission products are critically dependent on how much leaves the core, the gas flow in the plant and the temperature distribution, these aspects must be commented upon under this headline.

The core. MAAP displays a worrisome lack of chemistry within the core. Too much concern have been of the fission products. The mechanical effect of other materials metamorphosis have largely been neglected. The consequences of a formation of low-melting eutectica on the free path from fuel to the rest of the plant is not considered.

Flow and temperature. MAAP models that the upper downcomer does not receive any radiation energy from the core, in spite of its immediate vicinity, only the moderator tank shields the radiation from the core. Let us assume that the real temperature of the upper downcomer is higher than of the upper plenum. This may have interesting consequences on the flow of gas, as well as the transport of fission products and other materials, which will less easy condense in the upper downcomer than in upper plenum.

#### 8.8 Identified errors in MAAP

There is a general confusion in the definitions of, and data used for, the 6 fission product groups in various MAAP subroutines. This is further complicated by the possibility for the user to define the original core inventory mass in terms of various chemical compounds. Table 8.8.1 below summarizes the most important findings. The disparate definitions will lead to erroneous results from various calculations throughout MAAP. These coding mistakes must be corrected. Until then, any agreement between release data from MAAP and other codes or experiments must be purely accidental.

Table 8.8.1. Comparison of the definitions of the fission product groups and data used in MAAP subroutines and common blocks.

Routine	FP group						Comments
	1	2	3	4	5	6	
FPRATB	I	Cs	Te	Sr	Ru	-	Release rates
	126.9	132.9	127.6	87.6	101.1	-	Molar weights
GROSSE	??	CsI	TeO <sub>2</sub> ?	SrO?	Ru	CsOH	Vapor pressures
	??	CsI	Te	SrO	MoO <sub>3</sub>	CsOH	Vapor densities
BLOCK DATA	135	260	128	104	144 <sup>3</sup>	150	Molar weights
PARAMETER	Kr, Xe	CsI	TeO <sub>2</sub>	SrSiO <sub>2</sub>	K <sub>2</sub> MoO <sub>4</sub>	CsOH	Core inventory
FILE F3							mass (kg)

### 8.9 Conclusions

MAAP's model of chemistry assumes that the processes takes place in an oxidative milieu, with inert walls, and that only one compound (and also possibly water) is located at the same place and time since no chemical reactions are modeled to occur other than just before an element enters the calculations.

It might in the end turn out that MAAP's prediction of releases are reliable, but it would presumably be due to the possibilities of retention of all kinds of substances in the reactor.

### 8.10 Reference

- /1/ S. Kazikowski, L.-G. Johansson, U. Malmström and O. Lindqvist, Corrosion and Deposition Studies of Stainless Steel Exposed to Aerosols Containing Te, Cs, Mn, Ag, and B<sub>2</sub>O<sub>3</sub> at 300-1000°C in a Reducing (H<sub>2</sub>/H<sub>2</sub>O/N<sub>2</sub>) Environment, NUREG/CP0078 vol 3 (1986) p 79.



9 THE SOLGASMIX DATA BASE - SUITABILITY AS A BASIS FOR THE MODELING OF CHEMICAL BEHAVIOR IN CORE MELT ACCIDENTS

A chemical thermodynamic data base contains data which makes it possible to calculate the chemical potential ( $u_i = (dG/dn_i)_{n_j, T, P}$ ) for a compound "i", (G = Gibbs free energy), for at least one (T,P)-point, e.g. T = 298 K and P = 1 bar. In order to be of practical use in accident analysis, the data base have to contain data which makes possible the calculation of the chemical potential for "i" for arbitrary points in those (T,P)-interval which are of interest. For us it means temperatures between 400 K and well above 1300 K, and pressures ranging from 1 bar to 5 bar. Much of the needed data can be found in current compilations /1, 2/.

9.1 The extent of the database

Chemical thermodynamic data for all materials and compounds which might be of importance for the release of fission products, fuel and structural materials ought to be included. This means, among other things, that all elements which are present in significant amount shall be contained in the database. For BWR's, the elements Cs, H, O, Te, Ru, Fe, Cr, Ni, Sn, Zr, U, Sr, B, C, Cu, Cl, Al and Si are of interest, maybe also fluorine which originates from UF<sub>6</sub>. It is, however, not necessary that all chemical compounds which the above elements can form are included in the data base, but only those that are thermodynamically stable under conditions of severe accident sequences. To accomplish this, a computer program has been developed. This fact does to a high degree ease the computational burden. It is also possible to further reduce the computational burden by having the chemical model too, from the above mentioned reduced data base and for a given 3-dimensional interval T(low), P(low), (H<sub>2</sub>O/H<sub>2</sub>) ; T(high), P(high), (H<sub>2</sub>O/H<sub>2</sub>), choose only those compounds which might be thermodynamically stable in this interval. These intervals shall together cover the conditions of interest under a severe accident sequence. Presently there are no such data base, but as a start it will be produced from the JANAF tables.

9.2 Limitations of a database of only pure chemical compounds

It is not enough to only have data for pure chemical compounds. Other kinds of materials which arise during the lapse of a severe accident sequence are mixtures of various kinds. Mixtures like water solutions, alloys, solid solutions and complex gas mixtures with fairly low temperature in the containment. These mixtures are often nonideal, which means that activity coefficients have to be known from experiments. It is not likely that such coefficients are determined for all mixtures of interest during a severe accident sequence. Empirical knowledge of situations which, according to results from the use of the chemical model, arise may ease the drawback of lacking thermodynamic data.

There are only relatively few data for really high temperatures

which means that chemical modeling for very high temperatures are less reliable than for the middle range (600 to about 1300 K).

### 9.3 Consistency of the JANAF table

The JANAF table /2/ is a consistent chemical thermodynamic data base. This means that the functions of state (Gibbs, entropy etc.) for a certain total reaction from A to B are the same regardless of the way between A and B. As a consequence, chemical composition will be exactly the same regardless of the way between A and B.

Since the set of original experimental data do not fulfill this requirement, the data have to be adjusted a little. One of the drawbacks of this is that a single data in the literature, taken alone, may be more accurate than the corresponding JANAF value, but may taken together with other data to form a chemical system be of little value since the new set of data is not consistent.

The somewhat paradoxical effect of this is that a more accurate single datum will yield a less accurate result for a complex chemical system.

### 9.4 Recommendations for future development

Empirical knowledge have to be included, as a separate data base. Such knowledge is;

1. Kinetic stability
2. Phases formed under specified conditions, but without thermodynamic data.

Thermodynamic data for nonideal mixtures have to be added to the thermodynamic data base.

### 9.5 References

- /1/ I. Barin and O. Knacke, Thermodynamical properties of inorganic substances, 1973.
- /2/ JANAF Thermochemical tables, 3:rd ed., 1985.

## 10 CELSOL ANALYSES OF SEVERE LWR REACTOR ACCIDENTS

The computer code CELSOL /1//2//3/ used for calculation of chemical equilibria during severe reactor accidents was developed as a part of the common nordic safety study NKA/AKTI-150 and a danish reactor safety study /4/.

### 10.1 The CELSOL code

The CELSOL code performs a thermodynamic analysis on a prescribed system of elements and compounds to determine the most stable compounds as a function of elemental abundances, temperature and pressure. The analysis gives a detailed description of the system under the assumption that equilibrium is obtained.

The central part of the code is a set of subroutines solving the equilibrium equations. The code SOLGASMIX /5//6/ has been implemented for this purpose.

CELSOL has an option for specifying plate out. It is possible to specify a plate out fraction for each compound. The amount of plated out is collected in dummy boxes and is excluded from the subsequent equilibrium calculations.

For each time step and compartment the code requires information about temperature, pressure, flows and concentrations of elemental abundances. The information about concentrations should comprise both fission products, structural materials and hydrogen and oxygen.

The code system consisting of MARCH 3.0 /7/, RELCOND /8//9/ and CELSOL is illustrated below:

```
----- Thermohydraulic accident data such as temperature,
: MARCH 3.0 : pressure, flows etc. are calculated with the MARCH
----- 3.0 code from NRC and used as input to the Relcon
: code.
:
----- The release of material from the fuel during the
: RELCON : accident is calculated with the RELCON code.
----- Concentrations of the released elements in the
: reactor system are also calculated with the code
: and used as input to the CELSOL code.
:
----- The CELSOL code produces a listing of the calculat-
: CELSOL : ed equilibrium concentrations of the compounds
----- formed in the reactor system as a function of time
and compartment.
```

Thermodynamic data for a number of elements and compounds are present in the CELSOL data base /10//11//12//13/ and used as input to the code. The actual elements and compounds are given in table 10.1. If the thermodynamic data are available it is easy to extend the database.

Table 10.1 Elements and compounds in the CELSOL data base

	O(g)	H(g)	H <sub>2</sub> O(g)
	O <sub>2</sub> (g)	H <sub>2</sub> (g)	
C(g)	CO(g)	CH <sub>4</sub> (g)	
	CO <sub>2</sub> (g)		
Te(g)	TeO(g)	H <sub>2</sub> Te(g)	
Te(l)	(TeO) <sub>2</sub> (g)		
Te(s)	TeO <sub>2</sub> (g)		
Te <sub>2</sub> (g)	TeO <sub>2</sub> (l)		
	TeO <sub>2</sub> (s)		
Cs(g)	CsO(g)	CsH(g)	CsOH(g)
Cs(l)	Cs <sub>2</sub> O(g)		CsOH(s)
Cs <sub>2</sub> (g)	CsO <sub>2</sub> (g)		(CsOH) <sub>2</sub> (g)
I(g)	IO(g)	HI(g)	HOI(g)
I <sub>2</sub> (g)			
B(g)	B <sub>2</sub> O <sub>3</sub> (g)		H <sub>3</sub> BO <sub>3</sub> (g)
			HBO <sub>2</sub> (g)
B <sub>4</sub> C(l)			(g: gas)
B <sub>4</sub> C(s)			(l: liquid)
CsI(g)	CsBO <sub>2</sub> (s)		(s: solid)
CsI(l)			
CsI(s)			
(CsI) <sub>2</sub> (g)			

## 10.2 CELSOL analyses of the TB accident sequence

The analysed accident sequences are transients with complete failure of all electrical power supply system. They are called TB accidents. A short presentation of CELSOL analyses of 2 different TB accident sequences are given in the following. The analyzed sequences are characterised in table 10.2.

Table 10.2. Analyzed TB sequences

Sequence	Conditions
TB with ADS	No Boron Release
TB with ADS	H <sub>3</sub> BO <sub>3</sub> Data from Winfrith
TB with ADS	JANAF Boron Data
TB without ADS	No Boron Release
TB without ADS	H <sub>3</sub> BO <sub>3</sub> Data from Winfrith
TB without ADS	JANAF Boron Data

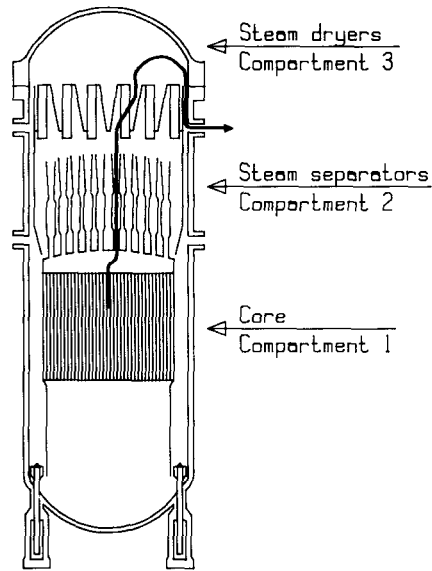


Figure 10.1. Reactor vessel compartments used in CELSOL.

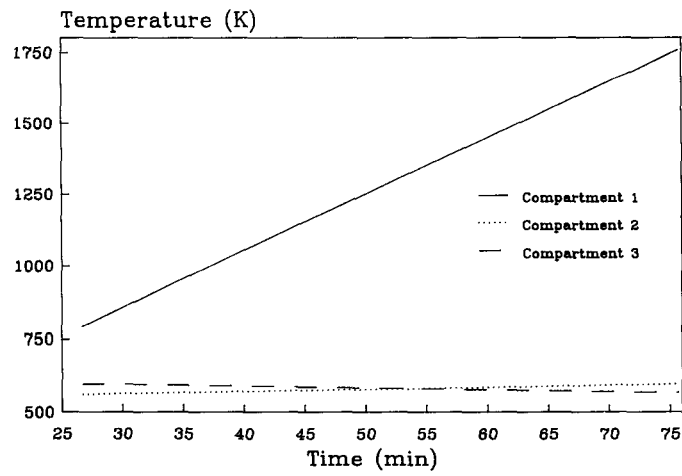


Figure 10.2. Temperature history for the TB accident with ADS.

The power plant used in the study is a Swedish BWR designed by ABB-ATOM. It is designated BWR-3000 and is almost identical to the Forsmark 3 and the Oskarshamn 3 plants.

In the CELSOL calculations the reactor vessel is divided into three compartments, the core, the steam separator and the steam dome inclusive the steam dryers as shown in figure 10.1.

#### 10.2.1 TB Accident sequence with automatic depressurization

Three different CELSOL analyses of the TB accident with automatic depressurization (ADS) have carried out as shown in table 10.2.

10.2.1.1 TB with ADS and no boron release. Figure 10.2 shows the temperature history for the TB accident with ADS in the 3 primary compartments. The CELSOL analysis starts 25.7 minutes after reactor scram. The pressure is assumed to be constant (0.44 MPa) after blow down.

The CELSOL analysis of this accident sequence without boron release shows that the dominant iodine compound in compartment 1 throughout the whole accident is cesium iodide gas. A few minutes before core slump, where the analysis is stopped, iodine and hydrogen iodide gas is formed because of the high temperature. Atomic cesium dominates

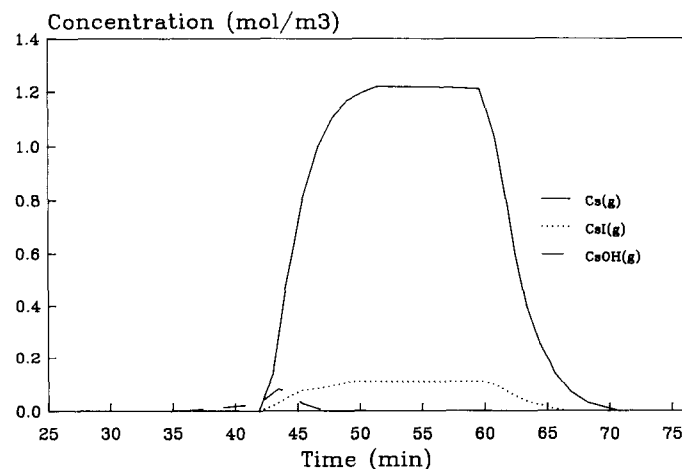


Figure 10.3. Concentrations of cesium compounds in compartment 1.

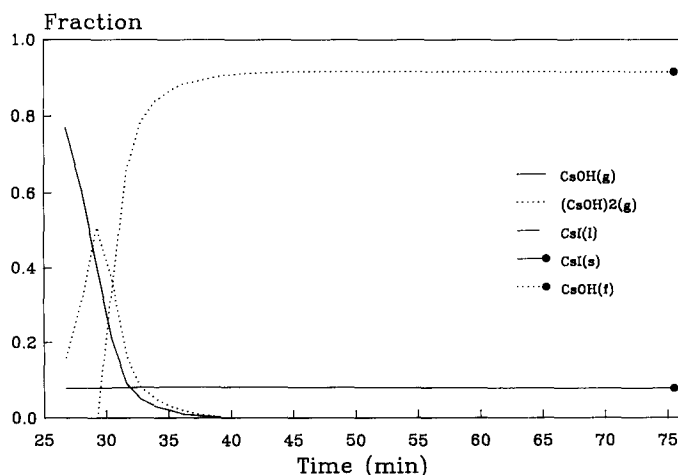


Figure 10.4. Distribution of cesium compounds in compartment 3.

the cesium compounds in compartment 1 but also cesium hydroxide and cesium iodide is present. Cesium dominates because of the lack of water.

Cesium iodide in liquid or solid form is the only iodine compound in the cooler parts of the reactor vessel in compartment 3. Cesium hydroxide is the important cesium compound in this compartment but also  $(\text{CsOH})_2$  is present.

Tellurium has also been analysed.  $\text{Te}$ ,  $\text{Te}_2$  and  $\text{H}_2\text{Te}$  gases are present in compartment 1, while  $\text{Te}_2$  gas and tellurium in condensed form dominates in the cooler parts of the vessel but also  $\text{H}_2\text{Te}$  is present. Figures 10.3 and 10.4 show CELSOL results for cesium.

10.2.1.2 TB with ADS and new Boron Data from Winfrith. The Boron release in this accident sequence is calculated with the RELCON code. The release constants are arbitrarily chosen in such a way that the accumulated release of Boron during the accident is 2 - 3 % of the  $\text{B}_4\text{C}$  inventory.

The thermohydraulic situation is identical to the one described above.

Cesium iodide gas is the most important iodine compound in compartment 1 and atomic cesium is dominating the cesium compounds

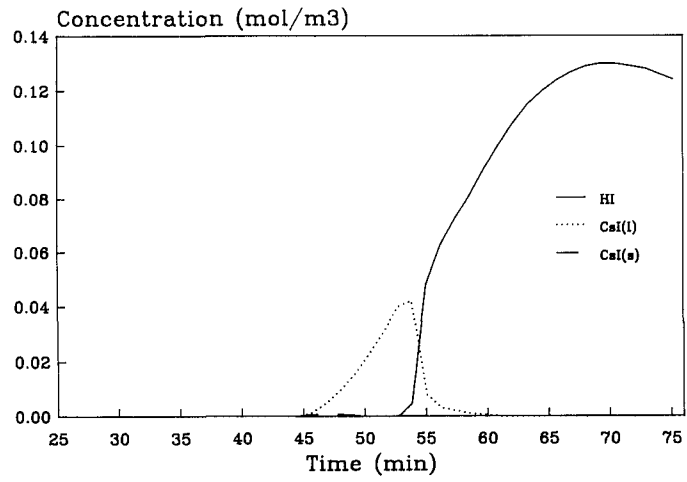


Figure 10.5. Concentrations of iodine compounds in compartment 3.

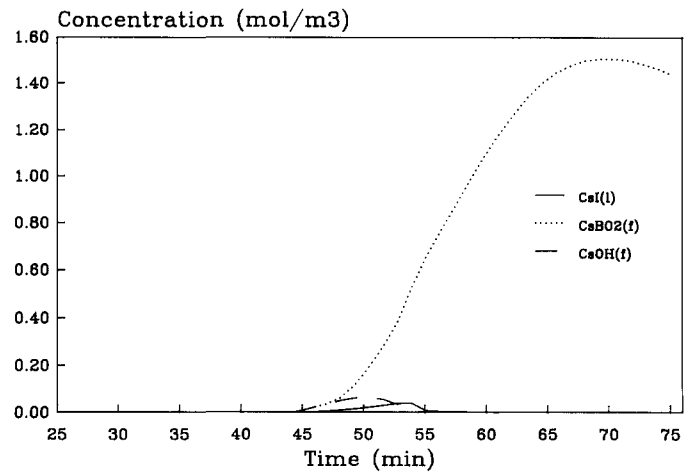


Figure 10.6. Concentrations of cesium compounds in compartment 3.

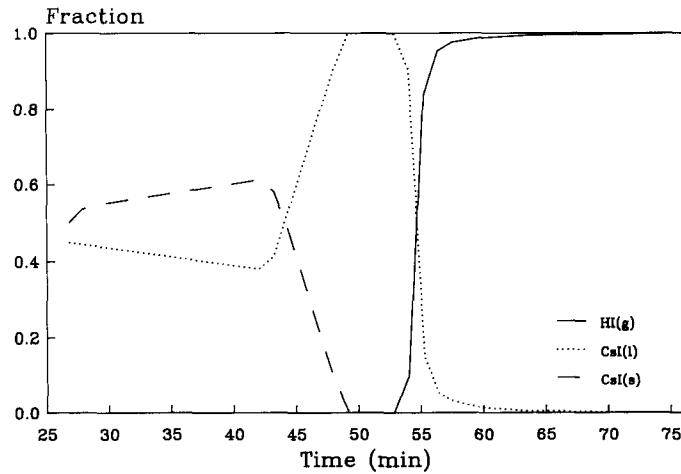


Figure 10.7. Distribution of iodine compounds in compartment 3.

but condensed  $\text{CsBO}_2$  and gaseous cesium hydroxide are also present.

The important iodine compound in compartment 3 is hydrogen iodide, while the amount of cesium iodide is small compared to the sequence without boron release. The dominant cesium compound is  $\text{CsBO}_2$ . Condensed phases of cesium iodide and cesium hydroxide is present in small amounts.

Figures 10.5 to 10.7 show characteristic results from the CELSOL analyses.

10.2.1.3 TB with ADS and JANAF boron data. The release of Boron is calculated with the RELCON code as above.

The important iodine compound in compartment 1 is cesium iodide gas. A small amount of condensed cesium iodide is also formed in compartment 1 during the accident.

The dominant cesium compound is atomic cesium. Cesium hydroxide gas and condensed  $\text{CsBO}_2$  is also present. In the cooler parts of the vessel in compartment 3 condensed  $\text{CsBO}_2$  and condensed cesium hydroxide are the important cesium compounds. The important iodine compound in compartment 3 is condensed cesium iodide.

It is clear from these CELSOL analyses of the TB accident with two

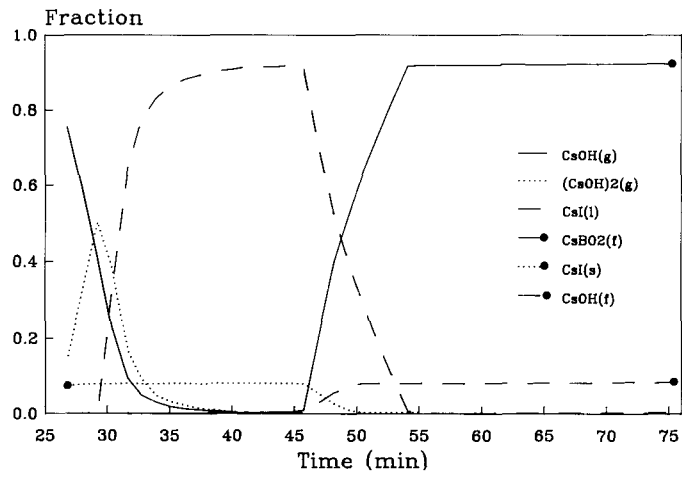


Figure 10.8. Distribution of cesium compounds in compartment 3.

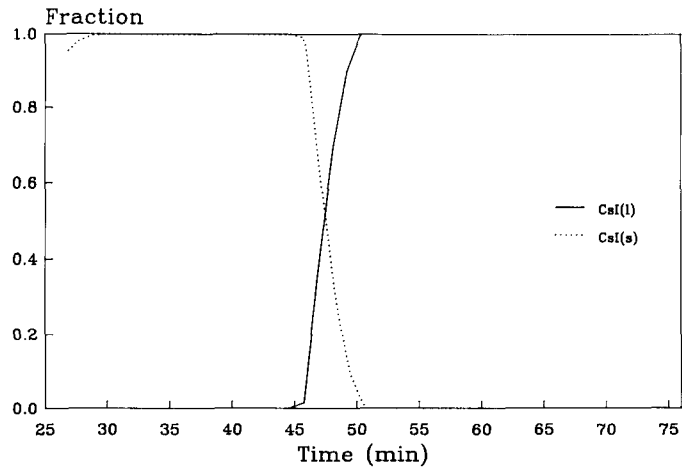


Figure 10.9. Distribution of iodine compounds in compartment 3.

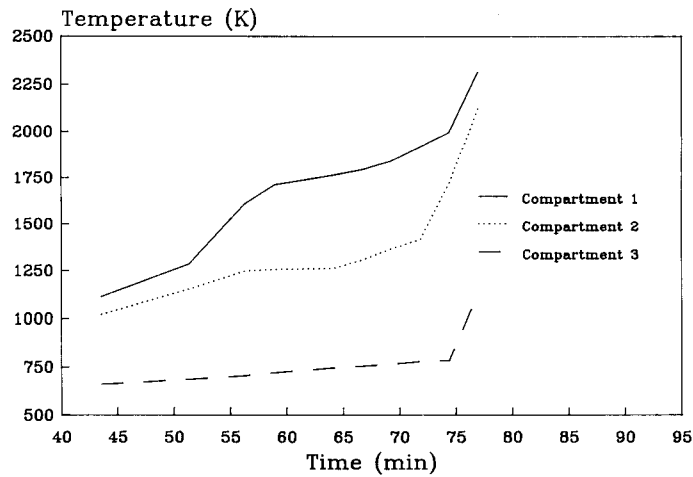


Figure 10.10. Temperature history for the TB accident without ADS.

different set of boron thermodynamic data that the stability of cesium iodide can be influenced by boron release. It is also very clear that the accuracy of the boron thermodynamic data is of decisive importance for the stability of cesium iodide as the CELSOL results are very different dependent on the boron data.

Figures 10.8 and 10.9 show the distributions of iodine and cesium compounds in compartment 3.

#### 10.2.2 TB accidents without automatic depressurization

10.2.2.1 TB without ADS and no boron release. Figure 10.10 shows the temperature history for the TB accident without ADS in the primary system. The pressure is constant (7.2 MPa) during the accident.

The important iodine compound is cesium iodide in this sequence without boron release but there is hydrogen iodide present in compartment 1 at high temperatures close to core slump.

Cesium hydroxide in the condensed phase is the dominant cesium compound. The gases cesium hydroxide and  $(\text{CsOH})_2$  are also present during the accident primarily in the beginning of and at the end of the accident sequence.

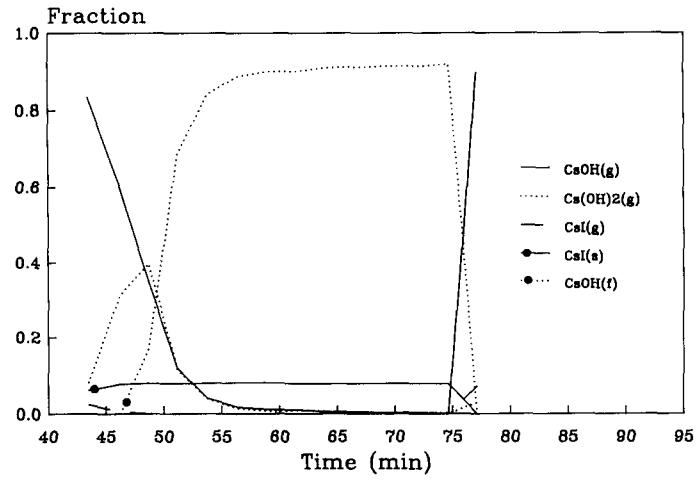


Figure 10.11. Distribution of cesium compounds in compartment 3.

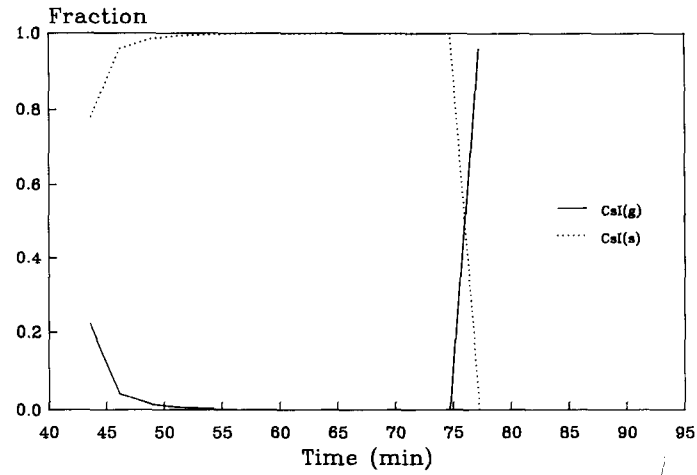


Figure 10.12. Distribution of iodine compounds in compartment 3.

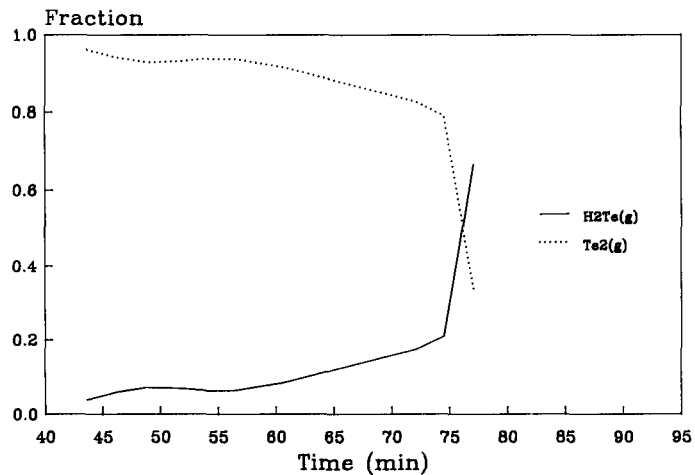


Figure 10.13. Distribution of tellurium compounds in compartment 3.

The CELSOL analysis shows further that  $Te_2$  and  $H_2Te$  are the important tellurium compounds.

Figures 10.11 to 10.13 show CELSOL results for cesium, iodine and tellurium.

10.2.2.2 TB without ADS and with boron data from Winfrith. The boron release is calculated with the RELCON code. We have used the same release constants as in the accident sequence with ADS but because of a different accident history the release of boron is approximately 1% of the inventory of boron in this case without ADS.

The thermohydraulic situation is as described above.

Cesium hydroxide gas and  $CsBO_2$  condensed are the important cesium compounds in compartment 1 but cesium iodide and cesium gases are also present. The dominant iodine compound is cesium iodide gas in compartment 1. There are very small amounts of hydrogen iodide in this compartment.

The dominant cesium compounds in compartment 3 are condensed  $CsBO_2$  and cesium hydroxide but gases of cesium hydroxide and  $(CsOH)_2$  are also present.

When it comes to iodine compounds in compartment 3 it is rather

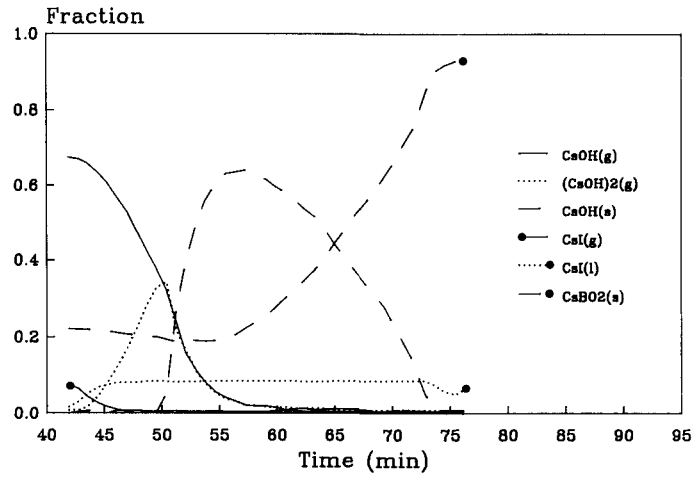


Figure 10.14. Distribution of cesium compounds in compartment 3.

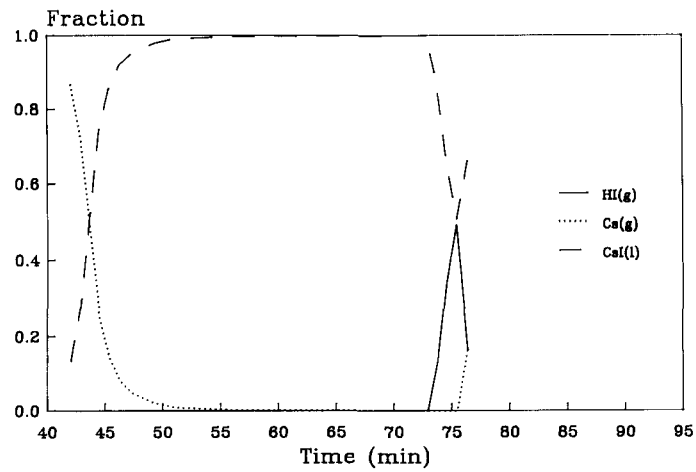


Figure 10.15. Distribution of iodine compounds in compartment 3.

interesting to notice that cesium iodide seems to be stable during the whole accident. Only at the very end and at rather high temperatures about 50% of the iodine is present as hydrogen iodide.

Figures 10.14 and 10.15 show CELSOL results for cesium and iodine.

10.2.2.3 TB without ADS and with JANAF boron data. The boron release is calculated as above.

The dominant cesium compound in compartment 1 is cesium hydroxide gas. The amount of  $\text{CsBO}_2$  condensed is much smaller here than in the previous sequence with the Winfrith boron data. Cesium gas is also present. Cesium iodide gas seems to be stable during the whole accident in compartment 1.

Cesium hydroxide condensed is totally dominating the cesium compounds in compartment 3. Condensed  $\text{CsBO}_2$ , cesium hydroxide gas,  $(\text{CsOH})_2$  gas are present in small amounts according to the CELSOL analysis.

The only iodine compound present in compartment 3 is cesium iodide.

Figures 10.16 and 10.17 show CELSOL results for cesium and iodine.

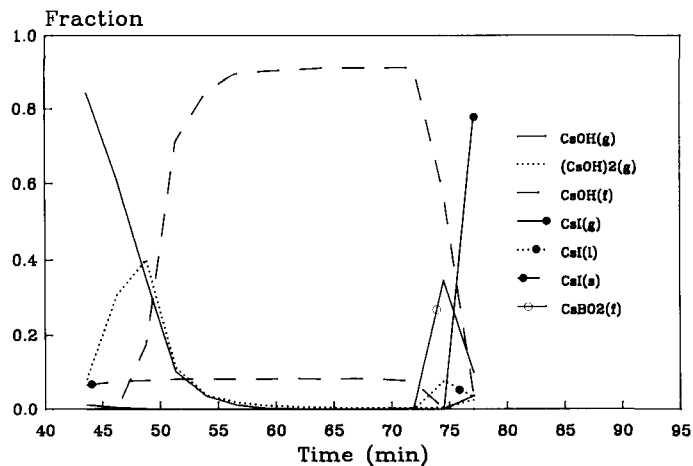


Figure 10.16. Distribution of cesium compounds in compartment 3.

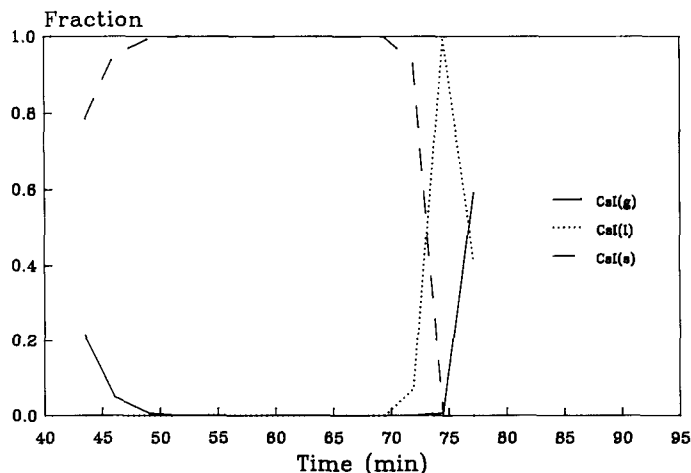


Figure 10.17. Distribution of iodine compounds in compartment 3.

#### 10.2.3 Analysis of the chemical importance of plate out

The Celsol code has an option for specifying plate out of condensed material, liquid or solid. The fraction of condensed material plated out (removed) in previous compartments is excluded from the subsequent equilibrium calculations. This means that changes in the gas phase may be expected, concerning both amounts and types of compounds present.

The analysis reported here deals with the TB accident sequence without ADS and is a comparison of the chemical behavior of the released elements in case of no plate out and 100% plate out of condensed material i.e. both liquid and solid material. The amount of released boron is the same in both cases. The used boron thermodynamic data are the Winfrith data.

We will concentrate on the behavior of iodine and caesium because of the radiological importance of these elements. Only results from the last compartment 3 is reported.

Figure 10.15 shows an analysis of the distribution of iodine containing compounds with no plate out in previous compartments. According to the Celsol calculations liquid cesium iodide dominates throughout the accident.

Figure 10.18 shows the distribution of iodine compounds with 100%

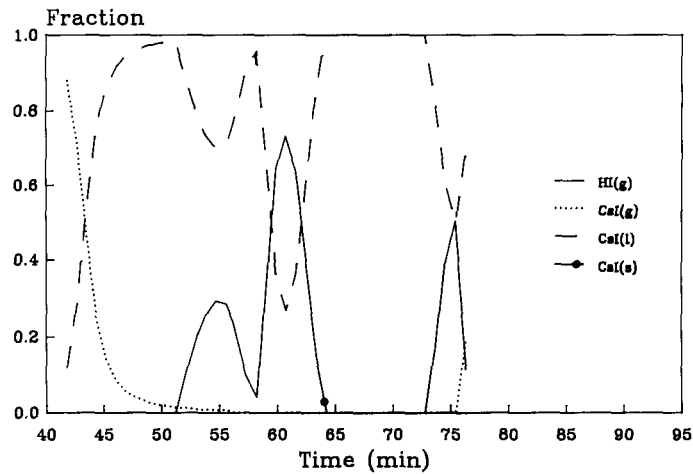


Figure 10.18. Iodine compounds in compartment 3 with plate out.

plate out of condensed material. At  $t = 10$  min. the amount of boron transported to compartment 3 is reduced due to plate out in compartment 1 and 2. As could be foreseen from the calculations without boron this results in a destabilization of liquid cesium iodide in favour of solid cesium iodide. The overall iodine behavior as cesium iodide and hydrogen iodide is not influenced.

Figure 10.14 shows the Celsol results for cesium compounds in compartment 3 without plate out. The most important cesium compounds are solid cesium hydroxide and solid  $\text{CsBO}_2$  but even gaseous cesium hydroxide is important.

Figure 10.19. shows the Celsol results for cesium compounds with plate out.

Solid cesium hydroxide and solid  $\text{CsBO}_2$  are again the dominant compounds but it is clear that the plate<sup>2</sup>out of boron in compartment 1 and 2 influences the chemical behavior in compartment 3 where a larger fraction of cesium is present as cesium hydroxide than in the case without plate out.

### 10.3 Conclusions concerning CELSOL Analyses

Two different TB accident sequences have been analysed with the CELSOL code.

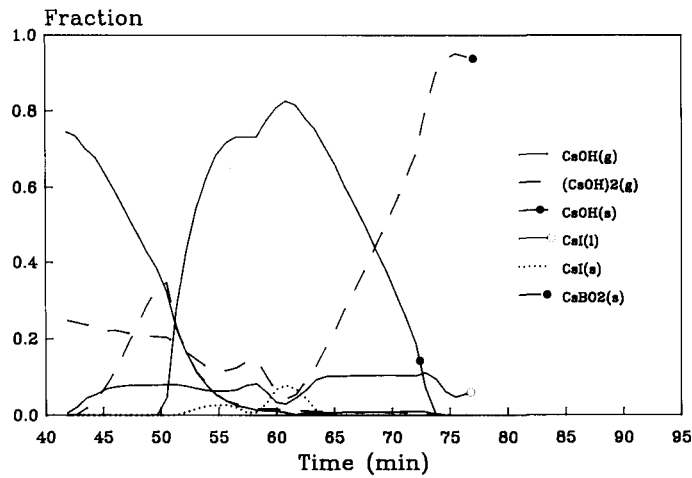


Figure 10.19. Cesium compounds in compartment 3 with plate out.

The CELSOL equilibrium calculations show a very strong influence from the release of boron from the control blades on the chemical behavior of iodine if the  $H_3BO_3$  thermodynamic data from Winfrith /12//13/ are used.

If e.g. boron is released in the TB accident without ADS it is calculated with the Celsol code using Winfrith thermodynamic data that between 15 and 20% of the iodine can be present as hydrogen iodide in the reactor vessel during the accident.

If no boron is assumed to be released or if boron thermodynamic data according to JANAF /10/ are used in the Celsol calculations more than 99% of the iodine is calculated to be cesium iodide.

The CELSOL analyses show that the accuracy and completeness of the thermodynamic data for boron is decisive for the results of chemical equilibrium calculations concerning cesium and iodine in reactor accident evaluations.

Plate out of condensed compounds within the reactor vessel can influence the chemical behavior of released material but for the analysed TB accident sequence without ADS it does not seem to change the overall chemical behavior.

#### 10.4 Recommendations for the future

A systematic testing - comparing CELSOL results with results from other code systems and results from experiments - could strongly be recommended.

Improvement of the CELSOL code itself is probably not recommendable, but a change of the manual preparation of input to the RELCON code from MARCH 3.0 output to a computerized preparation can be recommended. Such a change would make it much easier and faster to carry out analyses with the CELSOL code.

#### 10.5 References

- /1/ L. Schepper, CELSOL, Calculation of Chemical Equilibria in Reactor Accidents, Theory and User's Manual, Cowiconsult, Denmark.
- /2/ U. Steiner-Jensen, A. Pedersen, B. Fogh Schougaard, and L. Schepper, Chemical Reactions in LWR Reactor Vessels during Core Melt Accidents analysed with the Celsol Computer Code, Second American Chemical Society Symposium on Nuclear Reactor Severe Accident Chemistry, Toronto, Canada, June 5 - 10, 1988.
- /3/ U. Steiner-Jensen, A. Pedersen, B. Fogh Schougaard, and L. Schepper, Analyses of Chemical Reactions in LWR Reactor Vessels during Core Melt Accidents performed with the CELSOL Computer Code, International ENS/ANS Conference on thermal Reactor Safety, Avignon, France, October 2 - 7, 1988.
- /4/ A. Pedersen, K. E. Lindström-Jensen and U. Steiner-Jensen, The Safety of Nuclear Power Plants, Core Melt Accident Analyses for a BWR 3000 Reactor, Volume 1, ELSAM, DK-7000 Fredericia, Denmark.
- /5/ G. Eriksson, Thermodynamic Studies of High Temperature Equilibriums. XII SOLGAS-MIX, a Computer Program for Calculation of Equilibrium Compositions in Multiphase Systems, Chem. Scripta, 8 (1975) 100.
- /6/ T. M. Besmann, SOLGASMIX-PV, A Computer Program to Calculate Equilibrium Relationships in Complex Chemical Systems, ORNL/TM-5775, 1977.
- /7/ J. A. Giseke et al., Source Term Code Package, Users Guide, Mod 1, NUREG/CR-4587, BMI-2138, Batelle Columbus Division, 505 King Avenue, Columbus, OH 43201-2693, July 1986.
- /8/ U. Steiner-Jensen and K. E. Lindström-Jensen, RELCON, Calculation of Releases of Radioactive and non Radioactive Material during Core Melt Accidents, ELSAM, DK-7000 Fredericia, Denmark.
- /9/ Technical Bases for Estimating Fission Product Behavior during LWR Accidents, NUREG-0772, USNRC, June 1981.

- /10/ JANAF, Thermochemical Database, 1985, NBS, USA.
- /11/ E. H. P. Cordfunke, R. J. M. Konigs, G. Prins, P. E. Potter and M. H. Rand, Thermochemical Data for Reactor Materials and Fissions Products.
- /12/ B. R. Bowsher, S. Dickenson, J. S. Ogden and N. A. Young, New Estimates for the Thermodynamic Functions of Molecular Boric Acid, Chemistry Division, AEE Winfrith and Department of Chemistry, The University of Southampton, UK, March 1988.
- /13/ S. Dickenson, J. S. Ogden and N. A. Young, Vibrational Fundamentals and Thermodynamic Functions of Molecular Boric Acid: A Re-Evaluation of the  $\text{CsI} + \text{H}_2\text{BO}_3$  Reaction, Chemistry Division, AEE Winfrith and Department of Chemistry, The University of Southampton, UK, June 1988.

11 EXTENDED CHEMISTRY MODEL FOR THE MAAP CODE, BASED ON SOLGASMIX AND SIMPLISTIC SIMULATION OF REACTION RATE LIMITATIONS, FOR APPLICATIONS IN SENSITIVITY ANALYSIS.

The nordic countries have as the main analysis tool the MAAP code (Modular Accident Analysis Program, developed by Fauske & Assoc., INC., Illinois, USA). The chemistry model in this code is not very detailed, so we decided to develop a more realistic chemical model. The aim was not to exchange the ordinary MAAP chemical model for routine analysis, but to assess the consequences of the very simple chemical model in MAAP, and to gain a deeper understanding of phenomena of chemical importance during a severe accident sequence. Since the phenomena in the core are very complex we have concentrated our work on the modeling of chemistry in the vessel and later on in the containment.

11.1 Strategy for the development and implementation

Our aim was to develop and incorporate a chemical model into MAAP. We extract the thermal-hydraulic parameters of direct importance for chemical speciation from MAAP and also the steam to hydrogen ratio. The aerosol model of MAAP is left unchanged. Thus we did not attempt any large changes in the normal execution of MAAP.

11.2 Some thoughts about the modeling of chemistry during severe accident conditions

Generally, to be able to predict the future given some boundary conditions, it is necessary to know the possible ways the system may change with time. This means that a usable model of dynamic behavior is needed. Since MAAP has a decent modeling of the thermal-hydraulics, the aim of this work is thus to implement a chemical model with simplistic dynamics for chemical phenomena during severe accident conditions into MAAP.

Such a usable model might be divided into two parts.

1. Quantitative data for chemical phenomena.
2. A system of conditions and equations which utilize the above data to predict the chemical speciation as function of time and location in the reactor.

For such a model to be of practical use, there are at least three conditions which have to be fulfilled.

1. The data base must include all existing relevant data.
2. The conditions and equation system must include all necessary phenomena for the chosen approximation level.
3. Conditions 1 and 2 must not make the use of the model too

difficult to handle or demand too long execution time.

#### 11.2.1 Fulfillment of condition 1.

Since the only kind of data which are abundant enough are thermodynamic data a thermodynamic data base must be used.

#### 11.2.2 Fulfillment of condition 2.

The restriction of data to mainly thermodynamic data restricts the modeling of chemical reactions to chemical thermodynamics. This restriction is unlucky since it implies the use of thermodynamics, a static model of reality, to describe a dynamic process. The artificiality of using a static model for a dynamic process makes it necessary to use thermodynamics in the model in such a way that the model resembles a clumsy dynamic model, i.e. to model dynamic phenomena.

#### 11.2.3 Fulfillment of condition 3.

A selection has to be made among all available data for chemical compounds to make the equilibrium calculations manageable, see section 10. Also, the conversion of thermodynamics to a clumsy dynamic model must be carefully made, so that only the necessary conversions are made, and so that all necessary conversions are made.

### 11.3 The modeling of chemical phenomena

First follows a general description of the model, and thereafter a more detailed model for each main type of chemical system.

The condition of direct contact is fulfilled by a careful selection of chemical thermodynamic systems, such that each part (node) of the vessel is divided into four main systems, see below. Within each of them, the actual chemical systems is constructed so that only species in direct contact are in the same system and thus the number of actual chemical system varies from time step to time step.

The first of the main systems is the gas phase. The second system, the aerosol system, includes the gas and suspended particles. The third is the gas and surface system. This division is due to the fact that only a fraction of the suspended particles come into direct contact with the surface, but influence the surface indirectly via the gas phase. The fourth main system is the matter under the aerosol exposed surface material.

Starting amount for each specie for the gas and aerosol is the amount that has flowed into the node during the time step. The chemical potential is calculated with temperature equal to the gas temperature taken from MAAP.

After completed gas surface calculation the deposition of suspended particles is modeled by MAAP's aerosol model. The deposited particles enter as part of the surface in the next time step.

When the final chemical concentrations in the gas and aerosol systems are reached, i.e. when modeling have been performed for all necessary chemical systems, calculation starts for the third main system. Starting composition is taken as the gas composition calculated as above, together with the outer layer of deposited/condensed material on the surface. Temperatures for the chemical potential calculation are for the gaseous species the gas temperature, and for the surface located species the surface temperature, to ensure that the temperature difference is taken into account. No measures are taken to estimate the heat flow through the deposited layers, and thus all deposited substances are assumed to be of equal temperature. Simplistic initialization of matter transport, or lack of initialization, is performed.

The final composition of the aerosol is the composition that flows into the node down stream.

Since the effect of time on chemical reactions is that chemical equilibrium is not reached instantaneously, we have modeled the existence of a finite reaction time as a linear combination of calculated equilibrium composition  $C_{\text{equilibrium}}$  and the composition  $C_{\text{old}}$  in the previous time step.

$$C_{\text{new}} = (1-a) C_{\text{old}} + a C_{\text{equilibrium}}$$

where  $a$  is a real number between 0 and 1. This approach makes the final composition something between starting and equilibrium composition. An implicit assumption of this equation is that every reaction have the same reaction rate constant, which of course is not in accordance with scientific experience.

Inclusion of non-thermodynamical knowledge. An example which is easy to incorporate is kinetic stability. What is needed is a temperature interval and steam/hydrogen ratio interval between which a given species is kinetically stable. That species must not vary in amount during the equilibrium calculation. SOLGASMIX, the equilibrium program used, already contains this possibility.

#### 11.4 How to speed up the execution of the chemical model

Since the chemical model will be executed many times during a severe accident sequence, it is of great importance to have a high execution speed. If the execution speed is too slow, the model will not be of practical use. Two main measures can be taken to meet this need.

The first is to let the composition for the previous result of equilibrium calculation in the node be the starting estimate for the calculation to be done. This makes the start quite similar to the anticipated result and also minimizes the risk of failure to reach

the global minimum of chemical potential. This is already used in the current coding.

The second is to use a data base which contains only those species which may be thermodynamically stable during the prevailing conditions for each chemical system. We refer to section 10 for more information on such a data base. This has yet to be done.

#### 11.5 The specific descriptions for the main systems

The gas system consists of all gaseous species in the gas volume of the current node. As matter transport is fastest within the pure gas system this is treated first and separately from the remaining systems.

The gas and aerosol system consists of gas and aerosol particles. Reactions between gas and aerosol particles are assumed to be slower than pure gas phase reactions due to the existence of a stagnant boundary layer on the particle surfaces. Hence, these reactions are treated after the pure gas phase reactions.

The layer system consists of deposited material on the surfaces in the current node, each layer having a prescribed thickness. Solid-solid, solid-liquid and liquid-liquid reactions between adjoining deposited layers and between layers and underlying construction material are assumed to be fairly slow. They are thus treated after the previous systems.

The gas and surface system consists of the gaseous species and the outermost deposited layer or wall surface. Mass transfer is limited by the stagnant boundary layer. Reactions between the outermost layer and the gas phase are assumed to be the slowest and they are treated last.

#### 11.6 Summary of the chemical model

As decision of whether a chemical reaction between two materials in direct contact can take place, thermodynamics is used. This has as drawback that a static model (chemical thermodynamics) is used to describe a very dynamic process. A future desirable development would be to have a possibility to incorporate empirical knowledge, such as kinetic stability, in the model. This possibility would be especially important in the comparatively low temperatures in the containment.

The aerosol phase's chemical potentials are calculated for the gas temperature and the wall materials for the wall temperature. The time aspect is modeled in a qualitative way, and so is the condition of direct contact, which governs which chemical systems are formed. The formation and breakdown of chemical systems, and consequently the change of transport properties for a nuclide is only simplistically modeled. No attempts were made to model the balance between cohesive forces and gravity/convection.

There are important limitations of this model to bear in mind.

1. No detailed account can be taken of real reaction rates.
2. Phases which are nonideal are likely to form, especially due to solutions on wet vertical surfaces in the containment. Since it is not possible to model nonideal behaviour without experimental data on the specific mixture, we are prone to be short of thermodynamic data.
3. New, unknown compounds or mixtures may be formed, and obviously such occurrences are impossible to model without quantum chemical ab-initio calculations.
4. The time each compound and material is present in the gas and aerosol is short. This implies that metastable compounds (formed by the radiation or reaction intermediates) may exist in the aerosol for e.g. one minute. If the metastable compounds have different transport properties than the thermodynamically stable end products, the chemical model fails, as will every model which is based on thermodynamics.

#### 11.7 Functional description of the MAAP chemistry extension

Figure 11.7 shows the two new MAAP routines, CHTRAN (replacing FPTRAN), CHTRNP (replacing FPTRNP) and the modified version of INTGFP, acting as interfaces between MAAP and the new chemical model. The CHMODL routine executes the first level chemistry routines in order from left to right. Some of the first order routines execute in their turn second order routines etc. The Figure also indicates where subroutines from the SOLGASMIX library are used to compute the various chemical equilibria between reacting substances. The chemical model consists of 103 routines. A general description of the general logic and of individual first and second level routines is given below.

CHMODL is in principle called once for each node used by MAAP during the current time interval.

CHDBAS reads the chemical thermodynamics database as soon as any release from the core has begun.

CHFLOW computes the net flow of gas and aerosols into the current node.

##### 11.7.1 Gas phase reactions

The chemical modeling begins by treating reactions in the gas phase, module CHG, as the gas phase species in general are more mobile and reactive than condensed species.

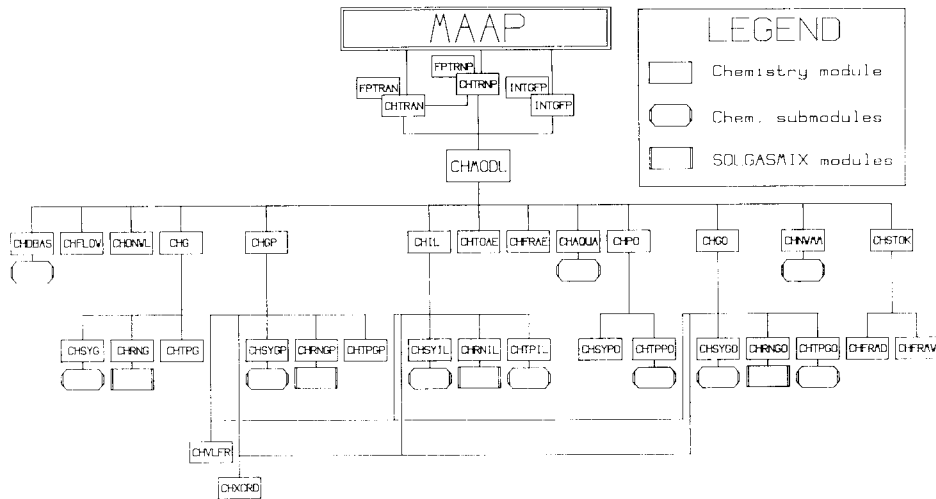


Figure 11.7. Top-down structure chart showing the chemistry extension to MAAAP developed within AKTI-150.

CHSYG determines the gaseous species present and their molar amounts from an internal book keeping of the previous composition of the standard MAAAP element groups and the current mass of each group. The routine then predicts possible, but yet nonexistent, reaction products. The temperature of the system is assumed to be the gas temperature in the current node.

CHRNG computes the concentrations corresponding to chemical equilibrium between reactants and reaction products. The new concentrations in the gas phase are then assumed to be a linear combination of starting and equilibrium concentrations.

$$C_{\text{new}} = (1-a) C_{\text{old}} + a C_{\text{equilibrium}}$$

This corresponds to a first order approximation of chemical kinetics when each reaction has its own a-value. So far, a universal a-value has been used for all reactions, which is a further approximation.

CHTPG finally computes the new chemical composition of the system, amount of each substance, resulting from the gas phase reactions. If condensed matter is formed, it is added to the aerosol mass in the current node.

### 11.7.2 Reactions between gas and aerosol

The second fastest reaction system is assumed to consist of aerosol particles and their surrounding gas. Mass transfer can usually be assumed to be faster in this system than for the other possible systems e.g. between gas and walls. Hence the reactions between the new gas phase and its aerosol particles are computed next by CHGP. The aerosol particles are assumed to consist of pure substances. Hence we have as many kinds of aerosol particles as there are condensed phases present. This model can be improved, if needed, by considering solid solutions.

CHVLFR computes the volume fraction of each kind of aerosol particle.

CHXCRD determines in which order the gas - particle reactions should be considered from the relative volume fractions of the various kinds of aerosol particles. Reactions with the particle kind having the largest volume fraction is computed first, the second largest next etc.

CHGP then loops over the three routines CHSYGP, CHRNGP and CHTPGP for all aerosol particle kinds present.

CHSYGP determines the amount of gas in direct contact with the current particle kind from the volume fraction occupied by this kind of particles and predicts the chemical reactions possible between this particle kind and the gas. The temperature is assumed to be the gas temperature in the current node.

CHRNGP computes the concentrations corresponding to chemical equilibrium between reactants and reaction products. The new concentrations in the gas phase are then assumed to be a linear combination of starting and equilibrium concentrations in the same manner as for the gas system. The new aerosol particle mass is also computed in the same way.

CHTPGP computes the new chemical composition of the system, amount of each substance, resulting from the gas - particle reactions. The routine then distributes the amounts of substances present as gas and condensed matter between gas phase and aerosol particles.

### 11.7.3 Reactions between deposited substances

Reactions between deposited substances not in direct contact with the gas phase and its aerosol particles are assumed to proceed independently of those in the gas and those between gas and aerosol. All deposits are assumed to have a layer structure. Each layer is assumed to be in contact with the next deeper and next outer layer only. When gases are formed they are assumed to be released to the gas phase.

Reactions in and between deposited layers are handled by the CHIL routine. This routine loops over the subordinate routines for all

heat sinks present in the current node, for all layers present on a heat sink and for all substances present in a layer.

CHVLFR computes the volume of each deposited substance in the current layer.

CHXCRD determines the order in which the substances should be considered from their volume fractions.

CHSYIL predicts the possible chemical reactions between the current substance and all other substances in direct contact with it, i.e. present in the current layer or in the two adjoining layers. The temperature is assumed to be the wall temperature of the current heat sink.

CHRNIL computes the concentrations corresponding to chemical equilibrium between reactants and reaction products. The new concentrations in the layer are then assumed to be a linear combination of starting and equilibrium concentrations.

CHTPIL determines the effect of the chemical reactions on the composition and mass of the current layer. Matter may be transferred between layers as a consequence of the reactions. Any gaseous substance formed is assumed to escape to the gas phase in the current node. As a consequence, layers may increase or decrease in thickness or even disappear.

#### 11.7.4 Aerosol deposition

The mass of newly deposited aerosol in the current node is converted to moles by the CHFRAE routine.

11.7.4.1 Nodes with liquid water present. When there is liquid water present in a node, all aerosol deposition is assumed to be in the water. Soluble gases are also assumed to be transferred to aqueous solution. Further transport of deposited material and dissolved gases is assumed to follow the flow of water. When all water present in a node evaporates the dissolved substances are assumed to form the same layer structure as they would have done if deposited without water ever present.

CHAQUA handles the dissolution of substances in water and the effects from dryout of a node. When water is present, the routines for layer formation and for reactions between gas and the upper deposited layer are bypassed by CHMODL.

11.7.4.2 Dry nodes. When there is no water present, aerosol particles are deposited on dry surfaces. The freshly deposited aerosol is assumed to form a new top layer on each surface when a prescribed layer thickness is exceeded else it is added to the current top layer.

The routine CHPO handles dry deposition on surfaces in a node.

CHSYPO determines the amount of aerosol particles to be deposited on the surface.

CHTPPO computes the thickness, volume and composition of the top layer and starts a new top layer if the prescribed layer thickness is exceeded for the current top layer.

#### 11.7.5 Reactions between gas and surfaces

All reactions between gas and dry surfaces are assumed to be limited to the exposed, top, layers in the node.

CHGO first uses CHVLFR and CHXCRD to determine the actual layer volumes, volume fractions and order of calculation. It then sets up a loop over all pure substances in the top layer. This loop spans the routines CHSYGO, CHRNGO and CHTPGO.

CHVLFR computes the volume fraction of each substance in the top layer.

CHXCRD determines the order in which the substances should be considered from their volume fractions.

CHSYGO determines the amount of gas in direct contact with the current substance from the volume fraction occupied by this substance in the layer and predicts the chemical reactions possible between the substance and the gas. The temperature of the top layer and of any condensed species is assumed to be the wall temperature in the current node and the temperature of the gas is assumed to be the gas temperature in the current node.

CHRNGO computes the concentrations corresponding to chemical equilibrium between reactants and reaction products. The new concentrations in the gas phase and condensed phases are then assumed to be a linear combination of starting and equilibrium concentrations.

CHTPGO computes the new chemical composition of the system, amount of each substance, resulting from the gas - top layer reactions. The routine then distributes the amounts of substances present as gas and condensed matter between gas phase and surface. Deposited matter forms a new layer as soon as the prescribed layer thickness is exceeded. Part or all of the existing top layer may also disappear in this process.

#### 11.7.6 Formation of new amounts in the MAAP groups

The results of chemical reactions may be transfer of mass between the classic MAAP chemical groups, addition of new mass or loss of existing mass. To be able to resume execution of MAAP after the chemical modeling the resulting distribution of mass between the MAAP groups in the current node is computed from the chemical com-

position and existing phases in the system. The information used for this transformation is also saved internally by the chemical model routines as this information is needed again to split the masses in the MAAP groups into individual substances next time.

CHNWMM converts the amount of each substance in moles to corresponding mass in the proper MAAP element group for the current node.

#### 11.7.7 Mass rate of change calculation

When the MAAP routines have dealt with all nodes, CHMODL calls on CHSTOK to convert previous and current masses and the timestep into mass rates for use by the INTGFP routine.

CHSTOK sets up a loop over all nodes. When a node is dry it calls upon CHFRMD to compute the rates of change in masses. When there is liquid water present in a node it calls instead on CHFRMW to do a similar calculation for this case.

### 11.8 Applications

The model, which might be used independent of MAAP, can be used in several different ways for analysis of severe accident chemistry.

1. For a separate node, without any flow between the nodes. This implies that the user specifies gas temperature, wall temperature, node volume,  $P(H_2O)/P(H_2)$  and either; a. number of elements and their respective molar amounts or b. aerosol composition, gas composition and the composition of the wall system.

This part is to be used for point analysis of possible states during an accident sequence and can be used to answer questions of type: With that and that composition and physical conditions, what happens? What happens if the composition is changed with respect to some element or some physical parameter?

2. To study the effect of a better chemical modeling of vapor pressure equilibria.

The chemical model is implemented in MAAP and the MAAP model of vapor pressure equilibrium is not used. Input to the extended MAAP version is identical to input to ordinary MAAP, unless the user wishes to change some of the default values. Default values consists of elements and the data base used.

3. For sensitivity analysis.

The model may of course be used for sensitivity analysis, due to its ability to take many important aspects of chemistry into account, as well as the availability of a well developed data base.

4. To assess future experiments of importance.

Together with the thermal-hydraulics the model facilitates a deeper understanding of the dynamics of what happens (or what may happen) during a severe accident sequence, and thus also what we ought to know more about. Experiments to enlighten the interaction between the thermal hydraulics and chemistry may be one spinoff effect of this model, as well as which nonideal mixtures should be studied.

5. To assess possible chemical actions for mitigation.

Another possible application is to improve the understanding of the dynamics of the whole accident sequence, and the sensitivity of various events to the release of fission products into the environment. A possible consequence of such a deeper understanding may be to know if any chemicals ought to be added during a certain transient in order to influence the chemistry in a releasing (in the benign sense) way.

#### 11.9 Recommendations for future development

There are four main tasks to accomplish in the future.

1. A better chemical model for core-phenomena than the one present in MAAP. Such a model must include direct coupling with the thermal-hydraulic model and flow properties.
2. A rationally chosen chemical thermodynamic data base with inclusion of relevant data for water solutions. Inclusion of kinetic data, such as reactivity of species.
3. Inclusion of all relevant structural material in the reactor.
4. Cooperation with specialists on thermal-hydraulics to formulate a better model for heat transfer between gas and surfaces, especially with regard to the insulating effect of deposits.

The reasons for these considerations are as follows.

For 1, consider the effect of formation of mixtures with low melting-points, such as eutectica which include boron and other construction materials. Drastically different flow properties result, compared with the original material. The TMI experience may be a good indicator of this.

For 2. it is obvious that much of the fission products get stuck in water pools, so we need knowledge of what may happen in the water. A rationally chosen thermodynamic data base greatly improves the speed of the model without diminishing the relevance. It also aids in deciding which substances may be formed under specific conditions. The effect of high activation energy may be negligible for very high temperatures, but become decisive in e.g. the containment.

For 3, very large amounts of different materials are present in reactor and containment and some of these may have a decisive in-

fluence on fission product behavior.

For 4, the temperature of matter is dependent on its heat conductivity, which probably is small for some deposits, e.g. oxides of tin and manganese.

## 12 COMPARISON BETWEEN THE CHMAAP AND MAAP CODES

One of the objectives of AKTI-150 was to assess the influence of chemical phenomena upon the course of an accident. To this end, two computer codes have been developed. CELSOL in Denmark and CHMAAP in Sweden, both codes have been described earlier in this report. A further objective with the development of CHMAAP was to obtain a tool to make a sensitivity analysis on the MAAP code possible with regard to chemical effects. As seen below there are important differences in fission product distribution as well as in chemical speciation for CHMAAP and MAAP 3.0. The sequence chosen was an AB sequence for the Swedish R1 plant.

### 12.1 How the comparison was performed

The differences between CHMAAP and MAAP may be considered to be grouped into two classes. One is the possibility to qualitatively model reaction time in CHMAAP, the other possibility includes all other differences such as the way to take into account the temperature difference between gas and wall, the possibility to model chemical reactions and the mass transfer considerations with respect to direct contact between matter. Two demonstration calculations were made with CHMAAP, one where high rates of the chemical changes were modeled and one with lower rates of the chemical changes. By this approach it was possible to get a feeling for the influence of phenomena in the two classes on the differences between CHMAAP and MAAP.

For CHMAAP the FP distributions for various times are given for high rates of chemical changes in tables 12.1.1 (1000 s), 12.1.2 (5633 s, vessel failure) and 12.1.3 (10 000 s) and for low rates in tables 12.1.4 (1000 s), 12.1.5 (5633 s, vessel failure) and 12.1.6 (10 000 s).

For MAAP the corresponding distributions are given in tables 12.1.7 (1000 s), 12.1.8 (5630 s, vessel failure) and 12.1.9 (10 000 s).

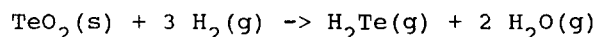
#### 12.1.1 Description of some of the differences observed

All observed differences will not be described. Instead some key effects were chosen and possible explanations for them in terms of different modeling discussed.

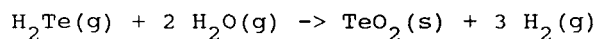
The differences between the case with high rates of chemical changes and the case with lower rates are significant but not striking. There is a tendency for the fission products to be more evenly distributed in the plant for the case with lower rates. This is to be expected since the distribution in case of lower rates imply less dependence on the conditions at the first place the species encounter, so the species are to a higher degree transported further on to other parts of the plant.

In spite of the small database used by CHMAAP, three chemical reactions of interest were observed. The result in terms of transport are of interest for all three of them. These reactions involved Te and Mo.

Tellurium can react as follows:

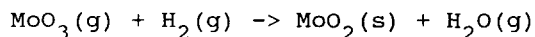


This reaction involves  $\text{TeO}_2(\text{s})$  aerosol particles and produces the gas  $\text{H}_2\text{Te}(\text{g})$ . All  $\text{TeO}_2(\text{s})$  aerosol particles formed  $\text{H}_2\text{Te}(\text{g})$ . The hydrogen telluride gas can react with excess water vapor again forming tellurium oxide and hydrogen in regions with a higher steam to hydrogen ratio or other temperature.



The  $\text{TeO}_2(\text{s})$  formed occurred as condensate on walls colder than the gas and it was the temperature difference between gas and wall that made the reaction thermodynamically possible. This reaction did not occur very frequently but its very existence is interesting. It occurred mainly in the lower downcomer. These two reactions involving Te provide another mode of Te transport than as  $\text{TeO}_2(\text{s})$  in aerosol particles.

The reaction with Mo was as follows.



This occurred both in the aerosol and between the walls and the gas phase. The stable condensed specie of Mo is thus not  $\text{MoO}_3(\text{s})$  but  $\text{MoO}_2(\text{s})$ . Since  $\text{MoO}_2(\text{s})$  has a higher chemical potential than  $\text{MoO}_3(\text{s})$  it is likely to undergo other chemical reactions more readily than  $\text{MoO}_3(\text{s})$ .

CHMAAP models less release than MAAP of CsOH and CsI from the pressure vessel to the containment. The explanation for this is not MAAP's inability to model chemical reactions but more complicated.

Initially CsOH and CsI are deposited mainly as aerosols on the same surface. The surface is then heated by thermal conduction through the construction material of the vessel. CsI and CsOH contribute to the heat by radioactive decay, causing the temperature of the surface to rise even more. CsOH evaporates and partly quickly forms aerosol particles in the gas, partly condenses on the other relatively cold surface. The aerosol particles are not in direct contact with the surfaces because they are suspended in the gas and cannot immediately deposit on surfaces. The condensing of CsOH(g) onto the colder surface is relatively fast and makes the CsOH(s) aerosol particles evaporate. The CsOH(s) in the aerosol particles which have not had time to evaporate and condense on the colder surface is partly blown out into the drywell. CsI is subject to the same phenomena as CsOH, but is less readily forming its gas phase, CsI(g), and hence remains a longer time as aerosol particles. The consequence is that a higher proportion of CsI than CsOH is found in

the containment. Since the gas flow into the drywell is low at this time the overall consequence is a retainment of CsOH and CsI in the upper head.

The most important reason for the different results between CHMAAP and MAAP for CsOH and CsI in the containment is that MAAP does not model the condition of direct contact. Also, MAAP does not distinguish properly between the different surface temperatures.

The resulting amounts of fission products are significantly different in the containment for CHMAAP and MAAP. These differences are mainly caused by the different modeling of phenomena in the pressure vessel mentioned above and not by differences in the modeling of processes in the containment.

There were no releases of fission products to the environment during the sequence so the eventual effects of chemistry on the external source term could not be evaluated.

## 12.2 Conclusions

Due to the small data base used and the limitation to a comparison for one sequence only it is impossible to draw any certain conclusions concerning the general importance of the findings reported above. However, phenomena were observed which seems to be important to take into account for an estimation of the fission product distribution and which are not modeled by MAAP.

The differences between the cases with fast chemical changes and with slower changes were largest in the very beginning. The longer the time since release from the core the less significant were the differences. The modeling of rates is likely to be most important during rapid changes in the plant, such as those occurring when the vessel or containment fails.

Chemical reactions are important for the transport behavior of the fission products. Even with the small data base used it was found that the hydrogen to steam ratio is important for the transport properties of Te and Mo.

The temperature differences between gas and wall made reactions possible which would be ruled out for systems with a homogenous temperature distribution.

If the different heat sinks in a node have significantly different temperatures it may give rise to a mass transfer, via aerosol particles and gas, from one heat sink to another. This phenomena implies that the fission products are not transported very far from the site wherefrom they evaporated when the gas flow is low.

It is important to model chemical changes only between phases which are in direct contact.

Finally a comment on the possibilities of informative output from

CHMAAP. The structure of CHMAAP provides data, not available from MAAP, which will make it easier to understand the reason for observed phenomena. The rates of gas to aerosol transition, the rate of condensation onto the walls etc are all important for an understanding of what is going on in the reactor. This gives a snapshot of ongoing processes. An example of this kind of information is given in table 12.3.1.

### 12.3 Recommendations for the future

- 1 Production of a rationally chosen database, see chapter 10.
- 2 Development of a model for the influence of e.g. boron carbide on the core geometry and consequently on the core source term.
- 3 Inclusion of the elements present in construction materials in the vessel and in the containment, and a corresponding chemical database.
- 4 Recognition of the effects on heat conductivity and mass transfer of the relatively thick layers of e.g. Sn and Mn compounds which are mainly deposited on the surfaces in the vessel. These layers have undoubtedly a large influence on the heat exchange between gas and wall. The chemical modeling can be used to calculate the amount of deposited matter which then can be used to estimate the corresponding heat transfer coefficient.

Table 12.1.1. AB sequence in R1 as modeled by CHMAAP at 1000 s into the accident assuming high reaction rates.

COMPARTMENT CONDITIONS: TIME= 1000 SECONDS					
FISSION PRODUCT MASS IN RPV (kg)					
		CORE	SHRD HEAD	SEPARATERS	UPP HEAD
GROUP 1	VAPOR	0.1024E-01	4.800	2.352	19.34
	AEROSOL	0.6647E-03	2.341	1.095	4.984
	DEPOSIT	0.7748E-05	0.3640	0.6436E-01	1.218
GROUP 2	VAPOR	0.000	0.1843E-01	0.4945E-02	0.3964E-02
	AEROSOL	0.000	0.3394	0.1578	1.006
	DEPOSIT	0.000	0.8035	0.1780	0.4136
GROUP 3	VAPOR	0.000	0.4015	0.2026	1.639
	AEROSOL	0.000	0.000	0.000	0.000
	DEPOSIT	0.000	0.3792E-02	0.000	0.000
GROUP 4	VAPOR	0.000	0.000	0.000	0.000
	AEROSOL	0.000	0.9037E-06	0.4359E-06	0.2137E-05
	DEPOSIT	0.000	0.1632E-06	0.2962E-07	0.5338E-06
GROUP 5	VAPOR	0.000	0.2258E-09	0.6183E-10	0.5015E-10
	AEROSOL	0.000	0.6171E-08	0.2610E-08	0.9765E-08
	DEPOSIT	0.000	0.2754E-08	0.1153E-08	0.2911E-08
GROUP 6	VAPOR	0.000	0.2768	0.3734E-01	0.3109E-01
	AEROSOL	0.000	1.591	0.8068	4.475
	DEPOSIT	0.000	9.624	1.357	2.218
SURF TEMP (K)		591.2	579.1	569.2	558.4
		568.6	583.1		559.7
CSI DEP MASS		0.000	0.4497	0.1780	0.7254E-01
(kg)		0.000	0.3538		0.3410
		UPP DWNCMR	LOW DWNCMR	LOW HEAD	RECIRC
GROUP 1	VAPOR	7.060	0.9647	0.2124	0.7392E-01
	AEROSOL	1.374	0.1342	0.1641E-01	0.8871E-02
	DEPOSIT	0.2639	0.2002E-02	0.2041E-03	0.3231E-03
GROUP 2	VAPOR	0.2895E-03	0.5529E-05	0.1906E-06	0.1583E-06
	AEROSOL	0.3692	0.5497E-01	0.1201E-01	0.4130E-02
	DEPOSIT	0.8775E-01	0.1329E-02	0.2499E-03	0.1842E-03
GROUP 3	VAPOR	0.5791	0.6962E-01	0.1333E-01	0.5144E-02
	AEROSOL	0.000	0.000	0.000	0.000
	DEPOSIT	0.000	0.000	0.000	0.000
GROUP 4	VAPOR	0.000	0.000	0.000	0.000
	AEROSOL	0.6198E-06	0.6407E-07	0.8431E-08	0.4315E-08
	DEPOSIT	0.1216E-06	0.1015E-08	0.1129E-09	0.1606E-09
GROUP 5	VAPOR	0.3748E-11	0.7177E-13	0.1811E-14	0.2034E-14
	AEROSOL	0.2331E-08	0.1927E-09	0.1889E-10	0.1199E-10
	DEPOSIT	0.4641E-09	0.3308E-11	0.1944E-12	0.4559E-12
GROUP 6	VAPOR	0.2286E-01	0.7739E-03	0.1063E-02	0.6235E-04
	AEROSOL	1.648	0.2279	0.4909E-01	0.1690E-01
	DEPOSIT	0.1788	0.1013E-01	0.7436E-04	0.7086E-03
SURF TEMP (K)		558.9	558.3	551.3	557.6
		569.2	591.2	440.8	
		559.2	441.6		
CSI DEP MASS		0.000	0.1864E-04	0.2499E-03	0.1842E-03
(kg)		0.000	0.000	0.000	

Continues on next page.

Table 12.1.1. Continued

FISSION PRODUCT	MASS (kg)	CONTAINMENT <sup>1)</sup>
	RPV	
GROUP 1 VAPOR	34.81	15.86
AEROSOL	9.954	1.660
DEPOSIT	1.913	0.5759E-01
CORIUM	0.000	0.000
GROUP 2 VAPOR	0.2764E-01	
AEROSOL	1.943	0.9262
DEPOSIT	1.485	
CORIUM	0.000	0.000
GROUP 3 VAPOR	2.911	
AEROSOL	0.000	0.9912
DEPOSIT	0.3792E-02	
CORIUM	0.000	0.000
GROUP 4 VAPOR	0.000	2)
AEROSOL	0.4173E-05	----
DEPOSIT	0.8495E-06	
CORIUM	0.000	0.000
GROUP 5 VAPOR	0.3416E-09	2)
AEROSOL	0.2110E-07	----
DEPOSIT	0.7287E-08	
CORIUM	0.000	0.000
GROUP 6 VAPOR	0.3699	
AEROSOL	8.814	3.757
DEPOSIT	13.39	
CORIUM	0.000	0.000

- 1) SINCE WE HAVEN'T YET FINISHED THE MODELING IN THE CONTAINMENT, WE ONLY DISPLAY TOTAL FIGURES FOR THE CONTAINMENT.
- 2) IT ISN'T POSSIBLE TO CALCULATE THE CONTAINMENT-CONTENT FOR THIS GROUP SINCE A TOO SMALL FRACTION OF THE GROUP HAS BEEN RELEASED.

Table 12.1.2. AB sequence in R1 as modeled by CHMAAP at vessel failure 5632 s into the accident assuming high reaction rates.

COMPARTMENT CONDITIONS: TIME= 5632 SECONDS VESSEL - FAILURE.  
FISSION PRODUCT MASS IN RPV (kg)

	CORE	SHRD HEAD	SEPARATERS	UPP HEAD
GROUP 1 VAPOR	0.6092E-03	0.3921E-02	0.2564E-02	3.370
AEROSOL	0.3429E-04	0.4777E-01	0.2955E-01	3.301
DEPOSIT	0.5697E-01	110.3	5.499	696.5
GROUP 2 VAPOR	0.000	0.1988E-04	0.4842E-03	0.1130E-01
AEROSOL	0.000	0.3754E-02	0.6569E-02	1.194
DEPOSIT	0.000	0.7513E-05	1.558	11.62
GROUP 3 VAPOR	0.000	0.2664E-03	0.1646E-03	0.7598E-01
AEROSOL	0.000	0.000	0.000	0.000
DEPOSIT	0.000	0.000	0.1341E-17	0.3817E-07
GROUP 4 VAPOR	0.000	0.000	0.000	0.000
AEROSOL	0.000	0.4586E-03	0.3535E-03	0.1600E-01
DEPOSIT	0.000	0.1250E-01	0.3590E-02	0.7883E-01
GROUP 5 VAPOR	0.000	0.6923E-05	0.2044E-04	0.8690E-04
AEROSOL	0.000	0.5713E-02	0.5054E-02	0.8441E-01
DEPOSIT	0.000	0.1780	0.8303E-01	0.4785
GROUP 6 VAPOR	0.000	0.9117E-04	0.9540E-04	0.2141
AEROSOL	0.000	0.1699E-02	0.3848E-02	1.014
DEPOSIT	0.000	0.6649E-06	0.2416E-09	93.23
SURF TEMP (K)	1351.	802.2	629.6	590.6
	781.1	809.2		970.4
CSI DEP MASS	0.000	0.1430E-10	1.558	11.60
(kg)	0.000	0.7513E-05		0.1328E-01
	UPP DWNCMR	LOW DWNCMR	LOW HEAD	RECIRC
GROUP 1 VAPOR	9.603	4.249	17.03	0.5879
AEROSOL	3.291	0.8290	0.9544	0.9078E-01
DEPOSIT	105.9	8.021	10.43	2.022
GROUP 2 VAPOR	0.1171E-01	0.2302E-01	0.6732E-05	0.4389E-04
AEROSOL	1.571	0.1426E-01	0.2432	0.1351E-01
DEPOSIT	1.710	1.522	0.6884	0.1437
GROUP 3 VAPOR	0.2536	0.6935E-02	0.2184	0.3344E-02
AEROSOL	0.000	0.000	0.000	0.000
DEPOSIT	0.000	7.928	0.000	0.000
GROUP 4 VAPOR	0.000	0.000	0.000	0.000
AEROSOL	0.1652E-01	0.3258E-02	0.1190E-02	0.2950E-03
DEPOSIT	0.1526E-01	0.1472E-02	0.1042E-02	0.2193E-03
GROUP 5 VAPOR	0.1516E-04	0.2713E-06	0.7117E-09	0.3635E-08
AEROSOL	0.9592E-01	0.2229E-01	0.1049E-01	0.2241E-02
DEPOSIT	0.9443E-01	0.1005E-01	0.4132E-02	0.1157E-02
GROUP 6 VAPOR	0.3349E-01	0.4771E-02	0.6531E-04	0.7964E-04
AEROSOL	0.1781	0.1473E-02	0.7924E-03	0.1056E-03
DEPOSIT	19.25	13.74	8.840	2.134
SURF TEMP (K)	584.9	812.5	542.7	566.4
	629.6	1351.	405.1	
	782.8	414.6		
CSI DEP MASS	0.8649	0.5917	0.6884	0.1437
(kg)	0.7520	0.000	0.000	
	0.9292E-01	0.9304		

Continued on next page.

Table 12.1.2. Continued

FISSION PRODUCT		MASS (kg)	CONTAINMENT <sup>1)</sup>
		RPV	
GROUP 1	VAPOR	34.84	341.04
	AEROSOL	8.543	25.92
	DEPOSIT	938.7	83.70
	CORIUM	0.000	0.000
GROUP 2	VAPOR	0.4658E-01	
	AEROSOL	3.046	12.18
	DEPOSIT	17.24	
	CORIUM	0.000	0.000
GROUP 3	VAPOR	0.5587	
	AEROSOL	0.000	20.49
	DEPOSIT	7.928	
	CORIUM	0.000	0.000
GROUP 4	VAPOR	0.000	
	AEROSOL	0.3807E-01	0.9873E-01
	DEPOSIT	0.1129	
	CORIUM	53.72	0.2137E-02
GROUP 5	VAPOR	0.1297E-03	
	AEROSOL	0.2261	0.1862
	DEPOSIT	0.8493	
	CORIUM	125.6	0.4995E-02
GROUP 6	VAPOR	0.2527	
	AEROSOL	1.200	56.71
	DEPOSIT	137.2	
	CORIUM	0.000	0.000

- 
- 1) SINCE WE HAVEN'T YET FINISHED THE MODELING IN THE CONTAINMENT, WE ONLY DISPLAY TOTAL FIGURES FOR THE CONTAINMENT.
  - 2) IT ISN'T POSSIBLE TO CALCULATE THE CONTAINMENT-CONTENT FOR THIS GROUP SINCE A TOO SMALL FRACTION OF THE GROUP HAS BEEN RELEASED.

Table 12.1.3. AB sequence in R1 as modeled by CHMAAP at 10 000 s into the accident assuming high reaction rates.

COMPARTMENT CONDITIONS: TIME= 10000 SECONDS  
FISSION PRODUCT MASS IN RPV (kg)

	CORE	SHRD HEAD	SEPARATERS	UPP HEAD
GROUP 1 VAPOR	1.577	0.7579	0.6054	6.093
AEROSOL	0.1486	0.7284E-01	0.1415E-01	0.1245
DEPOSIT	0.1117	110.9	5.541	697.1
GROUP 2 VAPOR	0.000	0.1994E-04	0.1296E-04	0.7011E-03
AEROSOL	0.000	0.1712E-02	0.1366E-03	0.4336E-03
DEPOSIT	0.000	0.8895E-04	1.528	12.17
GROUP 3 VAPOR	0.000	0.4967E-03	0.1444E-04	0.3093E-06
AEROSOL	0.000	0.000	0.000	0.000
DEPOSIT	0.000	0.000	0.000	0.000
GROUP 4 VAPOR	0.000	0.000	0.000	0.000
AEROSOL	0.000	0.3117E-02	0.9555E-04	0.3016E-03
DEPOSIT	0.000	0.6264E-01	0.4659E-02	0.8144E-01
GROUP 5 VAPOR	0.000	0.3299E-04	0.2085E-07	0.1369E-10
AEROSOL	0.000	0.2892E-02	0.1693E-03	0.1062E-02
DEPOSIT	0.000	0.5586	0.1032	0.5042
GROUP 6 VAPOR	0.000	0.3702E-02	0.2400E-03	0.7208E-04
AEROSOL	0.000	0.1221E-05	0.6926E-06	0.1153E-04
DEPOSIT	0.000	0.4083E-09	0.2178	96.26
SURF TEMP (K)	1485.	777.5	665.1	702.0
	794.2	788.0		904.2
CSI DEP MASS	0.000	0.000	1.528	12.17
(kg)	0.000	0.8895E-04		0.4537E-07
	UPP DWNCMR	LOW DWNCMR	LOW HEAD	RECIRC
GROUP 1 VAPOR	4.543	1.237	4.513	0.1749
AEROSOL	0.1106	0.3117E-01	0.3431	0.4295E-02
DEPOSIT	107.8	8.460	12.32	2.107
GROUP 2 VAPOR	0.4690E-04	0.1020E-03	0.4879E-04	0.4317E-05
AEROSOL	0.9265E-03	0.4746E-04	0.1447E-02	0.1372E-04
DEPOSIT	1.847	1.770	0.8182	0.1919
GROUP 3 VAPOR	0.4958E-04	0.9669E-05	0.6016E-03	0.1374E-05
AEROSOL	0.000	0.000	0.000	0.000
DEPOSIT	0.000	8.058	0.000	0.000
GROUP 4 VAPOR	0.000	0.000	0.000	0.000
AEROSOL	0.3004E-03	0.7517E-04	0.1942E-02	0.1018E-04
DEPOSIT	0.2881E-01	0.3677E-02	0.1020E-01	0.6280E-03
GROUP 5 VAPOR	0.6656E-08	0.5464E-09	0.8057E-05	0.4188E-10
AEROSOL	0.1061E-02	0.2995E-03	0.2106E-02	0.4127E-04
DEPOSIT	0.2369	0.3003E-01	0.6513E-01	0.4550E-02
GROUP 6 VAPOR	0.4140E-02	0.5219E-03	0.1160E-02	0.4224E-04
AEROSOL	0.9423E-06	0.6211E-07	0.2308E-06	0.6021E-08
DEPOSIT	14.11	15.15	10.24	2.527
SURF TEMP (K)	615.5	1077.	575.6	588.5
	665.1	1485.	426.2	
	775.8	546.0		
CSI DEP MASS	0.9938	0.2324E-07	0.8182	0.1919
(kg)	0.8536	0.000	0.000	
	0.6322E-06	1.770		

Continued on next page.

Table 12.1.3. Continued

FISSION PRODUCT		MASS (kg)	CONTAINMENT <sup>1)</sup>
		RPV	
GROUP 1	VAPOR	19.50	358.6
	AEROSOL	0.8493	6.188
	DEPOSIT	944.3	171.8
	CORIUM	0.000	0.000
GROUP 2	VAPOR	0.9360E-03	
	AEROSOL	0.4717E-02	14.36
	DEPOSIT	18.33	
	CORIUM	0.000	0.000
GROUP 3	VAPOR	0.1174E-02	
	AEROSOL	0.000	21.092
	DEPOSIT	8.058	
	CORIUM	0.000	0.000
GROUP 4	VAPOR	0.000	
	AEROSOL	0.5843E-02	0.2972
	DEPOSIT	0.1921	
	CORIUM	0.2625	207.9
GROUP 5	VAPOR	0.4107E-04	
	AEROSOL	0.7630E-02	0.4374
	DEPOSIT	1.503	
	CORIUM	0.6183	486.1
GROUP 6	VAPOR	0.9878E-02	
	AEROSOL	0.1469E-04	57.99
	DEPOSIT	138.5	
	CORIUM	0.000	0.000

- 
- 1) SINCE WE HAVEN'T YET FINISHED THE MODELING IN THE CONTAINMENT, WE ONLY DISPLAY TOTAL FIGURES FOR THE CONTAINMENT.
  - 2) IT ISN'T POSSIBLE TO CALCULATE THE CONTAINMENT-CONTENT FOR THIS GROUP SINCE A TOO SMALL FRACTION OF THE GROUP HAS BEEN RELEASED.

Table 12.1.4. AB sequence in R1 as modeled by CHMAAP at 1000 s into the accident assuming slow reactions.

COMPARTMENT CONDITIONS: TIME= 1000 SECONDS					
FISSION PRODUCT MASS IN RPV (kg)					
		CORE	SHRD HEAD	SEPARATERS	UPP HEAD
GROUP 1	VAPOR	0.1023E-01	4.791	2.352	19.34
	AEROSOL	0.6674E-03	2.340	1.098	5.008
	DEPOSIT	0.7771E-05	0.3595	0.6496E-01	1.214
GROUP 2	VAPOR	0.000	0.3132E-03	0.2597E-03	0.1313E-03
	AEROSOL	0.000	0.3904	0.1781	1.038
	DEPOSIT	0.000	1.038	0.6175E-01	0.3122
GROUP 3	VAPOR	0.000	0.3835	0.1960	1.662
	AEROSOL	0.000	0.000	0.000	0.000
	DEPOSIT	0.000	0.7573E-04	0.000	0.000
GROUP 4	VAPOR	0.000	0.000	0.000	0.000
	AEROSOL	0.000	0.9032E-06	0.4372E-06	0.2147E-05
	DEPOSIT	0.000	0.1611E-06	0.2988E-07	0.5324E-06
GROUP 5	VAPOR	0.000	0.2461E-19	0.3259E-11	0.1643E-11
	AEROSOL	0.000	0.7102E-08	0.3027E-08	0.1120E-07
	DEPOSIT	0.000	0.7608E-09	0.4114E-09	0.2691E-08
GROUP 6	VAPOR	0.000	0.1184	0.2136E-02	0.3589E-02
	AEROSOL	0.000	1.568	0.8414	4.306
	DEPOSIT	0.000	12.39	0.4281	1.415
SURF TEMP (K)		591.2	583.6	568.7	558.2
		568.7	588.6		559.4
CSI DEP MASS (kg)		0.000	0.6300	0.6175E-01	0.1724E-01
		0.000	0.4076		0.2950
		UPP DWNCMR	LOW DWNCMR	LOW HEAD	RECIRC
GROUP 1	VAPOR	7.061	0.9643	0.2123	0.7389E-01
	AEROSOL	1.390	0.1353	0.1651E-01	0.8951E-02
	DEPOSIT	0.2450	0.1958E-02	0.2001E-03	0.2976E-03
GROUP 2	VAPOR	0.5313E-05	0.7171E-07	0.6025E-07	0.3085E-08
	AEROSOL	0.3683	0.5230E-01	0.1119E-01	0.3897E-02
	DEPOSIT	0.7326E-01	0.1123E-02	0.2256E-03	0.1514E-03
GROUP 3	VAPOR	0.6034	0.7199E-01	0.1308E-01	0.5288E-02
	AEROSOL	0.000	0.000	0.000	0.000
	DEPOSIT	0.000	0.000	0.000	0.000
GROUP 4	VAPOR	0.000	0.000	0.000	0.000
	AEROSOL	0.6270E-06	0.6457E-07	0.8475E-08	0.4353E-08
	DEPOSIT	0.1125E-06	0.9921E-09	0.1106E-09	0.1476E-09
GROUP 5	VAPOR	0.6447E-13	0.4623E-15	0.4755E-17	0.5447E-17
	AEROSOL	0.2650E-08	0.2179E-09	0.2133E-10	0.1358E-10
	DEPOSIT	0.4519E-09	0.2747E-11	0.2042E-12	0.4327E-12
GROUP 6	VAPOR	0.3043E-01	0.5895E-03	0.9781E-03	0.5831E-04
	AEROSOL	1.535	0.1978	0.4133E-01	0.1453E-01
	DEPOSIT	0.1070	0.1500E-01	0.1782E-05	0.5189E-03
SURF TEMP (K)		558.8	558.3	551.3	557.6
		568.7	591.2	440.8	
		559.1	441.6		
CSI DEP MASS (kg)		0.000	0.5324E-05	0.2256E-03	0.1514E-03
		0.000	0.000	0.000	

Continued on next page

Table 12.1.4. Continued

FISSION PRODUCT MASS (kg)		CONTAINMENT <sup>1)</sup>	
	RPV		
GROUP 1	VAPOR	34.80	15.86
	AEROSOL	9.998	1.664
	DEPOSIT	1.885	0.5655E-01
	CORIUM	0.000	0.000
GROUP 2	VAPOR	0.7096E-03	
	AEROSOL	2.042	0.8531
	DEPOSIT	1.486	
	CORIUM	0.000	0.000
GROUP 3	VAPOR	2.936	
	AEROSOL	0.000	0.9699
	DEPOSIT	0.7573E-04	
	CORIUM	0.000	0.000
GROUP 4	VAPOR	0.000	2)
	AEROSOL	0.4192E-05	----
	DEPOSIT	0.8371E-06	
	CORIUM	0.000	0.000
GROUP 5	VAPOR	0.4966E-11	2)
	AEROSOL	0.2424E-07	----
	DEPOSIT	0.4318E-08	
	CORIUM	0.000	0.000
GROUP 6	VAPOR	0.1562	
	AEROSOL	8.504	3.331
	DEPOSIT	14.36	
	CORIUM	0.000	0.000

- 
- 1) SINCE WE HAVEN'T YET FINISHED THE MODELING IN THE CONTAINMENT, WE ONLY DISPLAY TOTAL FIGURES FOR THE CONTAINMENT.
- 2) IT ISN'T POSSIBLE TO CALCULATE THE CONTAINMENT-CONTENT FOR THIS GROUP SINCE TOO SMALL FRACTION OF THE GROUP HAS BEEN RELEASED.

Table 12.1.5. AB sequence in R1 as modeled by CHMAAP at vessel failure 5633 s into the accident assuming slow reactions.

COMPARTMENT CONDITIONS: TIME= 5633 SECONDS VESSEL-FAILURE					
FISSION PRODUCT MASS IN RPV (kg)					
		CORE	SHRD HEAD	SEPARATERS	UPP HEAD
GROUP 1	VAPOR	0.1052E-02	0.4295E-02	0.2962E-02	3.165
	AEROSOL	0.4048E-04	0.4389E-01	0.2777E-01	3.583
	DEPOSIT	0.3904E-01	94.40	6.270	715.5
GROUP 2	VAPOR	0.000	0.4871E-02	0.3345E-03	0.1011E-02
	AEROSOL	0.000	0.2412	0.1570	0.4463
	DEPOSIT	0.000	0.2087E-02	0.7565	9.653
GROUP 3	VAPOR	0.000	0.2664E-03	0.1679E-03	0.5501E-01
	AEROSOL	0.000	0.000	0.000	0.000
	DEPOSIT	0.000	0.000	0.000	0.4779E-08
GROUP 4	VAPOR	0.000	0.000	0.000	0.000
	AEROSOL	0.000	0.1112E-02	0.4623E-03	0.7651E-02
	DEPOSIT	0.000	0.1894E-01	0.2266E-02	0.8358E-01
GROUP 5	VAPOR	0.000	0.6868E-09	0.5996E-05	0.9961E-05
	AEROSOL	0.000	0.3268E-01	0.1215E-01	0.1077
	DEPOSIT	0.000	0.2127	0.5927E-01	1.088
GROUP 6	VAPOR	0.000	0.5280E-05	0.1361E-04	0.2580E-01
	AEROSOL	0.000	0.6489E-02	0.6853E-02	0.1539E-02
	DEPOSIT	0.000	0.1319E-03	0.1392E-11	88.45
SURF TEMP (K)		1351.	764.8	614.8	593.4
		890.1	908.4		962.3
CSI DEP MASS		0.000	0.1999E-02	0.7565	9.652
(kg)		0.000	0.8841E-04		0.2798E-03
		UPP DWNCMR	LOW DWNCMR	LOW HEAD	RECIRC
GROUP 1	VAPOR	8.846	3.877	16.25	0.5379
	AEROSOL	2.780	0.6002	0.6250	0.6102E-01
	DEPOSIT	111.8	7.892	8.083	1.513
GROUP 2	VAPOR	0.2418E-01	0.2108E-01	0.3960E-06	0.1051E-05
	AEROSOL	3.200	0.3197E-01	0.5103	0.2891E-01
	DEPOSIT	1.506	3.360	1.009	0.1886
GROUP 3	VAPOR	0.1859	0.2622E-02	0.1100	0.1498E-02
	AEROSOL	0.000	0.000	0.000	0.000
	DEPOSIT	0.000	8.563	0.000	0.000
GROUP 4	VAPOR	0.000	0.000	0.000	0.000
	AEROSOL	0.7904E-02	0.1925E-02	0.1167E-02	0.2004E-03
	DEPOSIT	0.1716E-01	0.1506E-02	0.9445E-03	0.2049E-03
GROUP 5	VAPOR	0.1678E-05	0.1406E-07	0.1000E-10	0.4146E-10
	AEROSOL	0.1401	0.3894E-01	0.1959E-01	0.4251E-02
	DEPOSIT	0.2159	0.1766E-01	0.5588E-02	0.2006E-02
GROUP 6	VAPOR	0.9525E-02	0.2302E-02	0.6290E-05	0.7109E-05
	AEROSOL	0.1622	0.1284E-03	0.1234E-03	0.5487E-04
	DEPOSIT	12.76	17.79	9.993	2.519
SURF TEMP (K)		582.8	814.6	545.1	566.9
		614.8	1351.	405.9	
		779.2	422.9		
CSI DEP MASS		0.6844	1.457	1.009	0.1886
(kg)		0.6137	0.000	0.000	
		0.2077	1.903		

Continued on next page.

Table 12.1.5. Continued

FISSION PRODUCT		MASS (kg)	CONTAINMENT <sup>1)</sup>
		RPV	
GROUP 1	VAPOR	32.68	343.3
	AEROSOL	7.721	25.98
	DEPOSIT	945.5	80.15
	CORIUM	0.000	0.000
GROUP 2	VAPOR	0.5148E-01	
	AEROSOL	4.616	11.38
	DEPOSIT	16.47	
	CORIUM	0.000	0.000
GROUP 3	VAPOR	0.3554	
	AEROSOL	0.000	20.07
	DEPOSIT	8.563	
	CORIUM	0.000	0.000
GROUP 4	VAPOR	0.000	
	AEROSOL	0.2042E-01	0.5301E-01
	DEPOSIT	0.1246	
	CORIUM	53.83	0.2111E-02
GROUP 5	VAPOR	0.1765E-04	
	AEROSOL	0.3555	0.2489
	DEPOSIT	1.601	
	CORIUM	125.1	0.4909E-02
GROUP 6	VAPOR	0.3766E-01	
	AEROSOL	0.1774	63.67
	DEPOSIT	131.5	
	CORIUM	0.000	0.000

- 
- 1) SINCE WE HAVEN'T YET FINISHED THE MODELING IN THE CONTAINMENT, WE ONLY DISPLAY TOTAL FIGURES FOR THE CONTAINMENT.
  - 2) IT ISN'T POSSIBLE TO CALCULATE THE CONTAINMENT-CONTENT FOR THIS GROUP SINCE TOO SMALL FRACTION OF THE GROUP HAS BEEN RELEASED.

Table 12.1.6. AB sequence in R1 as modeled by CHMAAP at 10 000 s into the accident assuming slow reactions.

COMPARTMENT CONDITIONS: TIME= 10000 SECONDS					
FISSION PRODUCT MASS IN RPV (kg)					
		CORE	SHRD HEAD	SEPARATERS	UPP HEAD
GROUP 1	VAPOR	1.576	0.7693	0.6185	6.139
	AEROSOL	0.1281	0.6430E-01	0.1403E-01	0.1268
	DEPOSIT	0.4472E-01	94.89	6.320	716.1
GROUP 2	VAPOR	0.000	0.8634E-05	0.1816E-05	0.2911E-03
	AEROSOL	0.000	0.9696E-03	0.6635E-04	0.8511E-04
	DEPOSIT	0.000	0.1207E-05	0.7246	10.52
GROUP 3	VAPOR	0.000	0.4995E-03	0.1813E-04	0.3850E-04
	AEROSOL	0.000	0.000	0.000	0.000
	DEPOSIT	0.000	0.000	0.000	0.000
GROUP 4	VAPOR	0.000	0.000	0.000	0.000
	AEROSOL	0.000	0.3553E-02	0.1066E-03	0.3588E-03
	DEPOSIT	0.000	0.4869E-01	0.3078E-02	0.8543E-01
GROUP 5	VAPOR	0.000	0.4669E-15	0.5083E-13	0.6072E-13
	AEROSOL	0.000	0.5861E-02	0.4506E-03	0.3303E-02
	DEPOSIT	0.000	0.5620	0.7274E-01	1.115
GROUP 6	VAPOR	0.000	0.2016E-02	0.1270E-03	0.2357E-04
	AEROSOL	0.000	0.4334E-07	0.4886E-07	0.8743E-06
	DEPOSIT	0.000	0.3171E-11	0.3345	89.80
SURF TEMP (K)		1488.	756.8	645.5	685.6
		888.1	880.3		896.1
CSI DEP MASS (kg)		0.000	0.000	0.7246	10.52
		0.000	0.1207E-05		0.4968E-08
		UPP DWNCMR	LOW DWNCMR	LOW HEAD	RECIRC
GROUP 1	VAPOR	4.652	1.229	4.486	0.1743
	AEROSOL	0.1127	0.3095E-01	0.2949	0.4265E-02
	DEPOSIT	113.4	8.211	9.867	1.578
GROUP 2	VAPOR	0.1299E-04	0.2863E-04	0.2118E-04	0.6480E-06
	AEROSOL	0.4430E-03	0.5377E-05	0.7143E-03	0.2186E-05
	DEPOSIT	1.469	4.357	1.222	0.2099
GROUP 3	VAPOR	0.1378E-03	0.5920	0.3585	0.7515E-01
	AEROSOL	0.000	0.000	0.000	0.000
	DEPOSIT	0.000	6.561	0.000	0.000
GROUP 4	VAPOR	0.000	0.000	0.000	0.000
	AEROSOL	0.4716E-03	0.1124E-03	0.2101E-02	0.1518E-04
	DEPOSIT	0.2412E-01	0.2659E-02	0.7804E-02	0.4416E-03
GROUP 5	VAPOR	0.5481E-13	0.1017E-10	0.8022E-06	0.1894E-13
	AEROSOL	0.3467E-02	0.9634E-03	0.4431E-02	0.1330E-03
	DEPOSIT	0.3262	0.3647E-01	0.1057	0.6107E-02
GROUP 6	VAPOR	0.2053E-02	0.1188E-03	0.2550E-03	0.4003E-05
	AEROSOL	0.2493E-07	0.1125E-08	0.4650E-08	0.9043E-10
	DEPOSIT	9.395	18.11	11.69	2.878
SURF TEMP (K)		604.0	1082.	582.8	589.7
		645.5	1488.	438.9	
		755.0	684.1		
CSI DEP MASS (kg)		0.7865	0.5551E-09	1.222	0.2099
		0.6823	0.000	0.000	
		0.2696E-06	4.357		

Continued on next page.

Table 12.1.6. Continued

FISSION PRODUCT MASS (kg)		CONTAINMENT <sup>1)</sup>	
GROUP	RPV		
GROUP 1	VAPOR	19.64	358.5
	AEROSOL	0.7760	6.628
	DEPOSIT	950.4	165.9
	CORIUM	0.000	0.000
GROUP 2	VAPOR	0.3650E-03	
	AEROSOL	0.2286E-02	14.20
	DEPOSIT	18.50	
	CORIUM	0.000	0.000
GROUP 3	VAPOR	1.026	
	AEROSOL	0.000	21.56
	DEPOSIT	6.561	
	CORIUM	0.000	0.000
GROUP 4	VAPOR	0.000	
	AEROSOL	0.6718E-02	0.2005
	DEPOSIT	0.1722	
	CORIUM	0.3075	208.2
GROUP 5	VAPOR	0.8022E-06	
	AEROSOL	0.1861E-01	1.403
	DEPOSIT	2.224	
	CORIUM	0.7240	485.1
GROUP 6	VAPOR	0.4597E-02	
	AEROSOL	0.9973E-06	64.30
	DEPOSIT	132.2	
	CORIUM	0.000	0.000

- 
- 1) SINCE WE HAVEN'T YET FINISHED THE MODELING IN THE CONTAINMENT, WE ONLY DISPLAY TOTAL FIGURES FOR THE CONTAINMENT.
  - 2) IT ISN'T POSSIBLE TO CALCULATE THE CONTAINMENT-CONTENT FOR THIS GROUP SINCE TOO SMALL FRACTION OF THE GROUP HAS BEEN RELEASED.

Table 12.1.7. AB sequence in R1 as modeled by MAAP 3.0 at 1000 s into the accident.

COMPARTMENT CONDITIONS: TIME= 1000 SECONDS, 0.28 HOURS					
FISSION PRODUCT MASS IN RPV (KG)					
		CORE	SHRD HEAD	SEPARATERS	UPP HEAD
GROUP 1	VAPOR	0.9358E-02	4.564	2.490	21.12
	AEROSOL	0.3267E-03	2.730	1.094	3.373
	DEPOSIT	0.5490E-05	0.3800	0.3395E-01	2.101
GROUP 2	VAPOR	0.6549E-03	0.6799E-02	0.4793E-07	0.1296E-06
	AEROSOL	-0.1048E-20	0.3628	0.1887	0.9749
	DEPOSIT	0.1789E-04	0.1432	0.2315E-01	1.077
GROUP 3	VAPOR	0.7172E-03	0.6730E-04	0.6693E-11	0.1045E-10
	AEROSOL	-0.8375E-21	0.4056	0.2071	1.070
	DEPOSIT	0.1943E-04	0.1613	0.2538E-01	1.182
GROUP 4	VAPOR	0.000	0.000	0.000	0.000
	AEROSOL	0.1951E-09	0.1047E-05	0.4298E-06	0.1432E-05
	DEPOSIT	0.3453E-11	0.1635E-06	0.1624E-07	0.9876E-06
GROUP 5	VAPOR	0.000	0.000	0.000	0.000
	AEROSOL	0.1922E-12	0.6739E-08	0.2526E-08	0.6299E-08
	DEPOSIT	0.2636E-14	0.6995E-09	0.4767E-10	0.2912E-08
GROUP 6	VAPOR	0.3935E-02	0.6927E-01	0.1661E-04	0.7251E-04
	AEROSOL	-0.4528E-20	2.152	1.134	5.858
	DEPOSIT	0.1061E-03	0.8618	0.1392	6.472
SURF TEMP (K )		591.2	574.2	567.9	558.2
		568.1	564.5		561.2
CSI DEP MASS		0.000	0.9262E-01	0.2315E-01	0.8012E-03
(KG)		0.1789E-04	0.5056E-01		1.076
		UPP DWNCMR	LOW DWNCMR	LOW HEAD	RECIRC
GROUP 1	VAPOR	6.675	0.9030	0.2118	0.6938E-01
	AEROSOL	0.6020	0.5178E-01	0.8252E-02	0.3555E-02
	DEPOSIT	0.2105	0.6711E-02	0.2014E-03	0.3013E-03
GROUP 2	VAPOR	0.1965E-07	0.2709E-07	0.2285E-07	0.1955E-08
	AEROSOL	0.3044	0.4957E-01	0.1422E-01	0.4009E-02
	DEPOSIT	0.1804	0.9129E-02	0.4538E-03	0.4567E-03
GROUP 3	VAPOR	0.4056E-30	0.2009E-11	0.1798E-30	0.1328E-12
	AEROSOL	0.3339	0.5433E-01	0.1557E-01	0.4394E-02
	DEPOSIT	0.1978	0.1000E-01	0.4968E-03	0.5003E-03
GROUP 4	VAPOR	0.000	0.000	0.000	0.000
	AEROSOL	0.2806E-06	0.2695E-07	0.4787E-08	0.1913E-08
	DEPOSIT	0.1082E-06	0.3735E-08	0.1225E-09	0.1714E-09
GROUP 5	VAPOR	0.000	0.000	0.000	0.000
	AEROSOL	0.8633E-09	0.5261E-10	0.5532E-11	0.3180E-11
	DEPOSIT	0.2200E-09	0.5300E-11	0.1100E-12	0.2167E-12
GROUP 6	VAPOR	0.1711E-04	0.1632E-04	0.1874E-04	0.1273E-05
	AEROSOL	1.829	0.2978	0.8543E-01	0.2409E-01
	DEPOSIT	1.084	0.5485E-01	0.2725E-02	0.2744E-02
SURF TEMP (K )		559.0	558.3	551.3	557.6
		567.9	591.2	440.8	
		560.3	441.1		
CSI DEP MASS		0.000	0.7554E-05	0.4538E-03	0.4567E-03
(KG)		0.000	0.000	0.000	

Continued on next page.

Table 12.1.7. Continued

FISSION PRODUCT MASS (KG)		RPV	CONTAINMENT <sup>1)</sup>
GROUP 1	VAPOR	36.05	14.83
	AEROSOL	7.864	0.9857
	DEPOSIT	2.733	0.1093
	CORIUM	0.000	0.000
GROUP 2	VAPOR	0.7455E-02	
	AEROSOL	1.898	1.060
	DEPOSIT	1.434	
	CORIUM	0.000	0.000
GROUP 3	VAPOR	0.7845E-03	
	AEROSOL	2.091	1.161
	DEPOSIT	1.577	
	CORIUM	0.000	0.000
GROUP 4	VAPOR	0.000	
	AEROSOL	0.3223E-05	0.1108E-06
	DEPOSIT	0.1280E-05	
	CORIUM	0.000	0.000
GROUP 5	VAPOR	0.000	
	AEROSOL	0.1649E-07	0.1239E-08
	DEPOSIT	0.3885E-08	
	CORIUM	0.000	0.000
GROUP 6	VAPOR	0.7335E-01	
	AEROSOL	11.38	6.3670
	DEPOSIT	8.617	
	CORIUM	0.000	0.000

---

1) SINCE WE HAVEN'T YET FINISHED THE MODELING IN THE CONTAINMENT,  
WE ONLY DISPLAY TOTAL FIGURES FOR THE CONTAINMENT.

Table 12.1.8. AB sequence in R1 as modeled by MAAP 3.0 at vessel failure 5642 s into the accident.

COMPARTMENT CONDITIONS: TIME= 5642 SECONDS, 1.57 HOURS					
FISSION PRODUCT MASS IN RPV (KG)					
		CORE	SHRD HEAD	SEPARATERS	UPP HEAD
GROUP 1	VAPOR	0.1770E-02	0.5415E-02	0.9064E-02	3.182
	AEROSOL	0.2375E-03	0.3912E-01	0.3136E-01	4.535
	DEPOSIT	0.3767E-01	126.4	7.180	636.3
GROUP 2	VAPOR	0.000	0.3744E-20	0.1140E-09	0.3470E-02
	AEROSOL	0.4639E-04	0.6162E-02	0.3830E-02	0.9183
	DEPOSIT	0.000	2.830	0.1709	5.910
GROUP 3	VAPOR	0.1749E-23	0.5910E-21	0.3245E-30	0.1149E-04
	AEROSOL	0.1149E-04	0.1214E-02	0.6435E-03	0.6935E-01
	DEPOSIT	0.2565E-02	3.968	0.1583	21.49
GROUP 4	VAPOR	0.000	0.5030E-30	0.000	0.2262E-29
	AEROSOL	0.1884E-05	0.4810E-03	0.7912E-04	0.9631E-02
	DEPOSIT	0.6444E-06	0.1735E-01	0.3414E-02	0.3621E-01
GROUP 5	VAPOR	0.000	0.4264E-31	0.000	0.4266E-30
	AEROSOL	0.2244E-03	0.5936E-01	0.2301E-02	0.8386E-01
	DEPOSIT	0.6358E-06	0.1249	0.2666E-01	0.2177
GROUP 6	VAPOR	0.3663E-09	0.6975E-09	0.2688E-06	0.8404E-01
	AEROSOL	0.2032E-03	0.2381E-01	0.1606E-01	4.112
	DEPOSIT	0.000	18.64	0.9917	52.39
SURF TEMP (K )		1351.	751.2	606.1	579.9
		971.0	1153.		1054.
CSI DEP MASS		0.000	0.5438	0.1709	2.334
(KG)		0.000	2.286		3.576
		UPP DWNCMR	LOW DWNCMR	LOW HEAD	RECIRC
GROUP 1	VAPOR	11.62	5.178	18.35	0.7116
	AEROSOL	4.320	1.079	0.9519	0.1242
	DEPOSIT	127.7	14.57	9.634	1.202
GROUP 2	VAPOR	0.1855E-03	0.1777	0.5048E-06	0.1833E-05
	AEROSOL	0.9244	0.1420	0.2523	0.3971E-01
	DEPOSIT	8.220	0.7932	0.6062	0.5577E-01
GROUP 3	VAPOR	0.2502E-06	0.5536E-02	0.8025E-10	0.1486E-08
	AEROSOL	0.7402E-01	0.1860E-01	0.1925E-01	0.2987E-02
	DEPOSIT	3.872	0.4477	0.2632	0.3346E-01
GROUP 4	VAPOR	0.000	0.000	0.000	0.000
	AEROSOL	0.1052E-01	0.2306E-02	0.8450E-03	0.2329E-03
	DEPOSIT	0.2127E-01	0.2011E-02	0.1335E-02	0.1172E-03
GROUP 5	VAPOR	0.000	0.000	0.000	0.000
	AEROSOL	0.1038	0.2634E-01	0.1234E-01	0.2932E-02
	DEPOSIT	0.1811	0.1568E-01	0.7447E-02	0.5162E-03
GROUP 6	VAPOR	0.9358E-02	1.078	0.1563E-03	0.1414E-03
	AEROSOL	4.127	0.4113	1.227	0.1859
	DEPOSIT	44.52	4.170	3.434	0.3299
SURF TEMP (K )		572.8	812.3	540.2	564.7
		606.1	1351.	403.9	
CSI DEP MASS		0.1369	0.2496	0.6062	0.5577E-01
(KG)		0.1811	0.000	0.000	

Continued on next page.

Table 12.1.8. Continued

FISSION PRODUCT MASS (KG)		RPV	CONTAINMENT <sup>1)</sup>
GROUP 1	VAPOR	39.06	337.0
	AEROSOL	11.08	34.78
	DEPOSIT	923.0	96.45
	CORIUM	0.000	0.000
GROUP 2	VAPOR	0.1813	
	AEROSOL	2.287	10.83
	DEPOSIT	18.58	
	CORIUM	0.000	0.000
GROUP 3	VAPOR	0.5548E-02	
	AEROSOL	0.1861	5.270
	DEPOSIT	30.24	
	CORIUM	0.000	0.000
GROUP 4	VAPOR	0.2765E-29	
	AEROSOL	0.2409E-01	0.8116E-01
	DEPOSIT	0.8171E-01	
	CORIUM	53.69	0.8502E-03
GROUP 5	VAPOR	0.4693E-30	
	AEROSOL	0.2912	0.7065
	DEPOSIT	0.5740	
	CORIUM	125.2	0.1983E-02
GROUP 6	VAPOR	1.172	
	AEROSOL	10.10	59.65
	DEPOSIT	124.5	
	CORIUM	0.000	0.000

---

1) SINCE WE HAVEN'T YET FINISHED THE MODELING IN THE CONTAINMENT,  
WE ONLY DISPLAY TOTAL FIGURES FOR THE CONTAINMENT.

Table 12.1.9. AB sequence in R1 as modeled by MAAP 3.0 at 10 013 s into the accident.

COMPARTMENT CONDITIONS: TIME= 10013 SECONDS, 2.78 HOURS  
FISSION PRODUCT MASS IN RPV (KG)

	CORE	SHRD HEAD	SEPARATERS	UPP HEAD
GROUP 1 VAPOR	1.593	0.7114	0.5993	5.743
AEROSOL	0.8636E-01	0.3871E-01	0.6618E-02	0.6195E-01
DEPOSIT	0.3767E-01	127.4	7.246	637.0
GROUP 2 VAPOR	0.5411E-01	0.6716E-04	0.5019E-05	0.5136E-01
AEROSOL	-0.6263E-19	0.3210E-01	0.1851E-01	-0.1141E-18
DEPOSIT	0.000	0.2380	0.1964	2.616
GROUP 3 VAPOR	0.3084E-02	0.1200E-06	0.3792E-08	0.1432E-02
AEROSOL	0.3160E-01	0.1730E-01	0.1157E-01	0.1084
DEPOSIT	0.000	3.467	0.2009	15.98
GROUP 4 VAPOR	0.9019E-29	0.2897E-27	0.000	0.8636E-77
AEROSOL	0.7348E-03	0.3311E-03	0.2027E-04	0.1985E-03
DEPOSIT	0.6443E-06	0.2341E-01	0.3639E-02	0.3765E-01
GROUP 5 VAPOR	0.1611E-29	0.2482E-28	0.000	0.000
AEROSOL	0.4769E-03	0.2143E-03	0.2186E-04	0.2078E-03
DEPOSIT	0.6358E-06	0.1798	0.2868E-01	0.2315
GROUP 6 VAPOR	0.3943	0.2687E-02	0.4106E-03	0.2589
AEROSOL	-0.9788E-18	0.2719	0.8096E-01	-0.1547E-17
DEPOSIT	0.000	2.754	1.315	15.41
SURF TEMP (K )	1488.	1034.	650.2	612.4
	1102.	1107.		995.7
CSI DEP MASS	0.000	0.2380	0.1964	2.616
(KG)	0.000	0.2974E-04		0.4702E-37
	UPP DWNCMR	LOW DWNCMR	LOW HEAD	RECIRC
GROUP 1 VAPOR	3.878	1.040	4.237	0.1510
AEROSOL	0.4838E-01	0.1445E-01	0.1984	0.2048E-02
DEPOSIT	129.8	15.28	12.93	1.303
GROUP 2 VAPOR	0.1016E-03	0.2146	0.3544E-03	0.5461E-05
AEROSOL	0.8413	-0.6281E-19	0.2480	0.2984E-01
DEPOSIT	4.393	0.6297	1.385	0.1374
GROUP 3 VAPOR	0.1099E-06	0.5131E-01	0.6015E-06	0.6599E-08
AEROSOL	0.1461	-0.6831E-19	0.1070	0.6824E-02
DEPOSIT	3.719	0.6162	0.5641	0.5066E-01
GROUP 4 VAPOR	0.3709E-27	0.2698E-09	0.000	0.000
AEROSOL	0.1156E-03	0.3004E-04	0.1603E-02	0.4178E-05
DEPOSIT	0.2710E-01	0.3706E-02	0.1236E-01	0.3461E-03
GROUP 5 VAPOR	0.1915E-28	0.2325E-10	0.000	0.000
AEROSOL	0.1484E-03	0.4296E-04	0.1062E-02	0.6063E-05
DEPOSIT	0.2443	0.3440E-01	0.1067	0.2983E-02
GROUP 6 VAPOR	0.6156E-02	0.8982	0.1479E-01	0.3018E-03
AEROSOL	3.503	-0.4508E-19	1.389	0.1246
DEPOSIT	29.36	2.810	11.08	0.7663
SURF TEMP (K )	602.0	1081.	589.0	586.3
	650.2	1488.	417.2	
	1108.	417.8		
CSI DEP MASS	0.3965	0.8167E-22	1.385	0.1374
(KG)	0.3902	0.000	0.000	
	3.607	0.6297		

Continued on next page.

Table 12.1.9. Continued

FISSION PRODUCT MASS (KG)		RPV	CONTAINMENT <sup>1)</sup>
GROUP 1	VAPOR	17.95	360.1
	AEROSOL	0.4570	3.955
	DEPOSIT	931.0	189.8
	CORIUM	0.000	0.000
GROUP 2	VAPOR	0.3206	
	AEROSOL	1.170	21.61
	DEPOSIT	9.596	
	CORIUM	0.000	0.000
GROUP 3	VAPOR	0.5582E-01	
	AEROSOL	0.4288	10.82
	DEPOSIT	24.59	
	CORIUM	0.000	0.000
GROUP 4	VAPOR	0.2698E-09	
	AEROSOL	0.3037E-02	0.1743
	DEPOSIT	0.1082	
	CORIUM	0.2756	208.2
GROUP 5	VAPOR	0.2325E-10	
	AEROSOL	0.2180E-02	1.192
	DEPOSIT	0.8283	
	CORIUM	0.6492	486.5
GROUP 6	VAPOR	1.576	
	AEROSOL	5.369	126.1
	DEPOSIT	63.50	
	CORIUM	0.000	0.000

1) SINCE WE HAVEN'T YET FINISHED THE MODELING IN THE CONTAINMENT,  
WE ONLY DISPLAY TOTAL FIGURES FOR THE CONTAINMENT.

Table 12.3.1. Snapshot of ongoing processes obtained from CHMAAP at an early stage of the AB sequence for R1.

THE TIME IS NOW, IN HOURS,MINUTES,SECONDS: 0 10 5.027

THE SHROUD HEAD

GAS AND WALLTEMPERATURE, RESPECTIVELY: 946.21 562.32  
 MOLAR STEAM TO HYDROGEN RATIO: 3.2787  
 PRESSURE, IN KILOPASCAL: 232.47

NET GAS FLOW RATES, MOLE/S		NET AEROSOL FLOW RATES, MOLE/S	
MoO3(g)	0.19979E-12	CsI	0.65277E-02
TeO2(g)	0.17379E-01	CsOH	0.14151E-07
CsOH(g)	0.10111	MoO2	0.95591E-13
CsI(g)	0.96142E-02	SrO	0.26272E-08
Cs2(g)	0.34436E-52		

DESTRUCTION OF GASES DUE TO PURE GAS REACTIONS. RATE OF CHANGE, MOLE/S, OF REACTING GASES

H2(g)	-0.52136E-01
I2(g)	-0.14614E-14
MoO3(g)	-0.19935E-12
TeO2(g)	-0.17379E-01
CsOH(g)	-0.25848E-01
CsI(g)	-0.70742E-02
Cs2(g)	-0.34436E-52

FORMATION OF GASES DUE TO PURE GAS REACTIONS. RATE OF CHANGE, MOLE/S, OF REACTING GASES

H2O(g)	0.34757E-01
H2Te(g)	0.17379E-01
MoO2(g)	0.69254E-19
(CsOH)2(g)	0.12924E-01

FORMATION OF AEROSOL PARTICLES SOLELY FROM GAS REACTIONS. RATE OF CHANGE, MOLE/S, OF FORMED AEROSOL PARTICLES

CsI	0.70742E-02
MoO2	0.19935E-12

DESTRUCTION OF AEROSOL PARTICLES DUE TO GAS FORMATION. RATE OF CHANGE, MOLE/S, OF DESTROYED AEROSOL PARTICLES

MoO2	-0.20195E-26
------	--------------

Continued on next page.

Table 12.3.1. Continued

GASES FORMED FROM AEROSOL PARTICLES. RATE OF CHANGE, MOLE/S, OF  
GASES FROM AEROSOL PARTICLES

H2 (g)	0.23235E-12
MoO3 (g)	0.19524E-28
TeO2 (g)	0.21836E-27
(CsOH)2 (g)	0.29948E-08
CsOH (g)	0.81611E-08
CsI (g)	0.52107E-15

AEROSOL PARTICLES FORMED BY REACTIONS BETWEEN THE GAS AND EXISTING  
AEROSOL PARTICLES. RATE OF CHANGE, MOLE/S, OF FORMED AEROSOL  
PARTICLES BY REACTIONS WITH THE GAS

MoO2	0.20195E-26
------	-------------

AEROSOL DEPOSITION: RATE OF DEPOSITION, MOLE/S, AEROSOL PARTICLES

CsI	0.67276E-03
MoO2	0.14588E-13
SrO	0.12994E-09

FORMATION OF THE OUTER LAYER DUE TO CONDENSATION OR CHEMICAL  
REACTIONS OF VARIOUS KINDS. RATE OF CHANGE, MOLE/S, OF GASES DUE  
TO REACTION OR CONDENSATION ONTO THE OUTER DEPOSITED LAYER

H2O (g)	-0.75279E-02
H2Te (g)	-0.37639E-02
MoO2 (g)	-0.70279E-19
MoO3 (g)	-0.47555E-15
TeO2 (g)	-0.57189E-15
(CsOH)2 (g)	-0.11881E-01
CsOH (g)	-0.69498E-01
CsI (g)	-0.25536E-02

RATE OF CHANGE, MOLE/S, OF FORMED OUTER LAYER, DUE TO CONDENSATION  
OR CHEMICAL REACTIONS

CsI	1	0.25536E-02
CsOH	1	0.93259E-01
MoO2	1	0.47562E-15
SrO	1	0.00000
TeO2	1	0.37639E-02

Continued on next page.

Table 12.3.1. Continued

PRESENT STATE IN THE SHROUD HEAD

THE GAS STATE		THE AEROSOL PARTICLES	
H2(g)	133.16969	CsI	0.25858
H2O(g)	439.84867	MoO2	0.56071E-11
H2Te(g)	0.37279	SrO	0.49945E-07
I2(g)	0.20536E-13		
MoO2(g)	0.12361E-18	THE OUTER LAYER	
MoO3(g)	0.83643E-15		
TeO2(g)	0.54786E-13	CsI	1 0.27231
(CsOH)2(g)	0.20897E-01	CsOH	1 9.14083
CsOH(g)	0.12224	MoO2	1 0.59880E-12
CsI(g)	0.44914E-02	SrO	1 0.56097E-08
		TeO2	1 0.64617

THE SEPARATORS AND STEAM DRYERS

GAS AND WALL TEMPERATURE, RESPECTIVELY:	594.09	562.30
MOLAR STEAM TO HYDROGEN RATIO:	3.2787	
PRESSURE, IN KILOPASCAL:	232.47	

NET GAS FLOW RATES, MOLE/S		NET AEROSOL FLOW RATES, MOLE/S	
I2(g)	0.51830E-15	CsOH	0.20296E-01
MoO2(g)	0.25547E-20		
MoO3(g)	0.70866E-13		
TeO2(g)	0.61618E-02		
CsOH(g)	0.35967E-01		
CsI(g)	0.34933E-02		

DESTRUCTION OF GASES DUE TO PURE GAS REACTIONS. RATE OF CHANGE, MOLE/S, OF REACTING GASES

H2(g)	-0.18486E-01
I2(g)	-0.51830E-15
MoO2(g)	-0.25547E-20
MoO3(g)	-0.70866E-13
TeO2(g)	-0.61618E-02
CsOH(g)	-0.35963E-01
CsI(g)	-0.34933E-02
Cs2(g)	-0.73790E-51

FORMATION OF GASES DUE TO PURE GAS REACTIONS. RATE OF CHANGE, MOLE/S, OF REACTING GASES

H2O(g)	0.12324E-01
H2Te(g)	0.61618E-02
(CsOH)2(g)	0.93256E-04

Continued on next page.

Table 12.3.1. Continued  
 FORMATION OF AEROSOL PARTICLES SOLELY FORMED FROM GAS REACTIONS.  
 RATE OF CHANGE, MOLE/S, OF FORMED AEROSOL PARTICLES

```
-----
CsI      0.34933E-02
CsOH     0.35777E-01
MoO2     0.70866E-13
```

GASES FORMED FROM AEROSOL PARTICLES. RATE OF CHANGE, MOLE/S, OF  
 GASES FROM AEROSOL PARTICLES

```
-----
H2(g)    0.11191E-11
H2O(g)   0.78160E-12
CsI(g)   0.51616E-22
```

AEROSOL DEPOSITION: RATE OF DEPOSITION, MOLE/S, AEROSOL PARTICLES

```
-----
CsI      0.60069E-04
CsOH     0.36960E-03
MoO2     0.86692E-15
SrO      0.81972E-11
```

FORMATION OF THE OUTER LAYER DUE TO CONDENSATION OR CHEMICAL  
 REACTIONS OF VARIOUS KINDS. RATE OF CHANGE, MOLE/S, OF GASES DUE  
 TO REACTION OR CONDENSATION ONTO THE OUTER DEPOSITED LAYER

```
-----
H2Te(g)  -0.27756E-17
(CsOH)2(g) -0.79874E-12
CsOH(g)  -0.79833E-13
CsI(g)   -0.36191E-20
```

RATE OF CHANGE, MOLE/S, OF FORMED OUTER LAYER, DUE TO CONDENSATION  
 OR CHEMICAL REACTIONS

```
-----
CsOH     1  0.16737E-11
MoO2     1  0.00000
SrO      1  0.00000
```

BREAKUP OF THE OUTER LAYER NUMBER 1 DUE TO EVAPORATION OR CHEMICAL  
 REACTIONS OF VARIOUS KINDS. RATE OF CHANGE, MOLE/S, OF OUTER  
 LAYER, DUE TO EVAPORATION OR CHEMICAL REACTIONS

```
-----
CsI      1 -0.86736E-19
```

PRESENT STATE IN THE SEPARATORS AND STEAM DRYERS

THE GAS STATE		THE AEROSOL PARTICLES	
-----		-----	
H2(g)	166.83188	CsI	0.18106
H2O(g)	548.45322	CsOH	1.11407
H2Te(g)	0.28307	MoO2	0.26131E-11
(CsOH)2(g)	0.28745E-02	SrO	0.24708E-07
CsOH(g)	0.28537E-03		
CsI(g)	0.30306E-06		

Continued on next page.

Table 12.3.1. Continued  
THE OUTER LAYER

```
-----
CsI      1  0.45101E-02
CsOH     1  0.32239E-01
MoO2     1  0.37128E-13
SrO      1  0.41210E-09
```

THE UPPER HEAD (UPPER PLENUM)

GAS AND WALL TEMPERATURE, RESPECTIVELY: 562.59 557.57  
MOLAR STEAM TO HYDROGEN RATIO: 3.2787  
PRESSURE, IN KILOPASCAL: 232.47

```
-----
NET GAS FLOW RATES, MOLE/S      NET AEROSOL FLOW RATES, MOLE/S
-----
H2Te(g)  0.49793E-02      CsI      0.20067E-01
I2(g)    0.65236E-15      CsOH     0.12771
MoO2(g)  0.32155E-20      MoO2     0.89294E-13
MoO3(g)  0.89196E-13      SrO      0.20920E-08
TeO2(g)  0.77557E-02
CsOH(g)  0.45279E-01
CsI(g)   0.43969E-02
```

DESTRUCTION OF GASES DUE TO PURE GAS REACTIONS. RATE OF CHANGE,  
MOLE/S, OF REACTING GASES

```
-----
H2(g)    -0.23267E-01
I2(g)    -0.65236E-15
MoO2(g)  -0.32155E-20
MoO3(g)  -0.89196E-13
TeO2(g)  -0.77557E-02
(CsOH)2(g) -0.75031E-04
CsOH(g)  -0.45286E-01
CsI(g)   -0.43969E-02
Cs2(g)   -0.57215E-49
```

FORMATION OF GASES DUE TO PURE GAS REACTIONS. RATE OF CHANGE,  
MOLE/S, OF REACTING GASES

```
-----
H2O(g)   0.15511E-01
H2Te(g)  0.77557E-02
```

FORMATION OF AEROSOL PARTICLES SOLELY FORMED FROM GAS REACTIONS.  
RATE OF CHANGE, MOLE/S, OF FORMED AEROSOL PARTICLES

```
-----
CsI      0.43969E-02
CsOH     0.45436E-01
MoO2     0.89196E-13
```

DESTRUCTION OF AEROSOL PARTICLES DUE TO GAS FORMATION. RATE OF  
CHANGE, MOLE/S, OF DESTROYED AEROSOL PARTICLES

```
-----
CsI      -0.49539E-08
CsOH     -0.55511E-16
Continued on next page.
```

Table 12.3.1. Continued

GASES FORMED FROM AEROSOL PARTICLES. RATE OF CHANGE, MOLE/S, OF GASES FROM AEROSOL PARTICLES

-----  
H2O(g) 0.27740E-11  
(CsOH)2(g) 0.23419E-17  
CsOH(g) 0.30358E-18  
CsI(g) 0.90659E-22

AEROSOL PARTICLES FORMED BY REACTIONS BETWEEN THE GAS AND EXISTING AEROSOL PARTICLES. RATE OF CHANGE, MOLE/S, OF FORMED AEROSOL PARTICLES BY REACTIONS WITH THE GAS

-----  
CsI 0.49539E-08  
CsOH 0.55511E-16

AEROSOL DEPOSITION: RATE OF DEPOSITION, MOLE/S, AEROSOL PARTICLES

-----  
CsI 0.35672E-04  
CsOH 0.24352E-03  
MoO2 0.32935E-15  
SrO 0.35437E-11

FORMATION OF THE OUTER LAYER DUE TO CONDENSATION OR CHEMICAL REACTIONS OF VARIOUS KINDS. RATE OF CHANGE, MOLE/S, OF GASES DUE TO REACTION OR CONDENSATION ONTO THE OUTER DEPOSITED LAYER

-----  
H2Te(g) -0.44409E-15  
(CsOH)2(g) -0.21503E-11  
CsOH(g) -0.10207E-12  
CsI(g) -0.24968E-20

RATE OF CHANGE, MOLE/S, OF FORMED OUTER LAYER, DUE TO CONDENSATION OR CHEMICAL REACTIONS

-----  
CsOH 1 0.37510E-11  
MoO2 1 0.00000  
SrO 1 0.00000

BREAKUP OF THE OUTER LAYER NUMBER 1 DUE TO EVAPORATION OR CHEMICAL REACTIONS OF VARIOUS KINDS. RATE OF CHANGE, MOLE/S, OF OUTER LAYER, DUE TO EVAPORATION OR CHEMICAL REACTIONS

-----  
CsI 1 -0.54210E-20

Continued on next page.

Table 12.3.1. Continued  
PRESENT STATE IN THE UPPER HEAD (UPPER PLENUM)

THE GAS STATE		THE AEROSOL PARTICLES	
H2(g)	2185.33727	CsI	0.67084
H2O(g)	7166.93899	CsOH	4.57958
H2Te(g)	1.18434	MoO2	0.61937E-11
(CsOH)2(g)	0.10169E-01	SrO	0.66642E-07
CsOH(g)	0.73975E-03		
CsI(g)	0.57802E-06		

THE OUTER LAYER

CsI	1	0.21478E-02
CsOH	1	0.16636E-01
MoO2	1	0.14193E-13
SrO	1	0.16863E-09

THE UPPER DOWNCOMER

GAS AND WALL TEMPERATURE, RESPECTIVELY	533.88	559.43
MOLAR STEAM TO HYDROGEN RATIO:	3.2787	
PRESSURE, IN KILOPASCAL:	232.47	

NET GAS FLOW RATES, MOLE/S		NET AEROSOL FLOW RATES, MOLE/S	
H2Te(g)	0.61767E-03	NONE	
I2(g)	0.12065E-16		
MoO2(g)	0.59471E-22		
MoO3(g)	0.16497E-14		
TeO2(g)	0.14344E-03		
(CsOH)2(g)	0.30889E-05		
CsOH(g)	0.83780E-03		
CsI(g)	0.81319E-04		
Cs2(g)	0.82394E-51		

DESTRUCTION OF GASES DUE TO PURE GAS REACTIONS. RATE OF CHANGE, MOLE/S, OF REACTING GASES

H2(g)	-0.43032E-03
I2(g)	-0.12065E-16
MoO2(g)	-0.59471E-22
MoO3(g)	-0.16497E-14
TeO2(g)	-0.14344E-03
(CsOH)2(g)	-0.13995E-04
CsOH(g)	-0.83853E-03
CsI(g)	-0.81320E-04
Cs2(g)	-0.36971E-50

FORMATION OF GASES DUE TO PURE GAS REACTIONS. RATE OF CHANGE, MOLE/S, OF REACTING GASES

H2O(g)	0.28688E-03
H2Te(g)	0.14344E-03

Continued on next page.

Table 12.3.1. Continued

FORMATION OF AEROSOL PARTICLES SOLELY FORMED FROM GAS REACTIONS.  
RATE OF CHANGE, MOLE/S, OF FORMED AEROSOL PARTICLES

-----  
CsI           0.81320E-04  
CsOH          0.86652E-03  
MoO2          0.16497E-14

DESTRUCTION OF AEROSOL PARTICLES DUE TO GAS FORMATION. RATE OF  
CHANGE, MOLE/S, OF DESTROYED AEROSOL PARTICLES

-----  
CsI           -0.42575E-09

GASES FORMED FROM AEROSOL PARTICLES. RATE OF CHANGE, MOLE/S, OF  
FORMED GASES FROM AEROSOL PARTICLES

-----  
H2O(g)        0.25921E-11  
(CsOH)2(g)    0.22850E-17  
CsOH(g)       0.77927E-19  
CsI(g)        0.72378E-23

AEROSOL PARTICLES FORMED BY REACTIONS BETWEEN THE GAS AND EXISTING  
AEROSOL PARTICLES. RATE OF CHANGE, MOLE/S, OF FORMED AEROSOL  
PARTICLES BY REACTIONS WITH THE GAS

-----  
CsI           0.42575E-09

AEROSOL DEPOSITION: RATE OF DEPOSITION, MOLE/S, AEROSOL PARTICLES

-----  
CsI           0.34772E-06  
CsOH          0.25431E-05  
MoO2          0.23925E-17  
SrO           0.28453E-13

FORMATION OF THE OUTER LAYER DUE TO CONDENSATION OR CHEMICAL  
REACTIONS OF VARIOUS KINDS. RATE OF CHANGE, MOLE/S, OF GASES DUE  
TO REACTION OR CONDENSATION ONTO THE OUTER DEPOSITED LAYER

-----  
H2(g)         -0.99760E-12  
H2Te(g)       -0.27756E-17  
(CsOH)2(g)    -0.34501E-12  
CsOH(g)       -0.93548E-14  
CsI(g)        -0.45081E-23

RATE OF CHANGE, MOLE/S, OF FORMED OUTER LAYER, DUE TO CONDENSATION  
OR CHEMICAL REACTIONS

-----  
MoO2         1   0.00000  
SrO          1   0.00000

Continued on next page.

Table 12.3.1. Continued

BREAKUP OF THE OUTER LAYER NUMBER 1 DUE TO EVAPORATION OR CHEMICAL REACTIONS OF VARIOUS KINDS. RATE OF CHANGE, MOLE/S, OF OUTER LAYER, DUE TO EVAPORATION OR CHEMICAL REACTIONS

-----  
 CsI 1 -0.33881E-21  
 CsOH 1 -0.11765E-17

PRESENT STATE IN THE UPPER DOWNCOMER

THE GAS STATE		THE AEROSOL PARTICLES	
-----		-----	
H2(g)	1410.37436	CsI	0.52851E-01
H2O(g)	4624.25272	CsOH	0.38653
H2Te(g)	0.97182E-01	MoO2	0.36364E-12
(CsOH)2(g)	0.16714E-02	SrO	0.43246E-08
CsOH(g)	0.90637E-04		
CsI(g)	0.52612E-07		

THE OUTER LAYER

-----

CsI	1	0.16780E-04
CsOH	1	0.13567E-03
MoO2	1	0.93400E-16
SrO	1	0.11730E-11

THE LOWER DOWNCOMER

GAS AND WALL TEMPERATURE, RESPECTIVELY: 551.60 532.14  
 MOLAR STEAM TO HYDROGEN RATIO: 3.2787  
 PRESSURE, IN KILOPASCAL: 232.47

NET GAS FLOW RATES, MOLE/S		NET AEROSOL FLOW RATES, MOLE/S	
-----		-----	
H2Te(g)	0.18266E-04	NONE	
I2(g)	0.49852E-19		
MoO2(g)	0.24572E-24		
MoO3(g)	0.68162E-17		
TeO2(g)	0.59267E-06		
CsOH(g)	0.33486E-05		
CsI(g)	0.33591E-06		
Cs2(g)	0.89013E-53		

DESTRUCTION OF GASES DUE TO PURE GAS REACTIONS. RATE OF CHANGE, MOLE/S, OF REACTING GASES

-----

H2(g)	-0.17780E-05
I2(g)	-0.49852E-19
MoO2(g)	-0.24572E-24
MoO3(g)	-0.68162E-17
TeO2(g)	-0.59267E-06
CsOH(g)	-0.35463E-05
CsI(g)	-0.33621E-06
Cs2(g)	-0.27205E-51

Continued on next page.

Table 12.3.1. Continued

FORMATION OF GASES DUE TO PURE GAS REACTIONS. RATE OF CHANGE,  
MOLE/S, OF REACTING GASES

-----  
H2O(g) 0.11853E-05  
H2Te(g) 0.59267E-06  
(CsOH)2(g) 0.17732E-05

FORMATION OF AEROSOL PARTICLES SOLELY FORMED FROM GAS REACTIONS.  
RATE OF CHANGE, MOLE/S, OF FORMED AEROSOL PARTICLES

-----  
CsI 0.33621E-06  
MoO2 0.68162E-17

GASES FORMED FROM AEROSOL PARTICLES. RATE OF CHANGE, MOLE/S, OF  
FORMED GASES FROM AEROSOL PARTICLES

-----  
H2(g) 0.63665E-12  
H2O(g) 0.25068E-11  
(CsOH)2(g) 0.20917E-06  
CsOH(g) 0.68211E-08

AEROSOL DEPOSITION: RATE OF DEPOSITION, MOLE/S, AEROSOL PARTICLES

-----  
CsI 0.64021E-08  
CsOH 0.20157E-07  
MoO2 0.39380E-19  
SrO 0.48584E-15

FORMATION OF THE OUTER LAYER DUE TO CONDENSATION OR CHEMICAL  
REACTIONS OF VARIOUS KINDS. RATE OF CHANGE, MOLE/S, OF GASES DUE  
TO REACTION OR CONDENSATION ONTO THE OUTER DEPOSITED LAYER

-----  
H2Te(g) -0.54210E-20  
CsI(g) -0.15551E-20

RATE OF CHANGE, MOLE/S, OF FORMED OUTER LAYER, DUE TO CONDENSATION  
OR CHEMICAL REACTIONS

-----  
CsI 1 0.15577E-20  
MoO2 1 0.00000  
SrO 1 0.00000

BREAKUP OF THE OUTER LAYER NUMBER 1 DUE TO EVAPORATION OR CHEMICAL  
REACTIONS OF VARIOUS KINDS. RATE OF CHANGE, MOLE/S, OF OUTER  
LAYER, DUE TO EVAPORATION OR CHEMICAL REACTIONS

-----  
CsOH 1 -0.20160E-07

Continued on next page.

Table 12.3.1. Continued  
PRESENT STATE IN THE LOWER DOWNCOMER

THE GAS STATE		THE AEROSOL PARTICLES	
H2(g)	587.33893	CsI	0.74768E-03
H2O(g)	1925.71845	CsOH	0.23541E-02
H2Te(g)	0.13832E-02	MoO2	0.45990E-14
(CsOH)2(g)	0.16489E-02	SrO	0.56739E-10
CsOH(g)	0.10750E-03		
CsI(g)	0.75242E-07		

THE OUTER LAYER

CsI	1	0.20615E-06
CsOH	1	0.40570E-10
MoO2	1	0.12343E-17
SrO	1	0.15356E-13

THE LOWER HEAD (LOWER PLENUM)

GAS AND WALL TEMPERATURE, RESPECTIVELY	544.73	510.45
MOLAR STEAM TO HYDROGEN RATIO:	3.2787	
PRESSURE, IN KILOPASCAL:	232.47	

NET GAS FLOW RATES, MOLE/S		NET AEROSOL FLOW RATES, MOLE/S	
H2Te(g)	0.58955E-06	NONE	
I2(g)	0.26784E-21		
MoO2(g)	0.13202E-26		
MoO3(g)	0.36622E-19		
TeO2(g)	0.31843E-08		
(CsOH)2(g)	0.88471E-06		
CsOH(g)	0.10511E-06		
CsI(g)	0.17912E-08		
Cs2(g)	0.15438E-50		

DESTRUCTION OF GASES DUE TO PURE GAS REACTIONS. RATE OF CHANGE, MOLE/S, OF REACTING GASES

H2(g)	-0.95520E-08
I2(g)	-0.26784E-21
MoO2(g)	-0.13202E-26
MoO3(g)	-0.36622E-19
TeO2(g)	-0.31843E-08
(CsOH)2(g)	-0.95213E-07
CsI(g)	-0.22403E-08
Cs2(g)	-0.15448E-50

FORMATION OF GASES DUE TO PURE GAS REACTIONS. RATE OF CHANGE, MOLE/S, OF REACTING GASES

H2O(g)	0.63701E-08
H2Te(g)	0.31843E-08
CsOH(g)	0.19043E-06

Continued on next page.

Table 12.3.1. Continued

FORMATION OF AEROSOL PARTICLES SOLELY FORMED FROM GAS REACTIONS.  
RATE OF CHANGE, MOLE/S, OF FORMED AEROSOL PARTICLES

-----  
CsI            0.22403E-08  
MoO2          0.36622E-19

GASES FORMED FROM AEROSOL PARTICLES. RATE OF CHANGE, MOLE/S, OF  
FORMED GASES FROM AEROSOL PARTICLES

-----  
H2O(g)        0.22737E-12  
(CsOH)2(g)   0.27746E-06  
CsOH(g)       0.79869E-07  
CsI(g)        0.25808E-22

AEROSOL DEPOSITION: RATE OF DEPOSITION, MOLE/S, AEROSOL PARTICLES

-----  
CsI            0.10358E-09  
MoO2          0.60446E-21  
SrO            0.75883E-17

FORMATION OF THE OUTER LAYER DUE TO CONDENSATION OR CHEMICAL  
REACTIONS OF VARIOUS KINDS. RATE OF CHANGE, MOLE/S, OF GASES DUE  
TO REACTION OR CONDENSATION ONTO THE OUTER DEPOSITED LAYER

-----  
H2O(g)        -0.28649E-11  
H2Te(g)       -0.50822E-21  
(CsOH)2(g)   -0.17247E-08  
CsI(g)        -0.54084E-20

RATE OF CHANGE, MOLE/S, OF FORMED OUTER LAYER, DUE TO CONDENSATION  
OR CHEMICAL REACTIONS

-----  
CsI            1   0.54220E-20  
CsOH          1   0.70758E-13  
MoO2          1   0.00000  
SrO            1   0.00000

PRESENT STATE IN THE LOWER HEAD (LOWER PLENUM)

THE GAS STATE		THE AEROSOL PARTICLES	
-----		-----	
H2(g)	1329.93890	CsI	0.95913E-05
H2O(g)	4360.49363	MoO2	0.55975E-16
H2Te(g)	0.17916E-04	SrO	0.70269E-12
(CsOH)2(g)	0.30043E-04		
CsOH(g)	0.17281E-04		
CsI(g)	0.10663E-06		

Continued on next page.

Table 12.3.1. Continued

THE OUTER LAYER

CsI	1	0.26353E-08
CsOH	1	0.21430E-11
MoO2	1	0.15080E-19
SrO	1	0.19210E-15

THE RECIRCULATION LOOPS

GAS AND WALL TEMPERATURE, RESPECTIVELY	556.00	557.80
MOLAR STEAM TO HYDROGEN RATIO:	3.2787	
PRESSURE, IN KILOPASCAL:	232.47	

NET GAS FLOW RATES, MOLE/S		NET AEROSOL FLOW RATES, MOLE/S	
H2Te(g)	0.10893E-05	CsI	0.68072E-06
I2(g)	0.96278E-21	CsOH	0.16470E-05
MoO2(g)	0.47456E-26	MoO2	0.40159E-17
MoO3(g)	0.13164E-18	SrO	0.51375E-13
TeO2(g)	0.11446E-07		
(CsOH)2(g)	0.10781E-05		
CsOH(g)	0.10072E-06		
CsI(g)	0.64506E-08		

DESTRUCTION OF GASES DUE TO PURE GAS REACTIONS. RATE OF CHANGE, MOLE/S, OF REACTING GASES

H2(g)	-0.34339E-07
I2(g)	-0.96278E-21
MoO2(g)	-0.47456E-26
MoO3(g)	-0.13164E-18
TeO2(g)	-0.11446E-07
CsOH(g)	-0.48618E-07
CsI(g)	-0.65069E-08
Cs2(g)	-0.55494E-50

FORMATION OF GASES DUE TO PURE GAS REACTIONS. RATE OF CHANGE, MOLE/S, OF REACTING GASES

H2O(g)	0.22892E-07
H2Te(g)	0.11446E-07
(CsOH)2(g)	0.24309E-07

FORMATION OF AEROSOL PARTICLES SOLELY FORMED FROM GAS REACTIONS. RATE OF CHANGE, MOLE/S, OF FORMED AEROSOL PARTICLES

CsI	0.65069E-08
MoO2	0.13164E-18

Continued on next page.

Table 12.3.1. Continued

GASES FORMED FROM AEROSOL PARTICLES. RATE OF CHANGE, MOLE/S, OF FORMED GASES FROM AEROSOL PARTICLES

```
-----
H2O(g)      0.28795E-12
(CsOH)2(g)  0.11126E-05
CsOH(g)     0.56682E-07
```

AEROSOL DEPOSITION: RATE OF DEPOSITION, MOLE/S, AEROSOL PARTICLES

```
-----
CsI         0.62012E-10
MoO2       0.36917E-21
SrO        0.45977E-17
```

FORMATION OF THE OUTER LAYER DUE TO CONDENSATION OR CHEMICAL REACTIONS OF VARIOUS KINDS. RATE OF CHANGE, MOLE/S, OF GASES DUE TO REACTION OR CONDENSATION ONTO THE OUTER DEPOSITED LAYER

```
-----
H2(g)      -0.91660E-13
H2Te(g)    -0.50822E-21
(CsOH)2(g) -0.13108E-08
```

RATE OF CHANGE, MOLE/S, OF FORMED OUTER LAYER, DUE TO CONDENSATION OR CHEMICAL REACTIONS

```
-----
MoO2      1  0.00000
SrO       1  0.00000
```

BREAKUP OF THE OUTER LAYER NUMBER 1 DUE TO EVAPORATION OR CHEMICAL REACTIONS OF VARIOUS KINDS. RATE OF CHANGE, MOLE/S, OF OUTER LAYER, DUE TO EVAPORATION OR CHEMICAL REACTIONS

```
-----
CsI       1 -0.23652E-23
```

PRESENT STATE IN THE RECIRCULATION LOOPS

THE GAS STATE		THE AEROSOL PARTICLES	
-----		-----	
H2(g)	53.83734	CsI	0.23337E-04
H2O(g)	176.51743	MoO2	0.13893E-15
H2Te(g)	0.43169E-04	SrO	0.17303E-11
(CsOH)2(g)	0.87117E-04		
CsOH(g)	0.86615E-05		
CsI(g)	0.92483E-08		

THE OUTER LAYER

```
-----
CsI       1  0.17499E-08
MoO2     1  0.10048E-19
SrO      1  0.12775E-15
```

Continued on next page.

Table 12.3.1. Continued

THE PEDESTAL  
 GAS AND WALL TEMPERATURE, RESPECTIVELY 378.86 372.00  
 MOLAR STEAM TO HYDROGEN RATIO: 253.7935  
 PRESSURE, IN KILOPASCAL: 234.28

NET GAS FLOW RATES, MOLE/S		NET AEROSOL FLOW RATES, MOLE/S	
H <sub>2</sub> Te(g)	0.23260E-05	CsI	0.76338E-05
(CsOH) <sub>2</sub> (g)	0.39064E-09	CsOH	0.70085E-04
CsOH(g)	0.57924E-11	MoO <sub>2</sub>	0.39485E-16
CsI(g)	0.80148E-15	SrO	0.51692E-12

DESTRUCTION OF GASES DUE TO PURE GAS REACTIONS. RATE OF CHANGE, MOLE/S, OF REACTING GASES

H <sub>2</sub> (g)	-0.28903E-10
H <sub>2</sub> Te(g)	-0.71151E-20
(CsOH) <sub>2</sub> (g)	-0.20030E-11

FORMATION OF GASES DUE TO PURE GAS REACTIONS. RATE OF CHANGE, MOLE/S, OF REACTING GASES

H <sub>2</sub> O(g)	0.38108E-10
CsOH(g)	0.40060E-11

DESTRUCTION OF AEROSOL PARTICLES DUE TO GAS FORMATION. RATE OF CHANGE, MOLE/S, OF DESTROYED AEROSOL PARTICLES

CsI	-0.20369E-15
-----	--------------

GASES FORMED FROM AEROSOL PARTICLES. RATE OF CHANGE, MOLE/S, OF FORMED GASES FROM AEROSOL PARTICLES

H <sub>2</sub> O(g)	0.45975E-10
(CsOH) <sub>2</sub> (g)	0.10792E-08
CsOH(g)	0.67060E-11
CsI(g)	0.28783E-15

AEROSOL PARTICLES FORMED BY REACTIONS BETWEEN THE GAS AND EXISTING AEROSOL PARTICLES. RATE OF CHANGE, MOLE/S, OF FORMED AEROSOL PARTICLES BY REACTIONS WITH THE GAS

CsI	0.20369E-15
-----	-------------

CONVECTIVE WATER TRANSPORT OF SUBSTANCES. GASES

H <sub>2</sub> Te(g)	0.90643E-04
(CsOH) <sub>2</sub> (g)	0.81000E-08
CsOH(g)	0.12209E-09
CsI(g)	0.17570E-13

Continued on next page.

Table 12.3.1. Continued

CONVECTIVE WATER TRANSPORT OF SUBSTANCES. AEROSOL PARTICLES

CsI	0.33584E-06
CsOH	0.25925E-05
MoO2	0.19315E-17
SrO	0.24469E-13

FORMATION OF OF WATER DISSOLVED GAS, MOLE/S

H2Te (g)	0.15082E-05
(CsOH)2 (g)	0.14921E-08
CsOH (g)	0.16906E-10
CsI (g)	0.83878E-15

FORMATION OF WATER DISSOLVED AEROSOL PARTICLES, MOLE/S

CsI	0.20467E-05
CsOH	0.16829E-04
MoO2	0.10798E-16
SrO	0.14034E-12

PRESENT STATE IN THE PEDESTAL

THE GAS STATE

H2 (g)	231.40151
H2O (g)	58728.19112
H2Te (g)	0.30165E-04
(CsOH)2 (g)	0.29842E-07
CsOH (g)	0.33811E-09
CsI (g)	0.16776E-13

THE AEROSOL PARTICLES

CsI	0.13508E-03
CsOH	0.11107E-02
MoO2	0.71267E-15
SrO	0.92620E-11

THE OUTER LAYER

CsI	1	0.17499E-08
MoO2	1	0.10048E-19
SrO	1	0.12775E-15

THE WATER: CONTENT OF SOLIDS

CsI	0.70067E-04
CsOH	0.58992E-03
MoO2	0.34808E-15
SrO	0.45926E-11

CONTENT OF GASES

H2Te (g)	0.25273E-02
(CsOH)2 (g)	0.48227E-06
CsOH (g)	0.67023E-08
CsI (g)	0.78030E-12

Continued on next page.

Table 12.3.1. Continued

THE DRYWELL

GAS AND WALL TEMPERATURE, RESPECTIVELY 406.39 391.70  
 MOLAR STEAM TO HYDROGEN RATIO: 49.9476  
 PRESSURE, IN KILOPASCAL: 232.67

NET GAS FLOW RATES, MOLE/S		NET AEROSOL FLOW RATES, MOLE/S	
H2Te (g)	0.52751E-02	CsI	0.59437E-02
I2 (g)	0.66901E-16	CsOH	0.42386E-01
MoO2 (g)	0.32976E-21	MoO2	0.39133E-13
MoO3 (g)	0.91473E-14	SrO	0.55292E-09
TeO2 (g)	0.79536E-03		
(CsOH)2 (g)	0.59836E-04		
CsOH (g)	0.46479E-02		
CsI (g)	0.45091E-03		
Cs2 (g)	0.58676E-50		

DESTRUCTION OF GASES DUE TO PURE GAS REACTIONS. RATE OF CHANGE, MOLE/S, OF REACTING GASES

H2 (g)	-0.23861E-02
I2 (g)	-0.66901E-16
MoO2 (g)	-0.32976E-21
MoO3 (g)	-0.91473E-14
TeO2 (g)	-0.79536E-03
(CsOH)2 (g)	-0.59667E-04
CsOH (g)	-0.46479E-02
CsI (g)	-0.45091E-03
Cs2 (g)	-0.58676E-50

FORMATION OF GASES DUE TO PURE GAS REACTIONS. RATE OF CHANGE, MOLE/S, OF REACTING GASES

H2O (g)	0.15907E-02
H2Te (g)	0.79536E-03

FORMATION OF AEROSOL PARTICLES SOLELY FORMED FROM GAS REACTIONS. RATE OF CHANGE, MOLE/S, OF FORMED AEROSOL PARTICLES

CsI	0.45091E-03
CsOH	0.47673E-02
MoO2	0.91473E-14

DESTRUCTION OF AEROSOL PARTICLES DUE TO GAS FORMATION. RATE OF CHANGE, MOLE/S, OF DESTROYED AEROSOL PARTICLES

CsI	-0.11378E-12
CsOH	-0.69389E-17

Continued on next page.

Table 12.3.1. Continued

GASES FORMED FROM AEROSOL PARTICLES. RATE OF CHANGE, MOLE/S, OF FORMED GASES FROM AEROSOL PARTICLES

H2(g)	0.39563E-11
H2O(g)	0.34852E-09
CsI(g)	0.28980E-26

AEROSOL PARTICLES FORMED BY REACTIONS BETWEEN THE GAS AND EXISTING AEROSOL PARTICLES. RATE OF CHANGE, MOLE/S, OF FORMED AEROSOL PARTICLES BY REACTIONS WITH THE GAS

CsI	0.11378E-12
CsOH	0.69389E-17

FORMATION OF WATER DISSOLVED GAS, MOLE/S

H2Te(g)	0.35665E-02
(CsOH)2(g)	0.17359E-06
CsOH(g)	0.25669E-08
CsI(g)	0.35398E-12

FORMATION OF WATER DISSOLVED AEROSOL PARTICLES, MOLE/S

CsI	0.40766E-04
CsOH	0.30065E-03
MoO2	0.30766E-15
SrO	0.35237E-11

PRESENT STATE IN THE DRYWELL

THE GAS STATE		THE AEROSOL PARTICLES	
H2(g)	5914.60338	CsI	0.12725
H2O(g)	295422.88622	CsOH	0.93849
H2Te(g)	0.71330E-01	MoO2	0.96037E-12
(CsOH)2(g)	0.34719E-05	SrO	0.11000E-07
CsOH(g)	0.51338E-07		
CsI(g)	0.70796E-11		

THE OUTER LAYER

CsI	1	0.17499E-08
MoO2	1	0.10048E-19
SrO	1	0.12775E-15

THE WATER: CONTENT OF SOLIDS		CONTENT OF GASES	
CsI	0.10534E-02	H2Te(g)	0.12091
CsOH	0.79282E-02	(CsOH)2(g)	0.85290E-05
MoO2	0.74253E-14	CsOH(g)	0.12632E-06
SrO	0.86900E-10	CsI(g)	0.17454E-10

Continued on next page.

Table 12.3.1. Continued

THE WETWELL

GAS AND WALL TEMPERATURE, RESPECTIVELY	298.27	294.74
MOLAR STEAM TO HYDROGEN RATIO:	752.0301	
PRESSURE, IN KILOPASCAL:	237.23	

DESTRUCTION OF GASES DUE TO PURE GAS REACTIONS. RATE OF CHANGE, MOLE/S, OF REACTING GASES

-----  
H2(g)            -0.25101E-09

CONVECTIVE WATER TRANSPORT OF SUBSTANCES. GASES

-----  
H2Te(g)        0.25767E-02  
(CsOH)2(g)    0.26397E-06  
CsOH(g)        0.39119E-08  
CsI(g)         0.54057E-12

CONVECTIVE WATER TRANSPORT OF SUBSTANCES. AEROSOL PARTICLES

-----  
CsI             0.12470E-04  
CsOH            0.10045E-03  
MoO2            0.66508E-16  
SrO             0.85905E-12

Continued on next page.  
Table 12.3.1. Continued

PRESENT STATE IN THE WETWELL

THE GAS STATE

-----  
H2(g)        291.70876  
H2O(g)      219373.77705

THE OUTER LAYER

-----  
CsI        1   0.17499E-08  
MoO2      1   0.10048E-19  
SrO        1   0.12775E-15

THE WATER: CONTENT OF SOLIDS

-----  
CsI            0.33519E-03  
CsOH          0.27835E-02  
MoO2          0.16883E-14  
SrO            0.22139E-10

CONTENT OF GASES

-----  
H2Te(g)      0.79421E-01  
(CsOH)2(g)   0.13057E-04  
CsOH(g)      0.19457E-06  
CsI(g)        0.27077E-10



### 13 CONCLUSIONS AND RECOMMENDATIONS

The ability of accident analysis codes to predict the course of events and the consequences of accidents with severe core damage can be expected to remain rather limited in spite of an increasing understanding of the pertinent phenomena and increasingly sophisticated mathematical modeling. In case of codes intended for practical safety analysis, like the MAAP code, this limitation is even more obvious in view of the modeling simplifications which have been necessary for practical reasons.

The shortcomings of the MAAP code are due to phenomenological uncertainties and to a complexity of the problem well beyond any reasonably workable mathematical model. Chemistry is indeed an important factor contributing to the complexity, but cannot always be distinctly separated from other factors, all together governing the course of events in the accident. This is particularly evident when trying to account for the progressing damage to the core structure during heat up during the accident, with ballooning and bursting of the fuel cladding while simultaneously oxidizing and undergoing a variety of reactions between various metallic and oxidic phases producing melts and gases and causing further deformation and segregated relocation of molten materials, possible build-up of an intermediate 'crucible' formation, temporarily holding up a melt pool, and final meandering towards the lower plenum of the pressure vessel.

Obviously, when applying the MAAP code to analysis of certain accident sequences in order to assess aspects of safety and risk, e.g. the proper functioning of consequence mitigating features and the anticipated mitigation achieved by means of various operator actions, the uncertainties in the calculated results have to be anticipated and allowed for in terms of added safety margins. These uncertainties are indeed appreciable as demonstrated by the practice in Sweden to apply an added safety margin of at least 100 % to the quantities of elemental hydrogen predicted by the MAAP code for an accident. It must be realized, however, that the implications of the uncertainties may extend beyond clearly realized risk factors under consideration, like the risks associated with larger amounts of hydrogen produced. Thus, in the example given, the important matter of the progress and timing of the core melting will be expected to bear a close relation to the amount of hydrogen produced, in view of the associated heat of reaction.

The purpose of the studies in the AKTI-150 project may accordingly be expressed as being one of assessing whether chemistry may actually in any respect entail predictable variations in the calculated results beyond the already rather considerable uncertainty limits assumed hitherto and be important as well in regard of risks and safety.

One important conclusion of the Swedish RAMA Project, expected to be confirmed by the Finnish VARA Project, is that the MAAP code can be recommended as a tool for safety analysis in connection with safety assessments of provisions for mitigation of severe accidents in the

Swedish BWR- and PWR-reactors provided proper allowance is made for the uncertainties. This conclusion is based on extensive studies of the code itself, sensitivity studies for various input parameters and modeling options and comparisons with another code system, the NRC Source Term Code Package (STCP), particularly the MARCH module.

In this project, a certain basis has been achieved for pointing out factors of chemical nature which could be significant in the sense indicated, i.e. by reviewing possible chemical influences (Chapter 4) in view of the modeling adopted in the MAAP code (Chapter 8), by experiments investigating hygroscopicity as one factor of importance with regard to aerosol behavior (Chapter 3.1-2) and the behavior of boron carbide with regard to melt progression and iodine chemistry (Chapter 3.3), and, finally, by attempting improved modeling of chemistry in code calculations (Chapters 10-12).

The following conclusions have been reached.

1. On the whole, also in consideration of the effects listed above, there appears to be no definite indication of any chemical effect, thus far poorly modeled or unaccounted for, which would entail an influence to a degree necessitating reconsideration of the current safety assessments or the current accident mitigating systems and accident mitigating strategies.
2. The influence of hygroscopicity of cesium hydroxide on aerosol behavior is partly of mitigating nature, as it implies enhanced particle growth and reduced shape factors which lead to an increased settling rate. Another anticipated effect under certain conditions close to the saturation temperature of the steam would be increased tendency of the cesium containing deposits to run off the surfaces in the primary system after absorption of water. As the run-off may lead into hotter regions, this may result in an increased re-evaporation. This may influence the retention of radioactivity in the primary system after meltthrough of the pressure vessel.
3. The experiments with boron carbide have confirmed the large influence of boron carbide on the melting of control rods containing this neutron absorbing material, thereby in turn causing further damage on adjacent fuel assemblies, by vigorously reacting with stainless steel as previously observed in the DF-4 experiment in the ACRR reactor at Sandia National Laboratory and in the CORA experiments at KfK, Karlsruhe.
4. The influence on iodine chemistry of borates and boric acid is not fully resolved. Recent experimental work indicates that, if borates are formed, there will be a substantial formation of volatile HI in the primary system. However, HI, as well as CsI, would be retained in the water sump in the containment and not spread to the environment.
5. The appreciable potential for hydrogen production in the containment due to the usually large surfaces of corrodable aluminium and zinc should be recognized and measures taken to

ensure that materials like mercury, which catalyzes the corrosion, will not be released to the containment atmosphere under accident conditions.

6. Organic and inorganic gases and vapors evolved in pyrolysis and vaporization of electric equipment and cables, particularly abundant in the region below the pressure vessel, may have appreciable influence on the speciation of radioactive iodine with consequent effects on the formation of organic iodine compounds and the capacity of the MVSS filters to retain this part of the radioactivity. This will also be important in some of the low probability events normally included in the residual risk.
7. The CELSOL calculations have demonstrated that plateout and chemical reactions with surface material can be important for the retainment of radioactive compounds in the primary system. Furthermore, these calculations have also shown that the predicted speciation of iodine is highly sensitive to the set of thermodynamic data for boron carbide used.
8. Preliminary calculations with CHMAPP on the AB sequence have shown that considerable chemical reactions are driven by the hydrogen generated in the core. In some cases, Te and Mo, it was observed that different chemical species dominated in the gas phase and on surfaces in the primary system. The results also show that it is possible to change the final amounts of some materials deposited in the containment considerably by changes in the assumed reaction-rate parameters.

As a consequence of this study it is recommended that appropriate chemical models are developed and implemented in the accident analysis codes. It is also very important to include all really occurring materials in the analysis.